Supplementary Information

for

Investigation of a Bacteriochlorin-Containing Pentad Array for

Panchromatic Light-Harvesting and Charge Separation

Haoyu Jing,[1] Nikki Cecil M. Magdaong,[2] James R. Diers,[3]

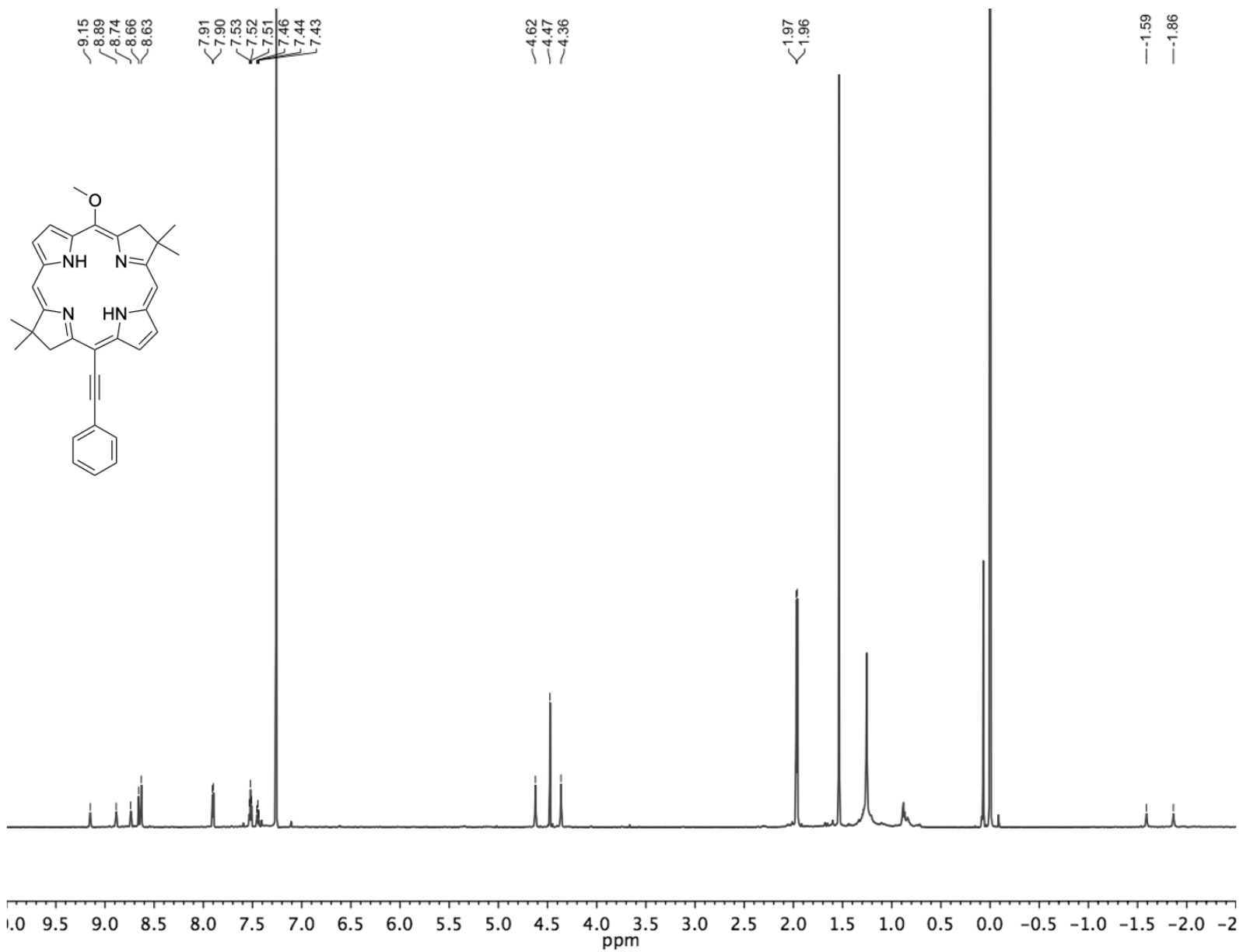Christine Kirmaier,[2] David F. Bocian,[3] Dewey Holten,[2] and Jonathan S. Lindsey[1]

[1] Department of Chemistry
North Carolina State University
Raleigh, North Carolina 27695-8204
E-mail: jlindsey@ncsu.edu

[2] Department of Chemistry
Washington University
St. Louis, Missouri 63130-4889
E-mail: holten@wustl.edu

[3] Department of Chemistry
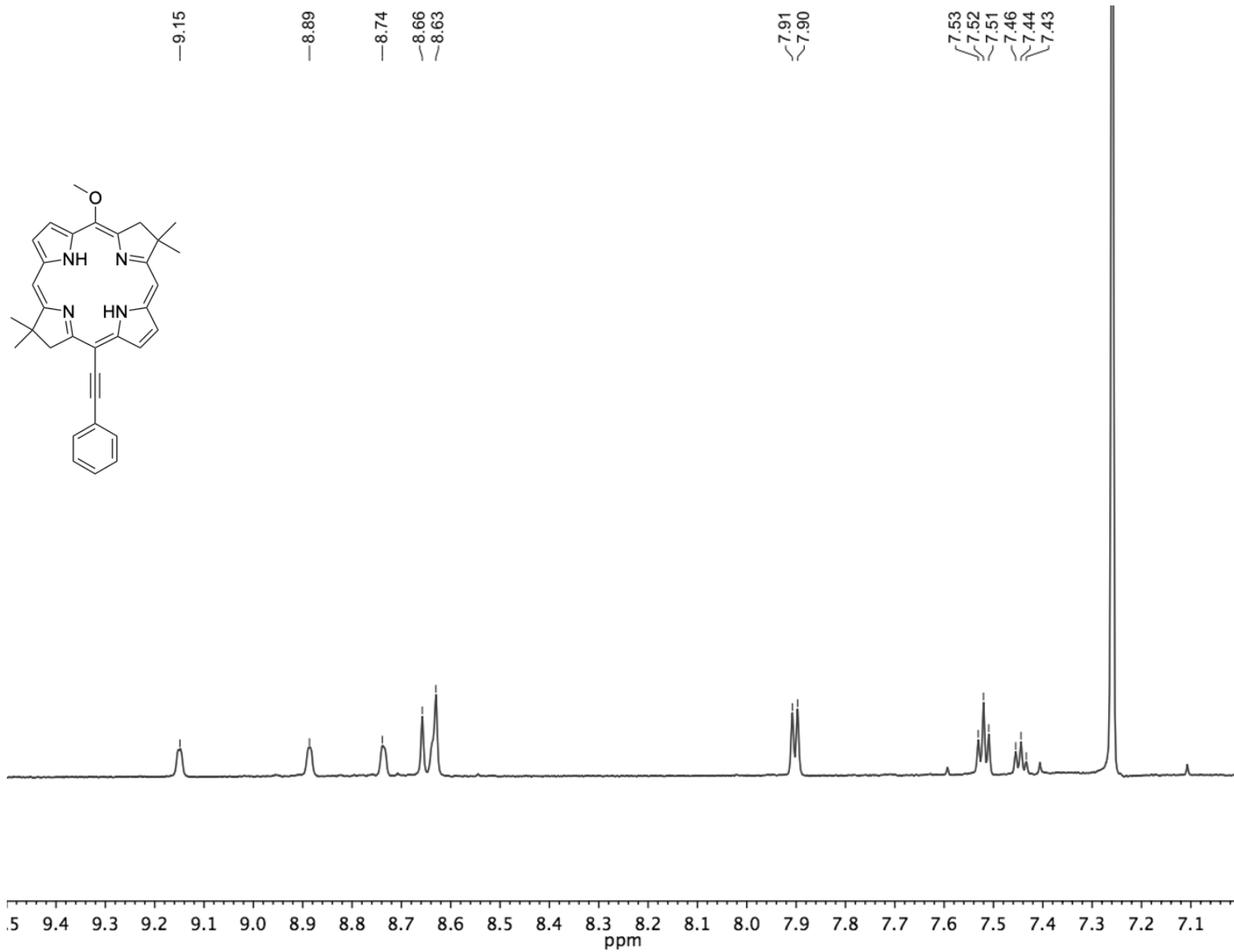University of California
Riverside, California 92521-0403
E-mail: david.bocian@ucr.edu

Table of Contents

Figure S1. ¹H NMR spectrum of **MeOBC-1**.

Figure S2. ¹H NMR spectrum of **MeOBC-1**.
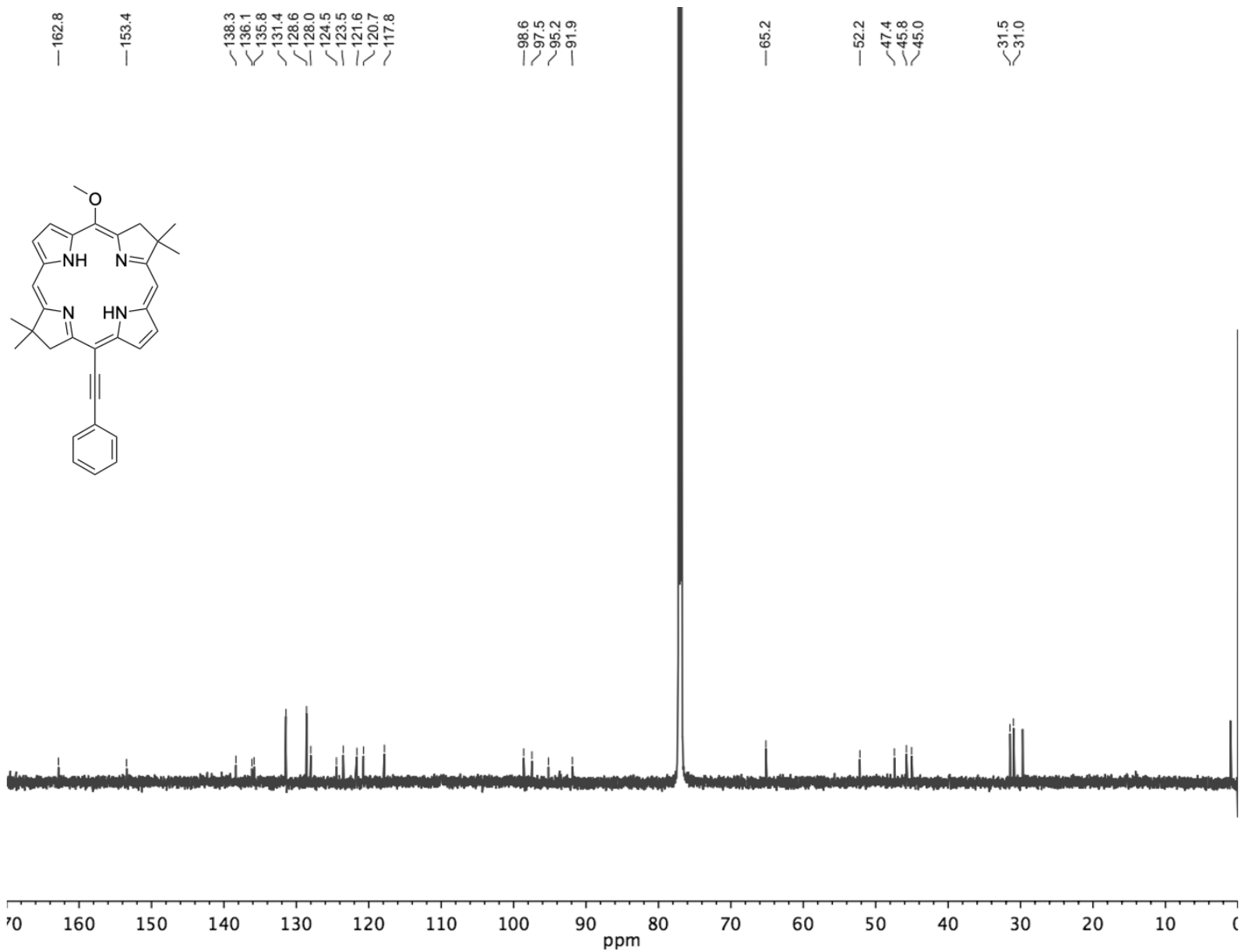
Figure S3. $^{13}C\{^1H\}$ NMR spectrum of **MeOBC-1**.
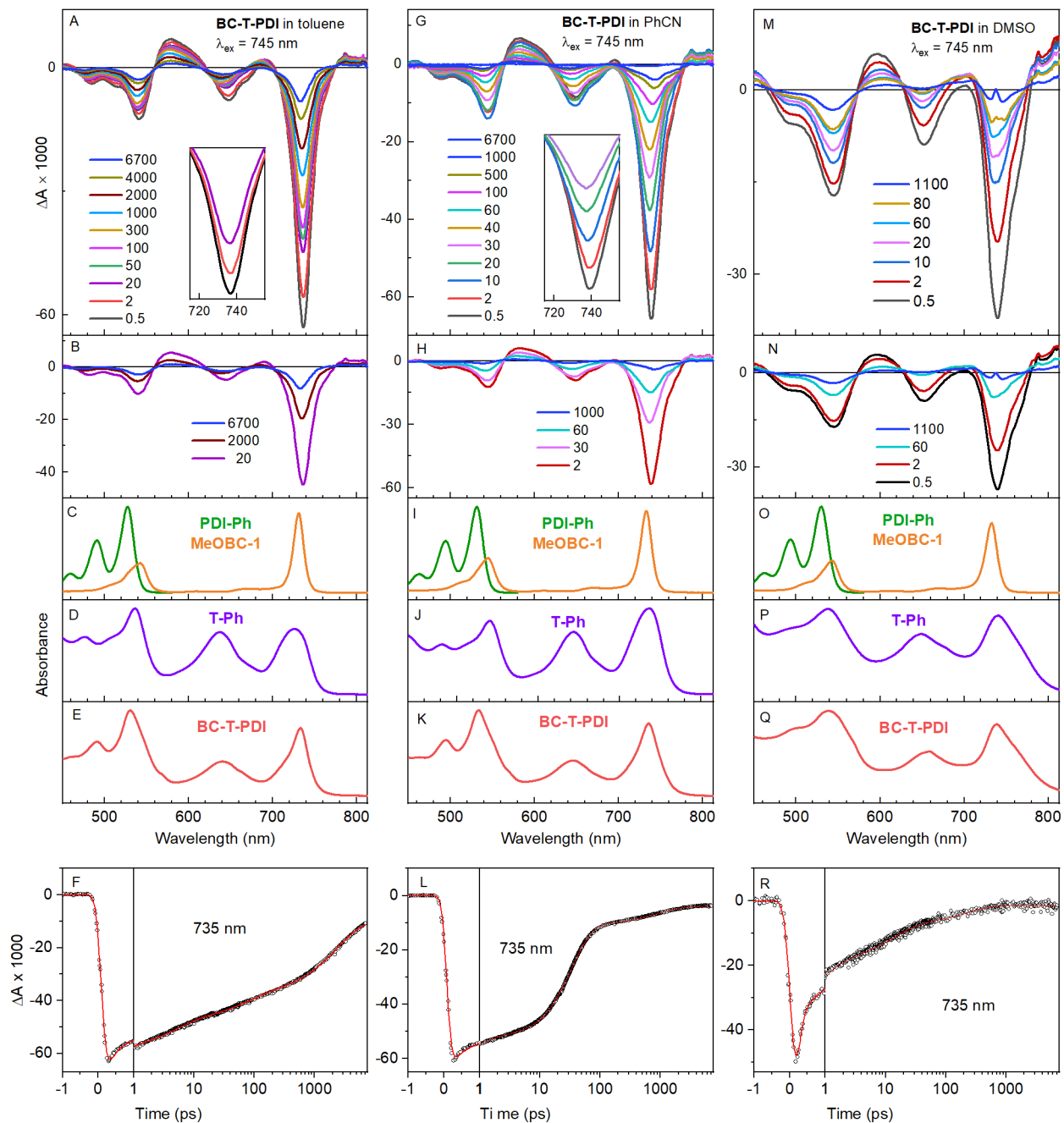
Figure S4. TA data for pentad **BC-T-PDI** in toluene (left), PhCN (middle), and DMSO (right). For each column of data, the top two panels show TA data at various times after excitation with a 100-fs flash at 745 nm; the middle three panels show ground-state absorption spectra of monomers **PDI-Ph** and **MeOBC**-1, benchmark triad **T-Ph** and the pentad; the bottom panel shows a kinetic profile for decay of combined $S_0 \rightarrow S_1$ bleaching and $S_1 \rightarrow S_0$ stimulated emission of the central panchromatic triad (T) of the pentad. The insets to panels A and G show evolution of this composite near-infrared feature at early times.
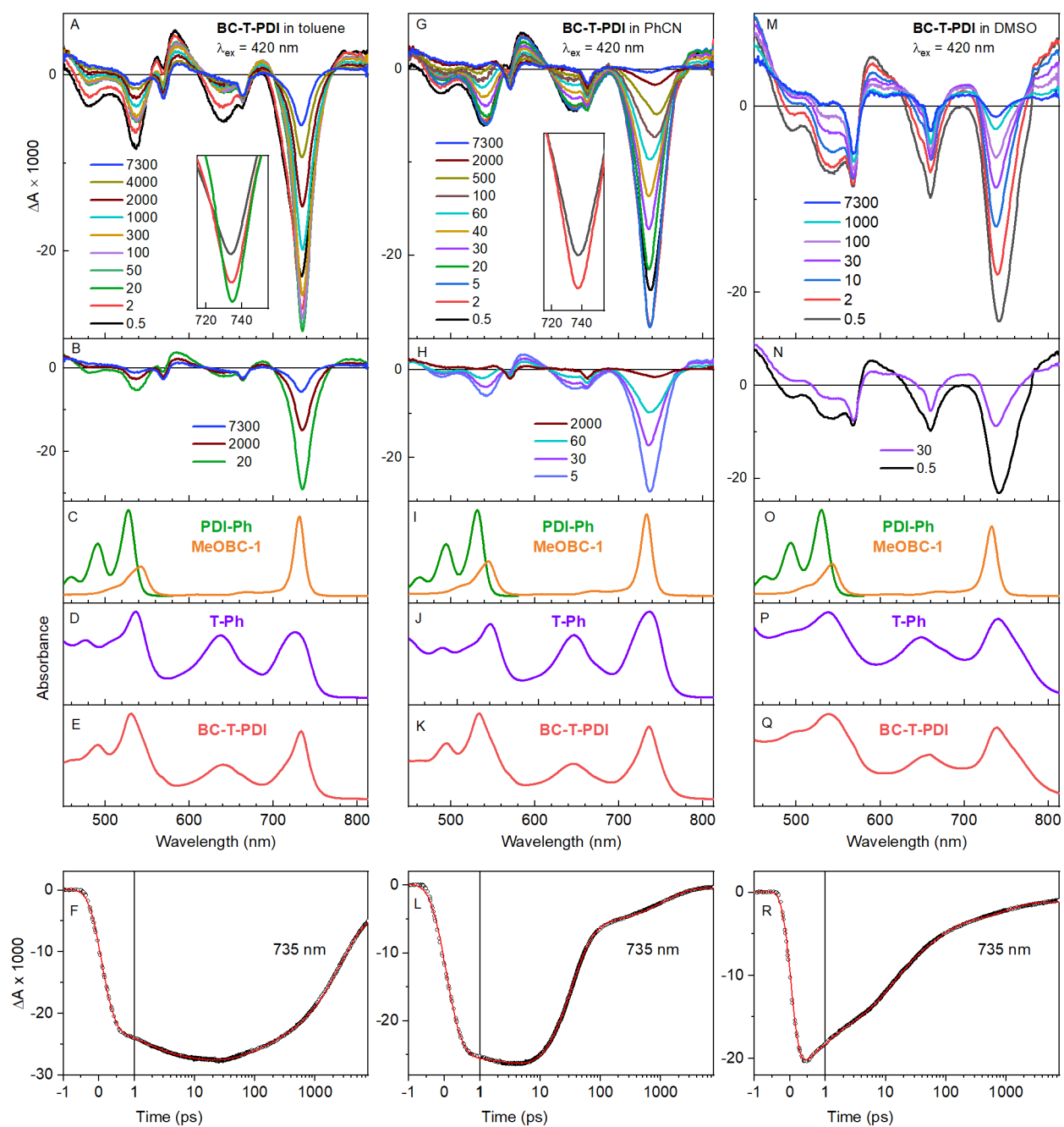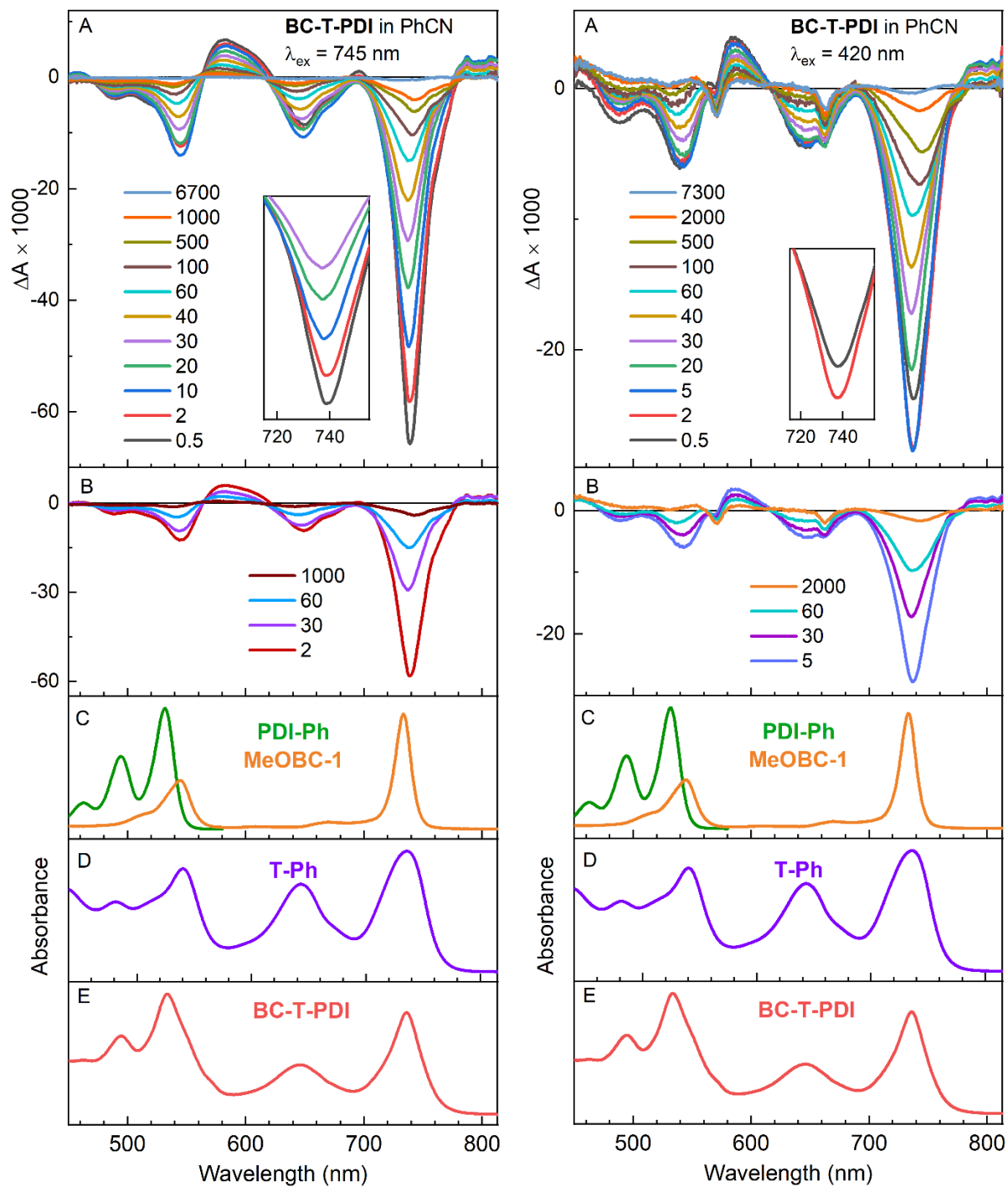
Figure S5. TA data for pentad **BC-T-PDI** in toluene (left), PhCN (middle), and DMSO (right). For each column of data, the top two panels show TA data at various times after excitation with a 100-fs flash at 420 nm; the middle three panels show ground-state absorption spectra of monomers **PDI-Ph** and **MeOBC**-1, benchmark triad **T-Ph** and the pentad; the bottom panel shows a kinetic profile for decay of combined $S_0 \rightarrow S_1$ bleaching and $S_1 \rightarrow S_0$ stimulated emission of the central panchromatic triad (T) of the pentad. The insets to panels A and G show evolution of this composite near-infrared feature at early times. The raw TA data obtained using 420 nm excitation flashes show small sharp features at ~570 and ~660 nm due to a small amount of putative chlorin in the **BC-T-PDI** samples. This impurity partially absorbs the 420 nm excitation light along with the majority absorption by the triad (T) component of the pentad; the putative chlorin is not excited using 745 nm excitation flashes.
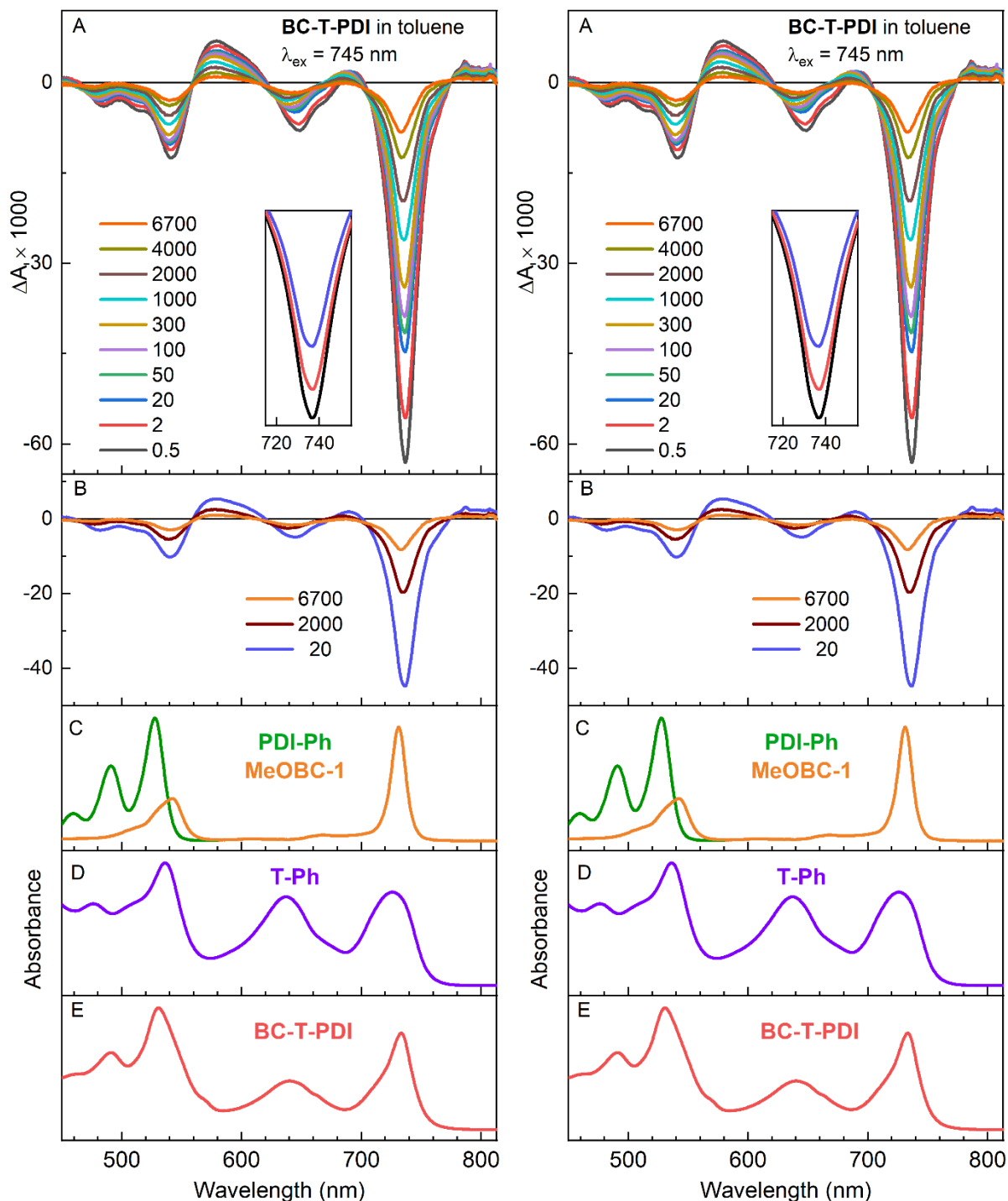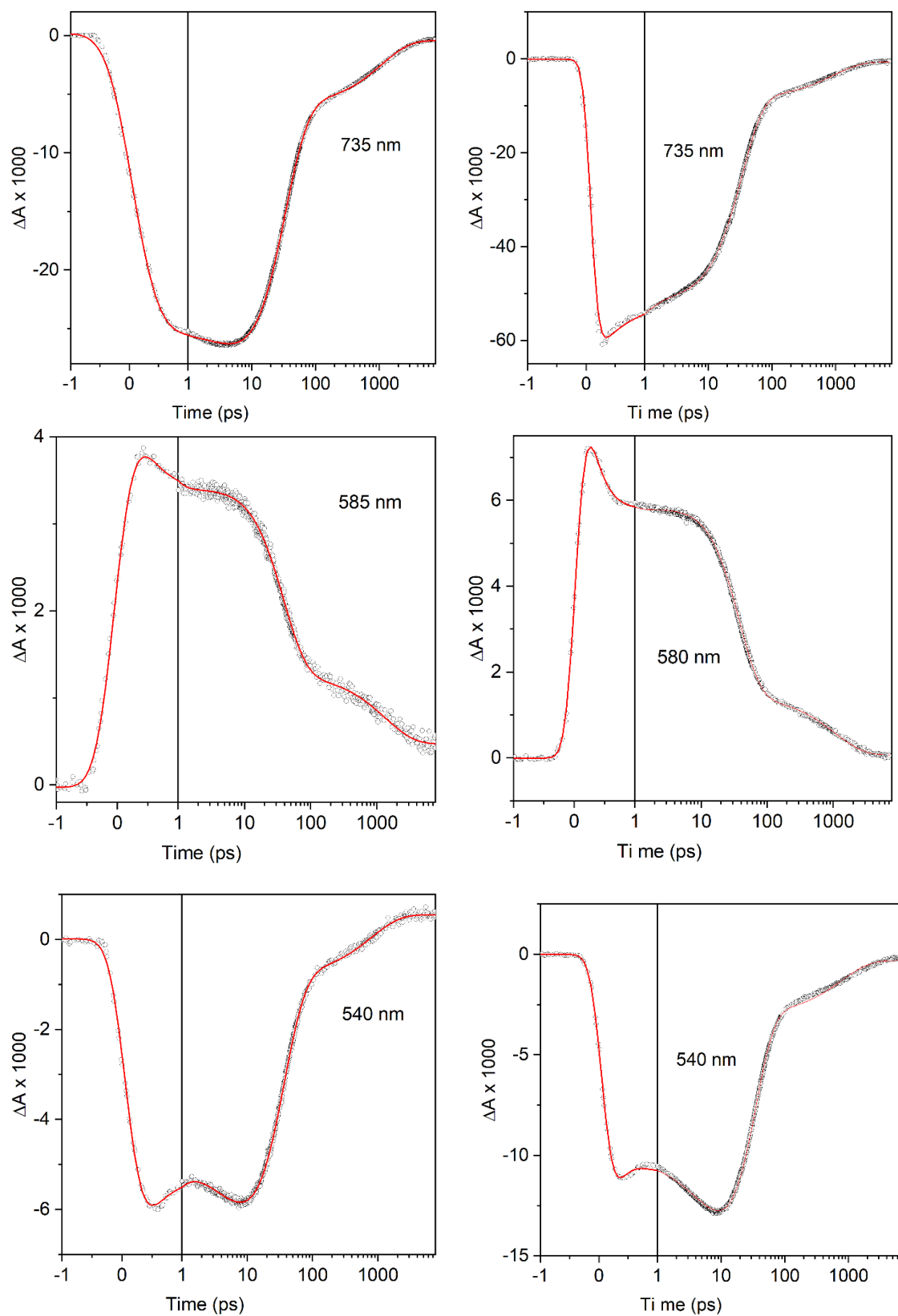
Figure S6. Time-resolved and static absorption data for arrays in toluene using λ_{ex} = 745 nm (left panels) and λ_{ex} = 430 nm (right panels). Both columns of panels show TA difference spectra for pentad **BC-T-PDI** in toluene (A, B) and ground-state absorption spectra of monomers **PDI-Ph** and **MeOBC-**1 (C), benchmark triad **T-Ph** (D) and the pentad (E). The TA data show small sharp features at ~570 and ~660 nm due to excitation of a small amount of putative chlorin impurity using λ_{ex} = 420 nm but not λ_{ex} =745 nm. See the next Figure for kinetic traces.
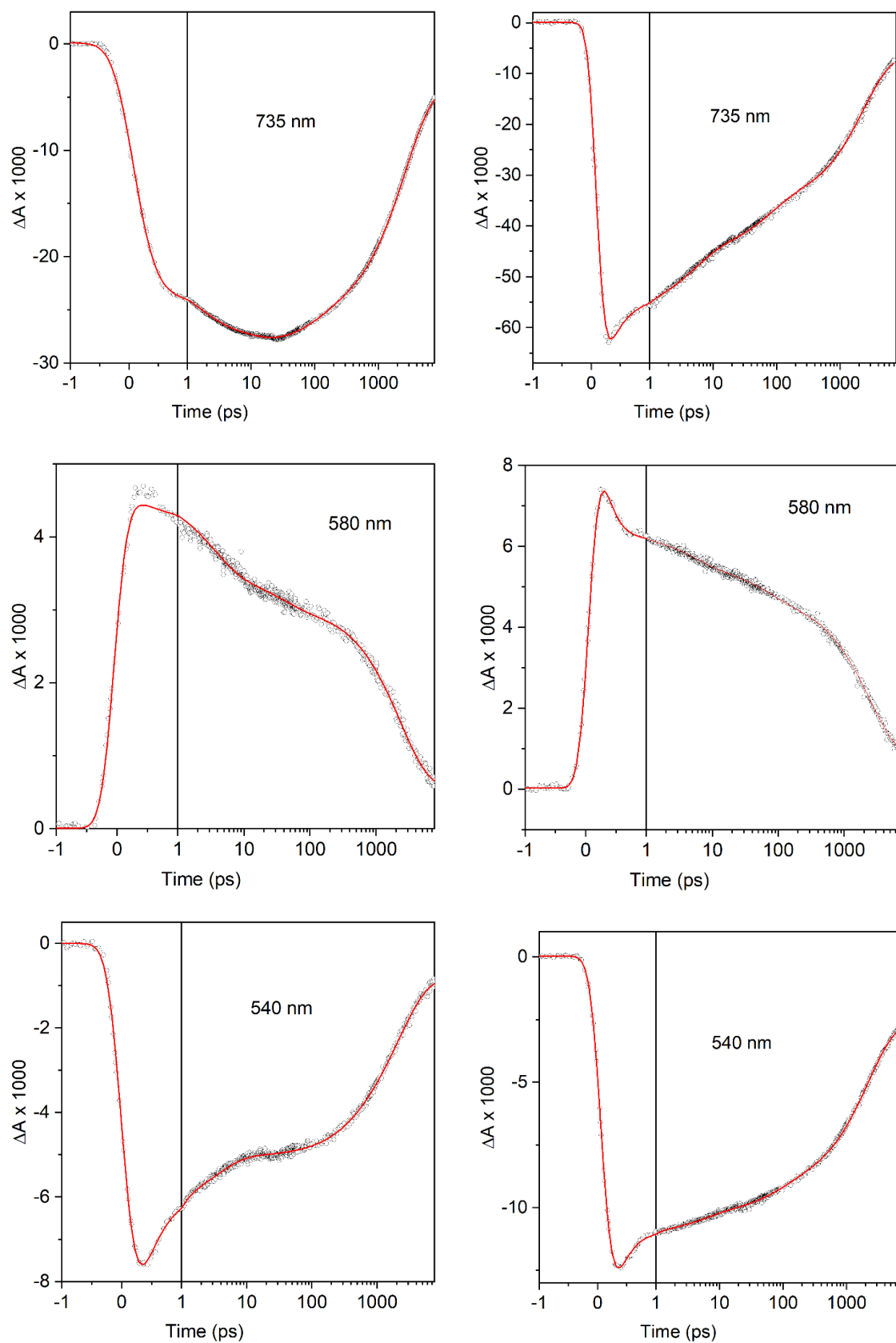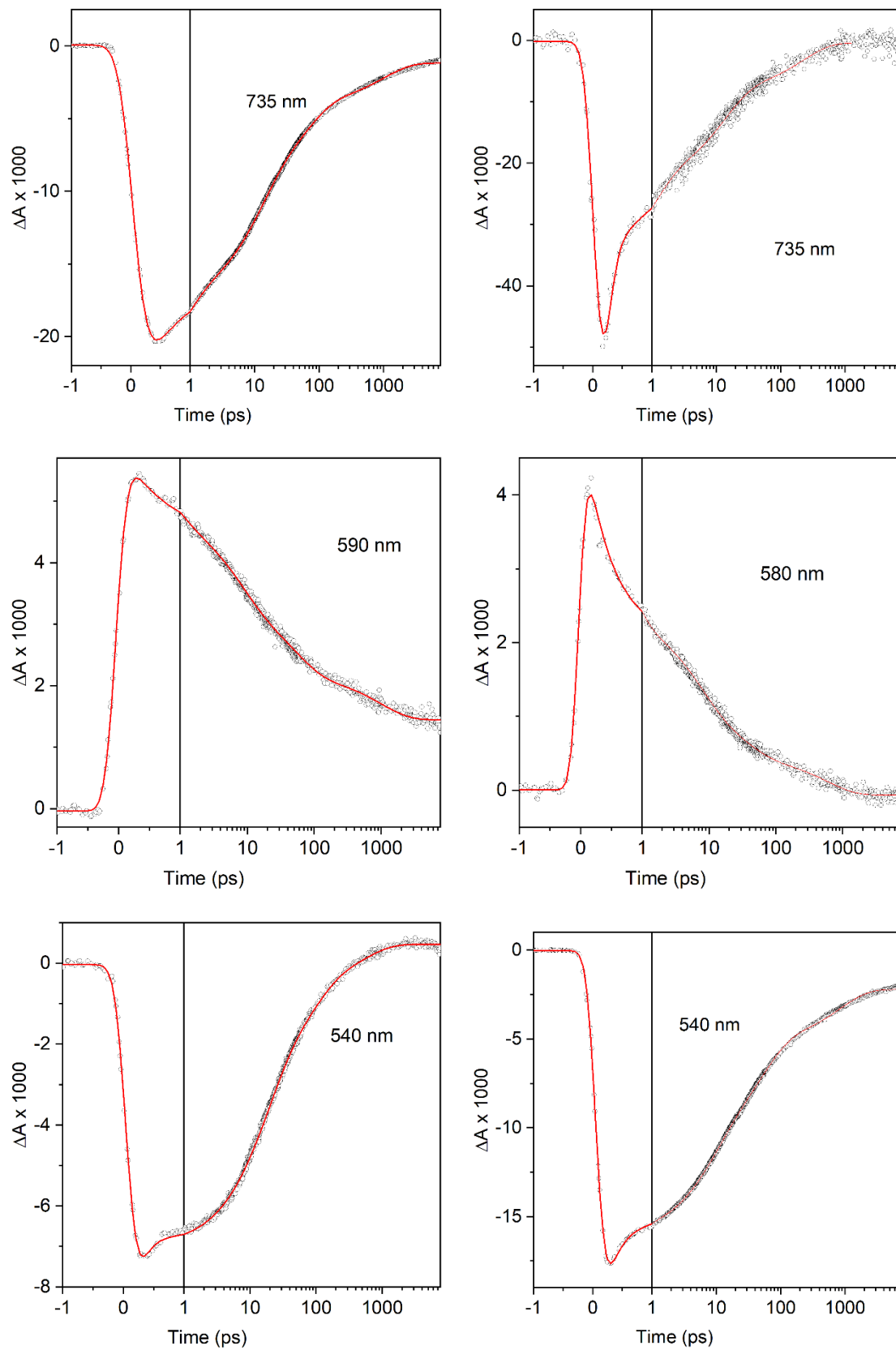
Figure S7. TA kinetic profiles and fits for **BC-T-PDI** in toluene at various probe wavelengths using λ_{ex} = 745 nm (left panels) and λ_{ex} = 420 nm (right panels). See the prior Figure for TA spectra.
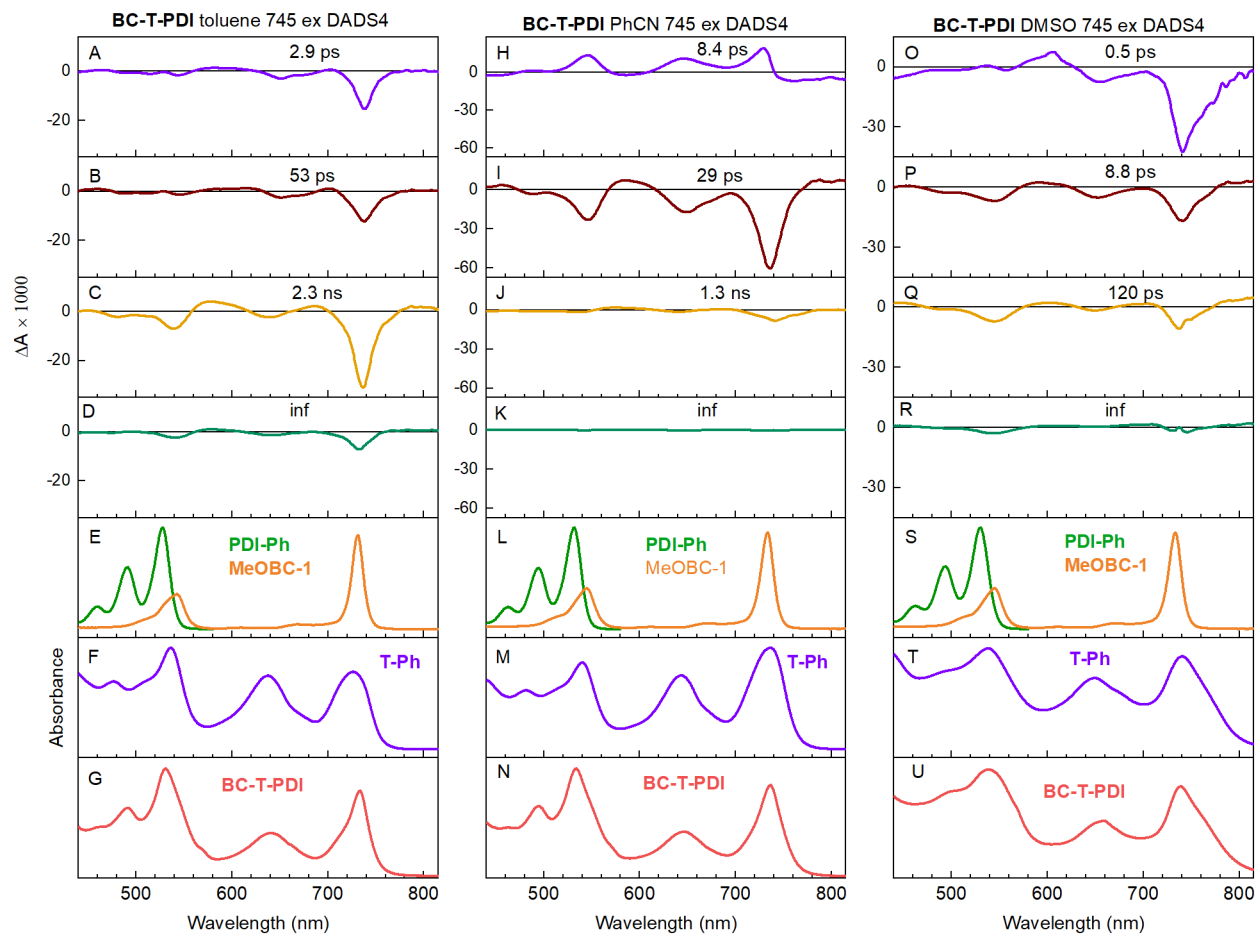
Figure S8. Time-resolved and static absorption data for arrays in PhCN using λ_{ex} = 745 nm (left panels) and λ_{ex} = 420 nm (right panels). Both columns of panels show TA difference spectra for pentad **BC-T-PDI** in toluene (A, B) and ground-state absorption spectra of monomers **PDI-Ph** and **MeOBC-**1 (C), benchmark triad **T-Ph** (D) and the pentad (E). The TA data show small sharp features at ~570 and ~660 nm due to excitation of a small amount of putative chlorin impurity using λ_{ex} = 420 nm but not λ_{ex} =745 nm. See the next Figure for kinetic traces.

Figure S9. TA kinetic profiles and fits for **BC-T-PDI** in PhCN at various probe wavelengths using $\lambda_{ex} =$ 745 nm (left panels) and $\lambda_{ex} = 420$ nm (right panels). See the prior Figure for TA spectra.
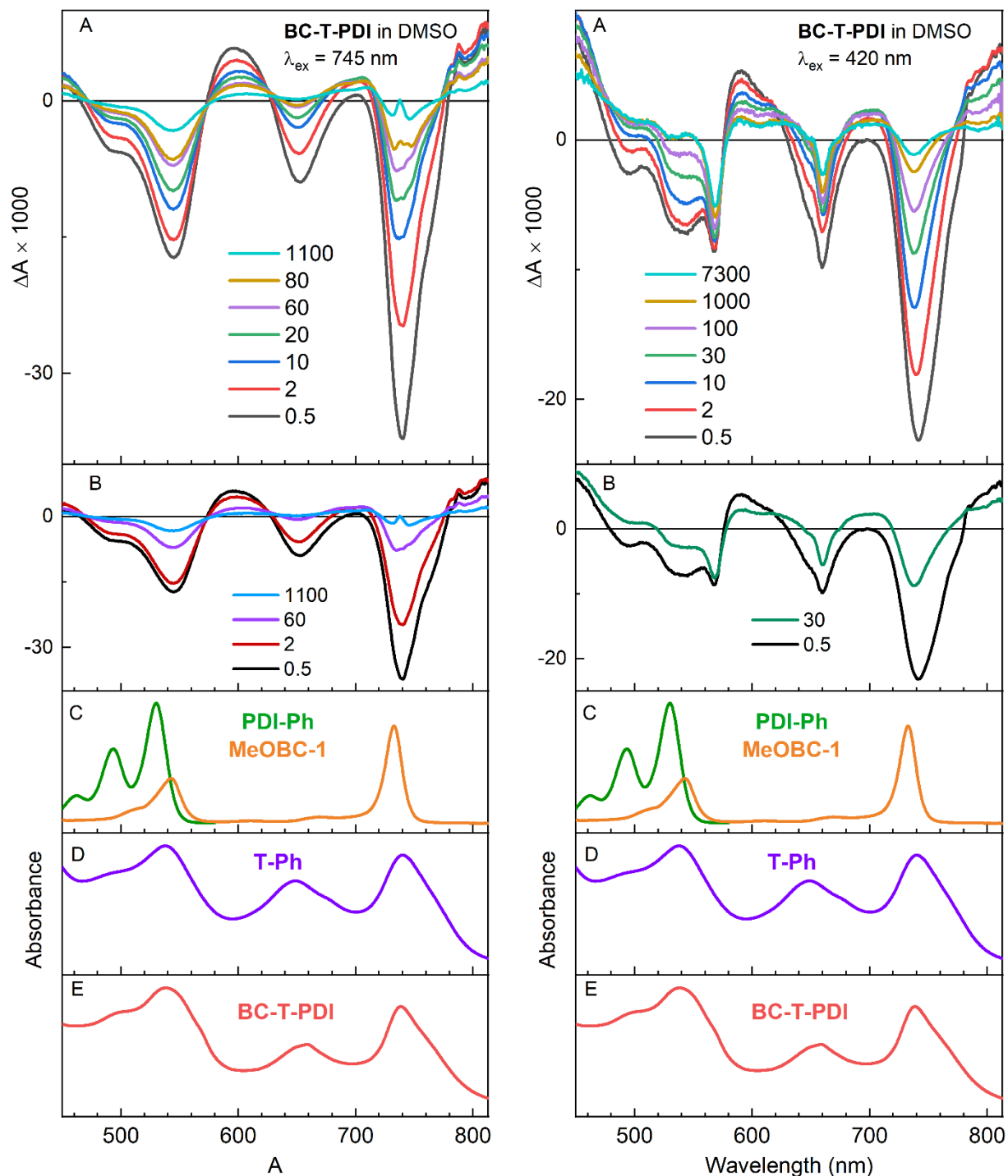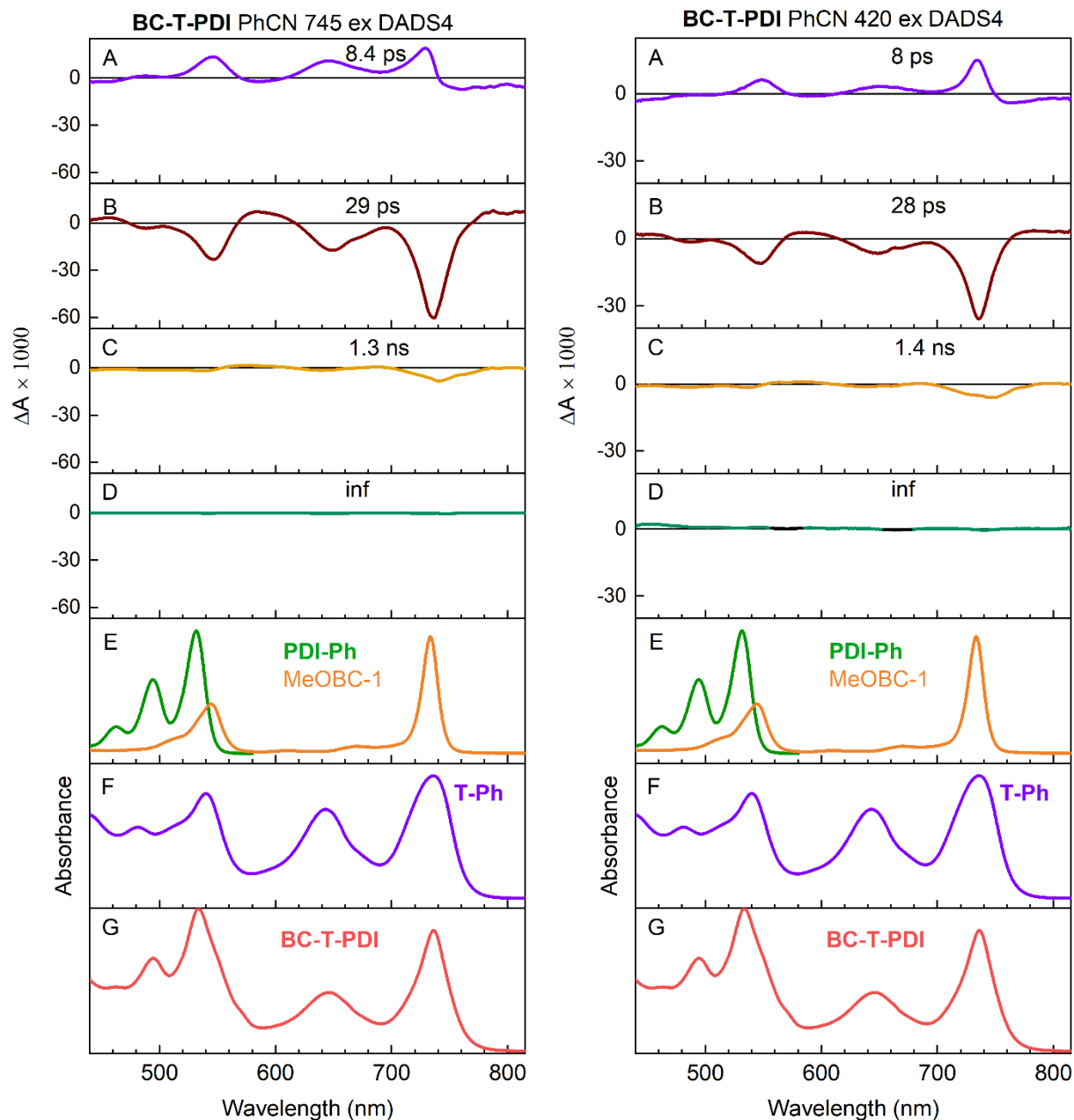
Figure S10. Time-resolved and static absorption data for arrays in DMSO using λ_{ex} = 745 nm (left panels) and λ_{ex} = 420 nm (right panels). Both columns of panels show TA difference spectra for pentad **BC-T-PDI** in toluene (A, B) and ground-state absorption spectra of monomers **PDI-Ph** and **MeOBC-1** (C), benchmark triad **T-Ph** (D) and the pentad (E). The TA data show small sharp features at ~570 and ~660 nm due to excitation of a small amount of putative chlorin impurity using λ_{ex} = 420 nm but not λ_{ex} =745 nm. See the next Figure for kinetic traces.

Figure S11. TA kinetic profiles and fits for **BC-T-PDI** in DMSO at various probe wavelengths using λ_{ex} = 745 nm (left panels) and λ_{ex} = 420 nm (right panels). See the prior Figure for TA spectra.

Figure S12. DADS summary for **BC-T-PDI** in toluene (left), PhCN (middle) and DMSO (right) obtained using 745 nm excitation flashes.
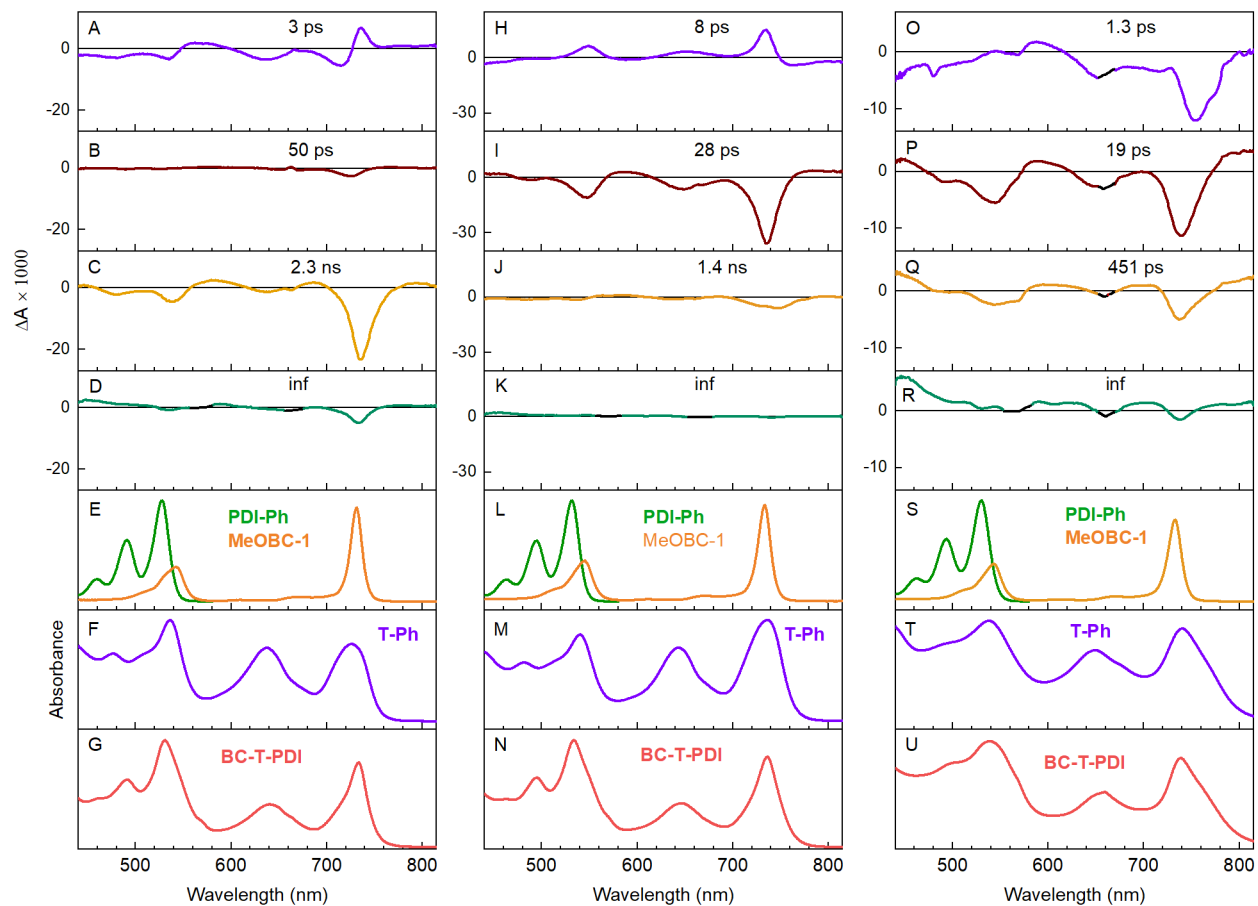
Figure S13. DADS summary for **BC-T-PDI** in toluene (left), PhCN (middle) and DMSO (right) using λ_{ex} = 420 nm. Small sharp features at ~570 and ~660 nm associated with a small putative chlorin impurity excited at 420 nm were removed from the long-lived DADS to avoid confusion and the spectra in those regions are colored black.
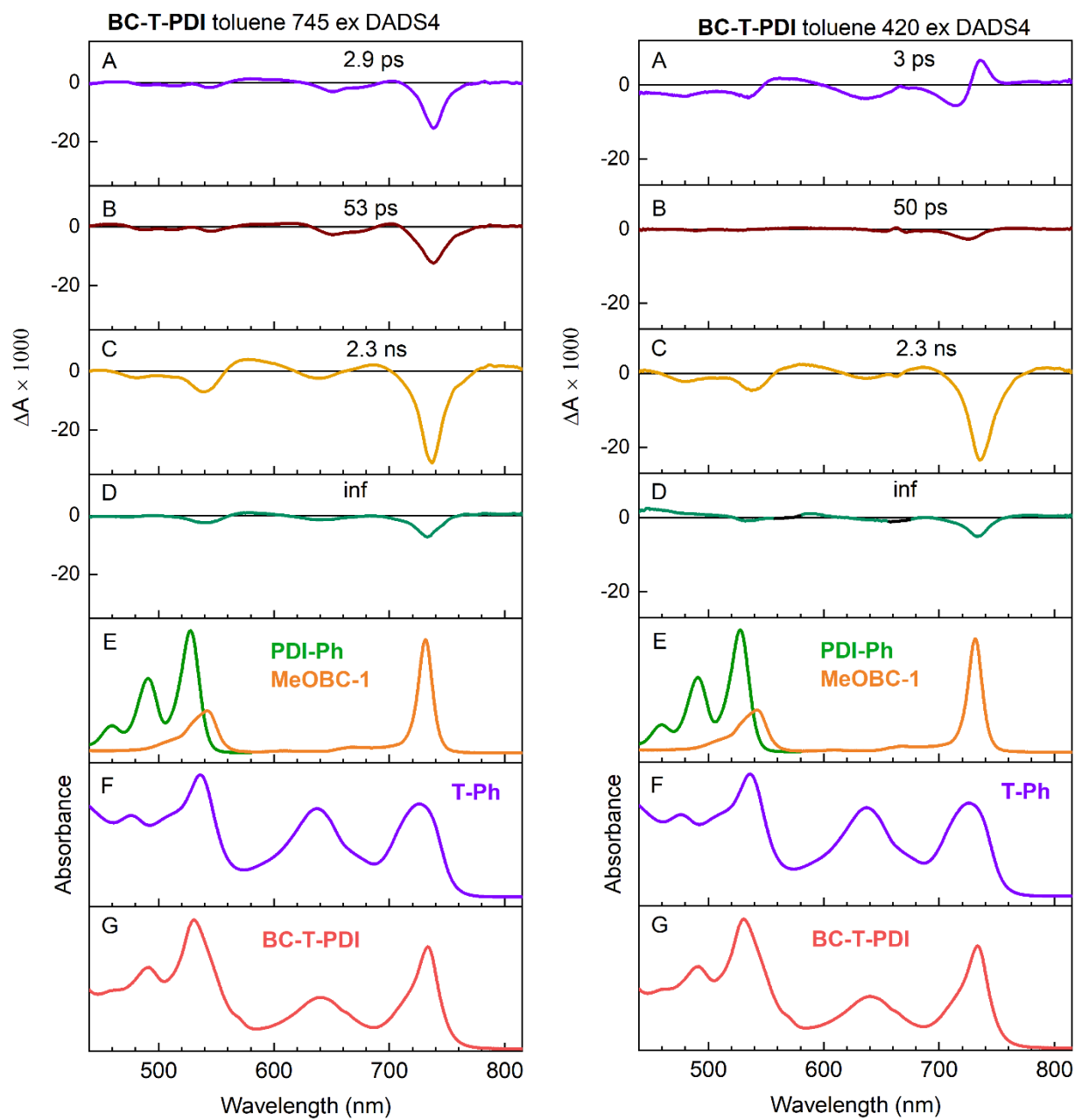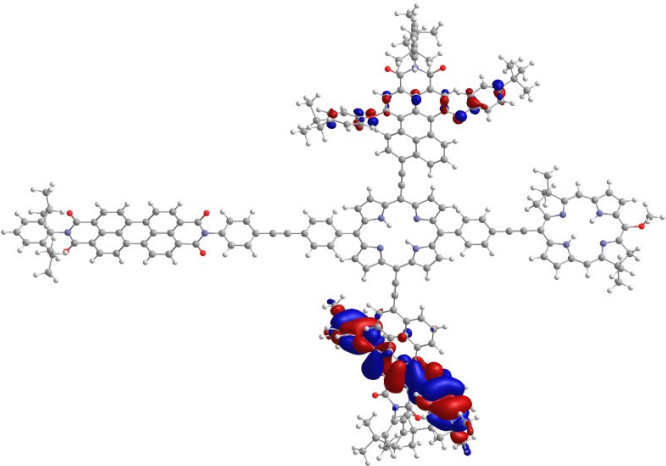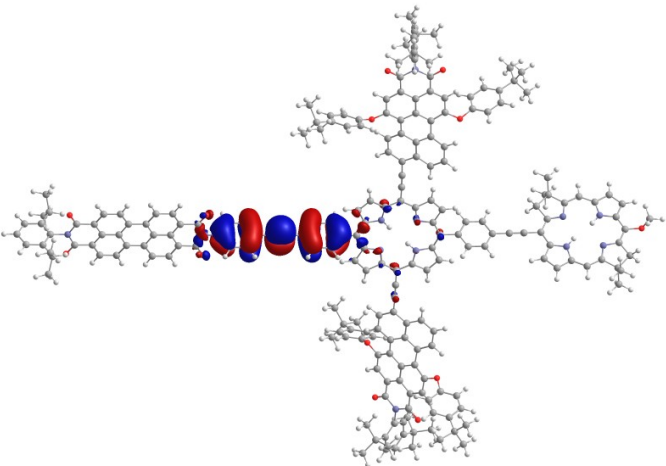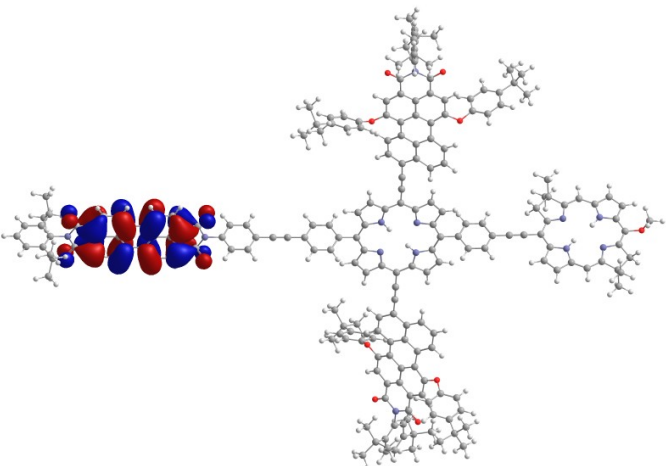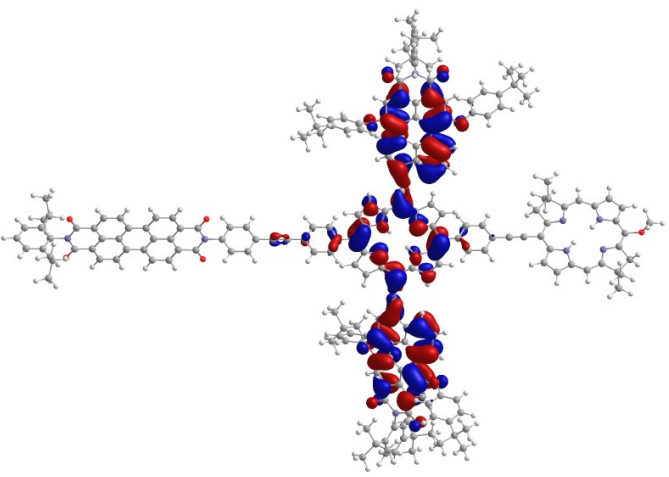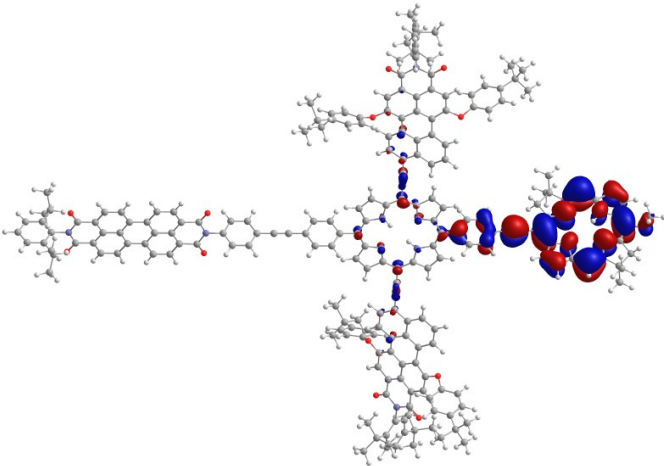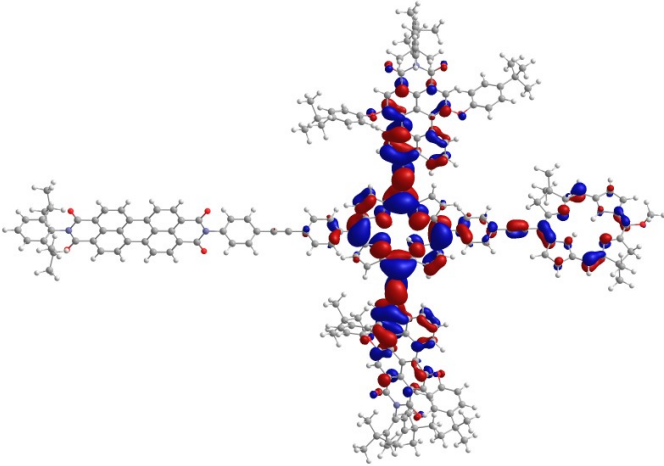
Figure S14. DADS for pentad **BC-T-PDI** in toluene using λ_{ex} = 745 nm (left panels) and λ_{ex} = 420 nm (right panels). Small sharp features at ~570 and ~660 nm associated with a small putative chlorin impurity excited at 420 nm were removed from the long-lived DADS to avoid confusion and the spectra in those regions are colored black.

Figure S15. DADS for pentad **BC-T-PDI** in PhCN using λ_{ex} = 745 nm (left panels) and λ_{ex} = 420 nm (right panels). Small sharp features at ~570 and ~660 nm associated with a small putative chlorin impurity excited at 420 nm were removed from the long-lived DADS to avoid confusion and the spectra in those regions are colored black.

Figure S16. DADS for pentad **BC-T-PDI** in DMSO using λ_{ex} = 745 nm (left panels) and λ_{ex} = 420 nm (right panels). Small sharp features at ~570 and ~660 nm associated with a small putative chlorin impurity excited at 420 nm were removed from the long-lived DADS to avoid confusion and the spectra in those regions are colored black.
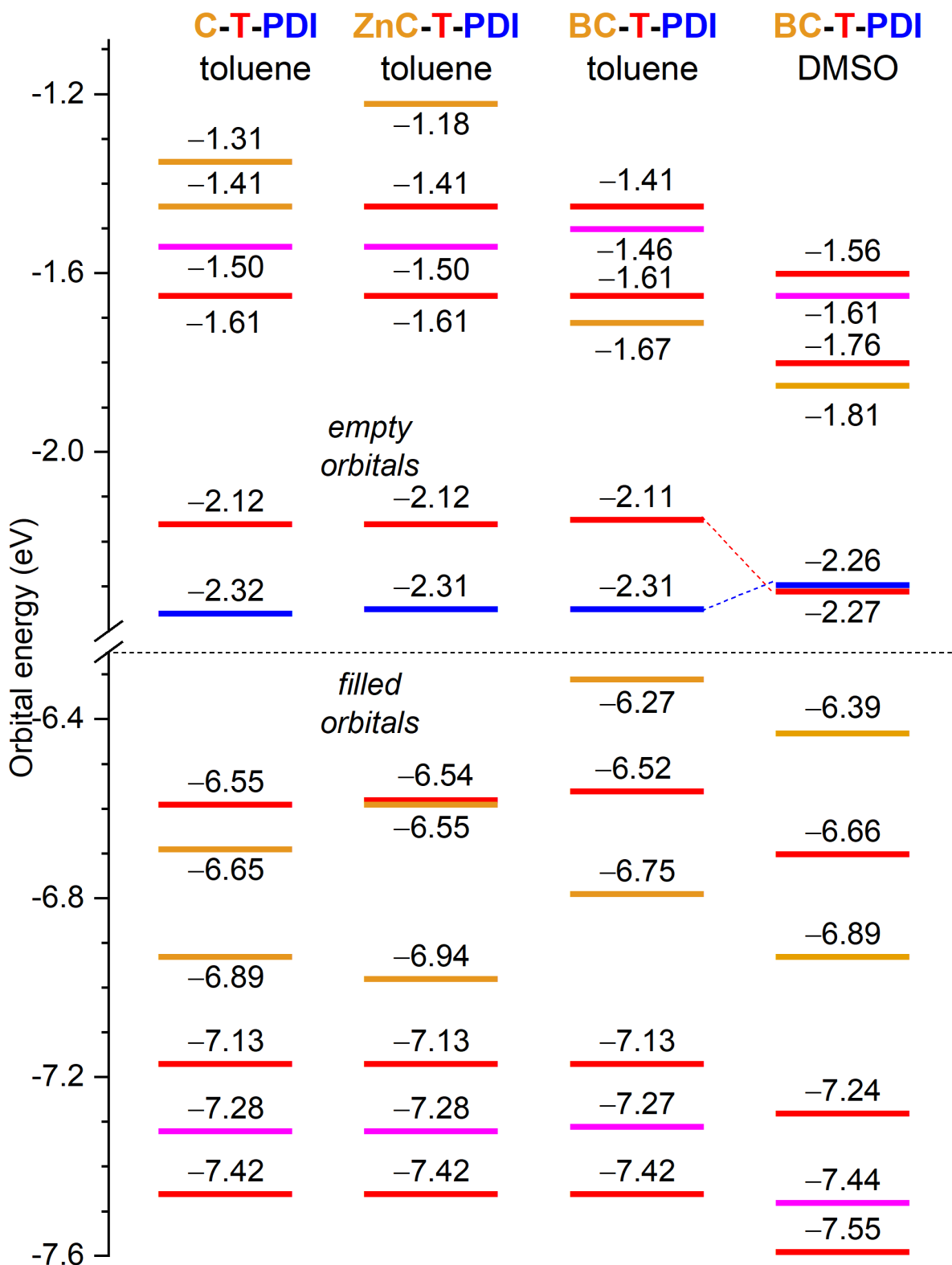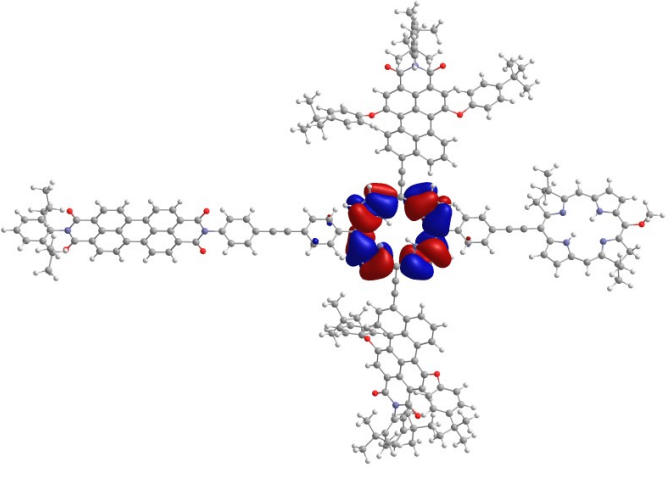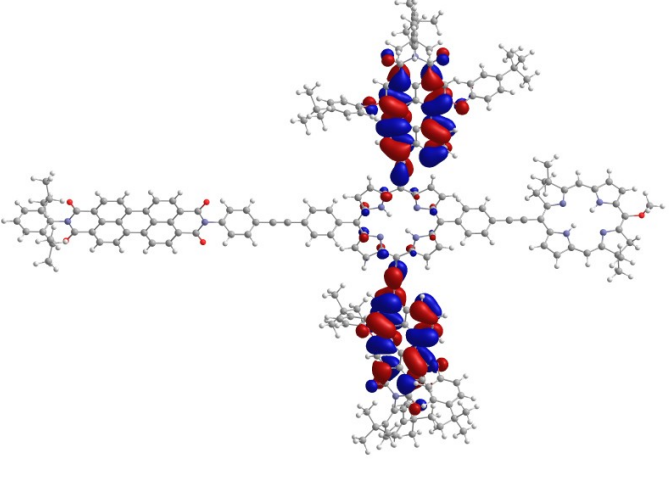
Figure S17. MO energies for pentads **ZnC-T-PDI** and **C-T-PDI** studied previously (Chart 1)[60] and pentad **BC-T-PDI** studied here (Chart 2), in the solvents indicated. The lines at the MO energies are colored to match the constituent: (bacterio)chlorin (gold), perylene-diimide (blue), and central panchromatic triad [red (derived from the porphyrin HOMO or LUMO and magenta (derived from the porphyrin HOMO-1 or LUMO+1)].
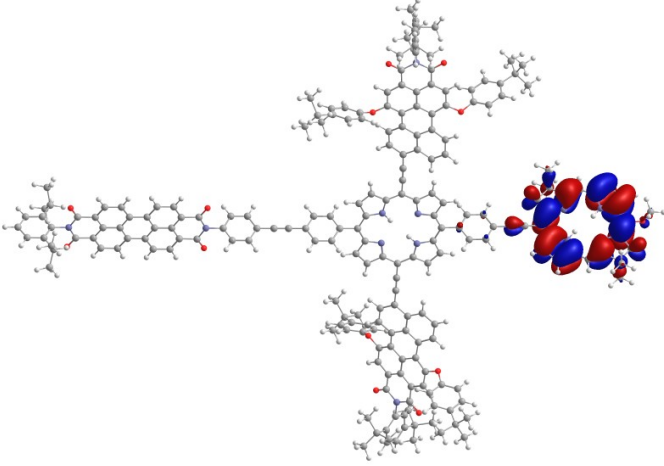
Table S1. MOs for pentad **BC-T-PDI** in toluene.
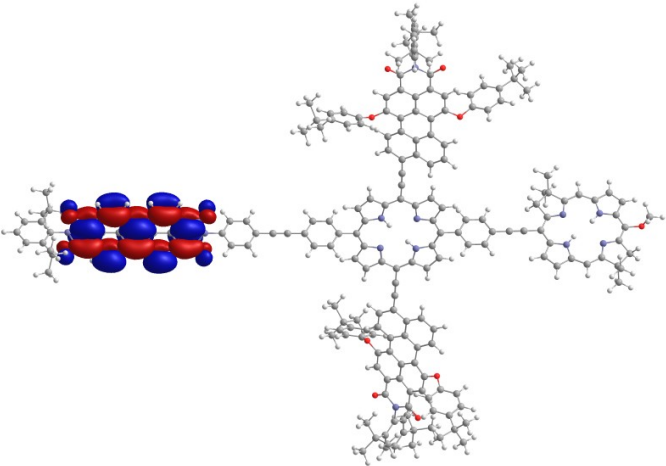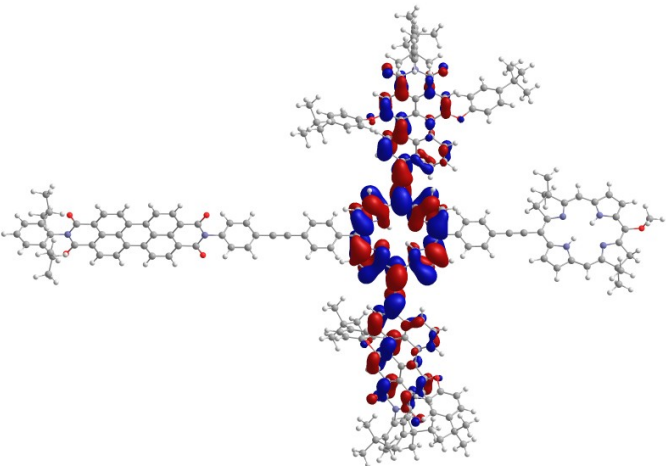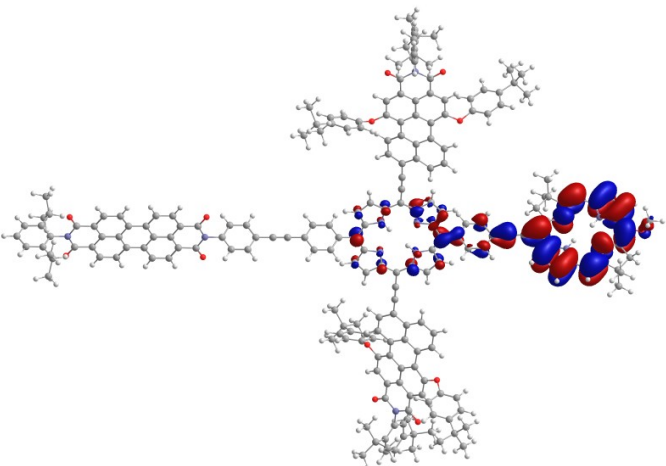
MO	Energy (eV)	MO Image
HOMO-11	-8.47	
HOMO-10	-8.32	
HOMO-9	-8.21	
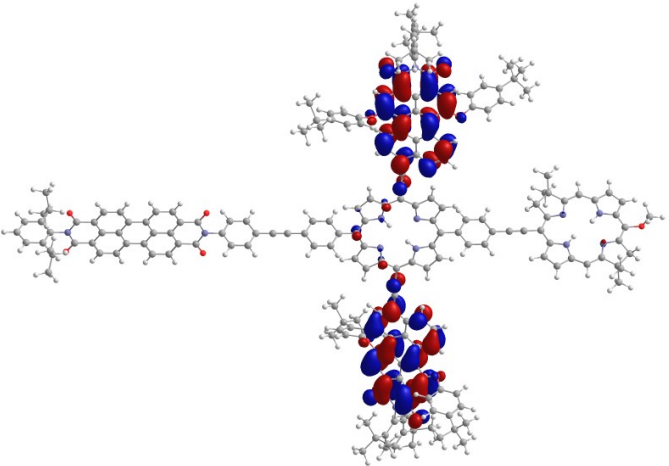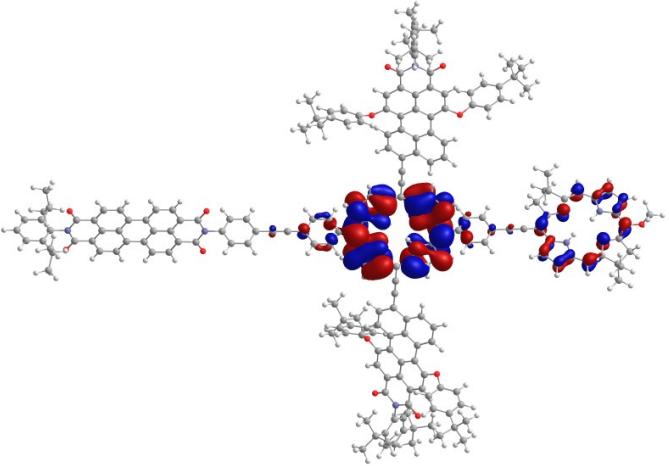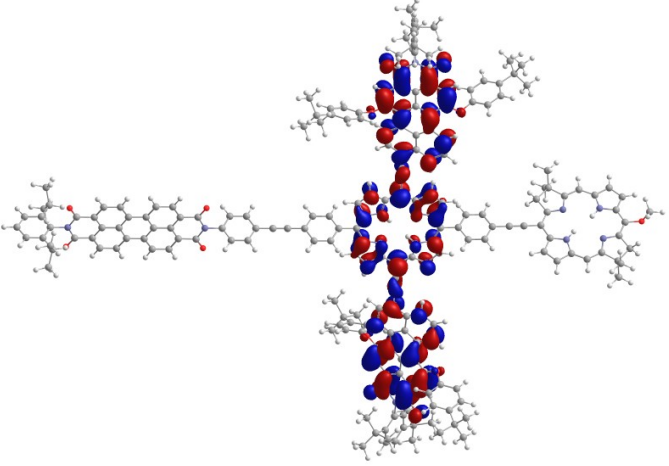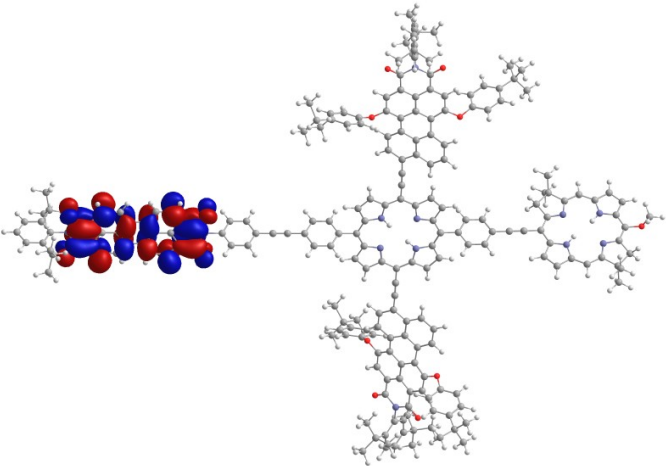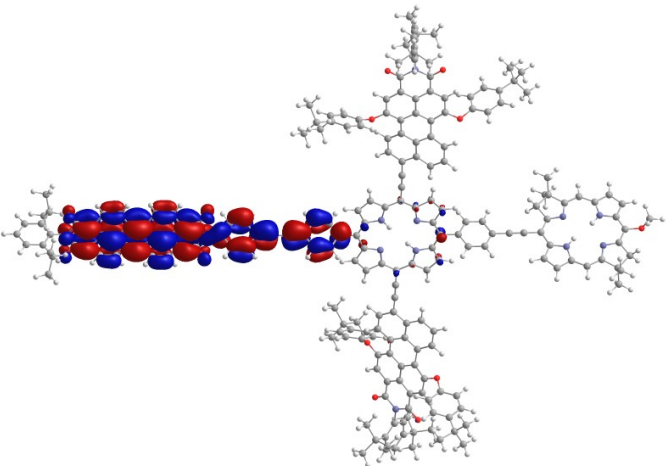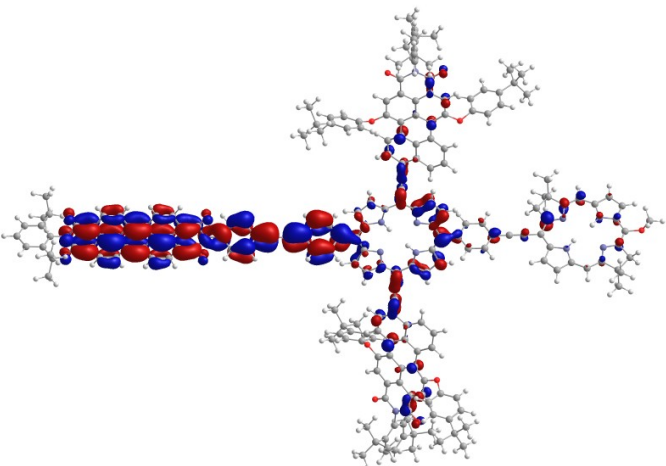
HOMO-8	-8.21	
HOMO-7	-8.03	
HOMO-6	-7.88	
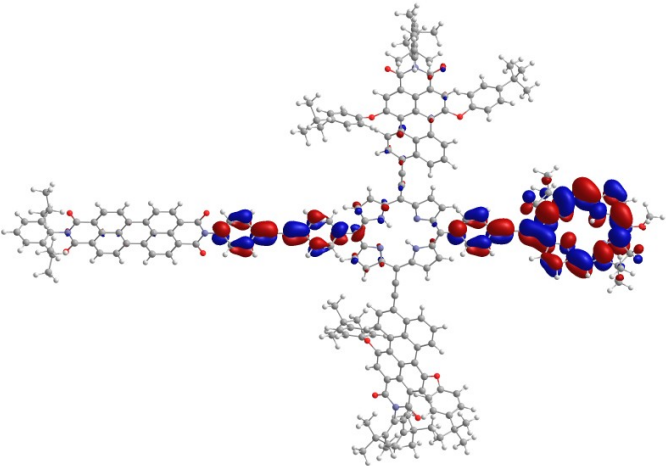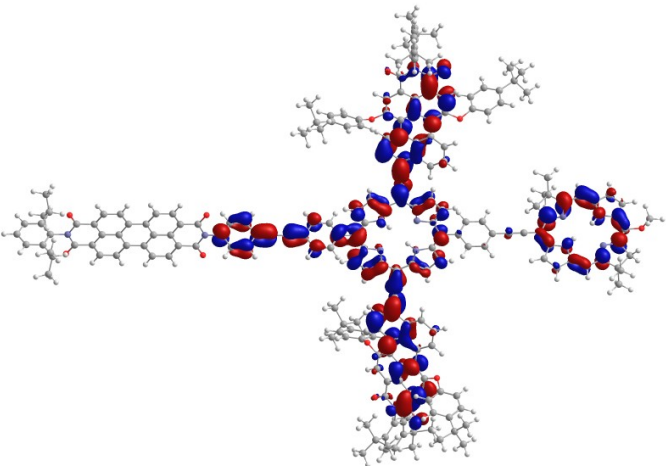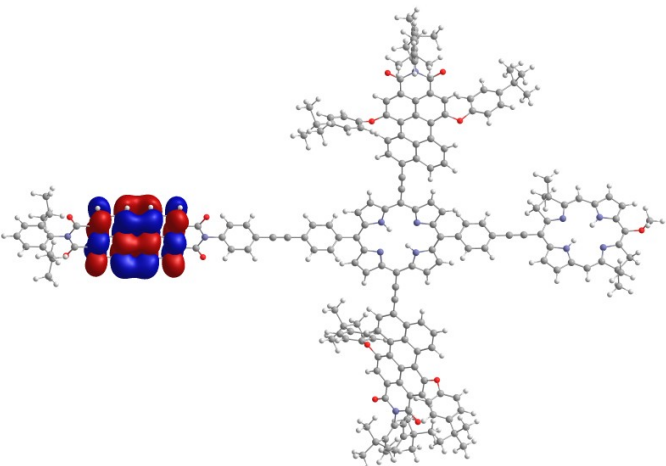
HOMO-5	-7.42	
HOMO-4	-7.27	
HOMO-3	-7.13	

HOMO-2	-6.75	
HOMO-1	-6.52	
HOMO	-6.27	
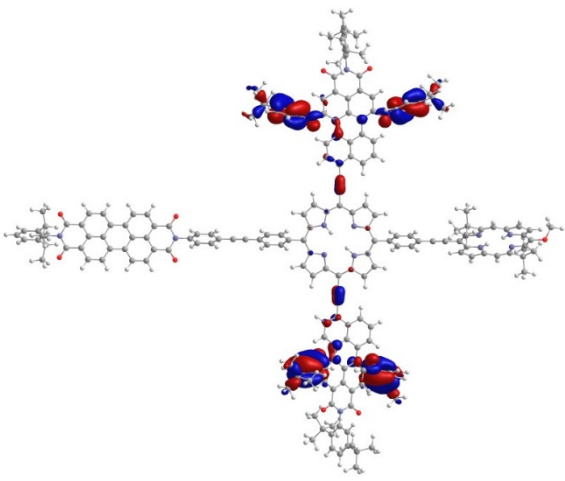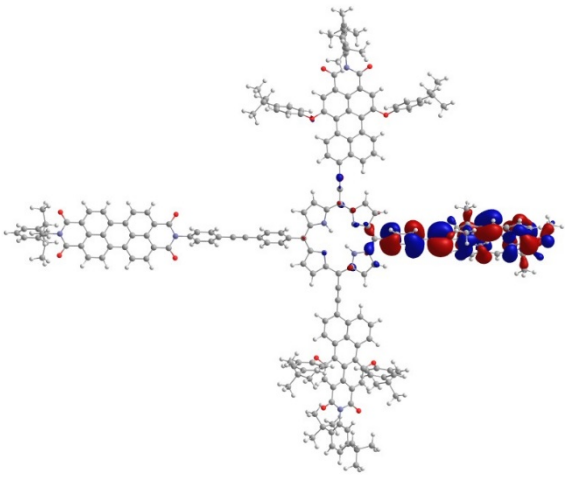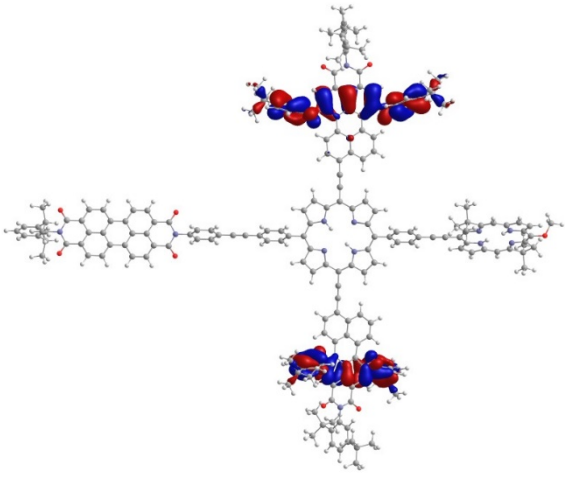
LUMO	-2.31	
LUMO+1	-2.11	
LUMO+2	-1.67	

LUMO+3	-1.61	
LUMO+4	-1.46	
LUMO+5	-1.41	
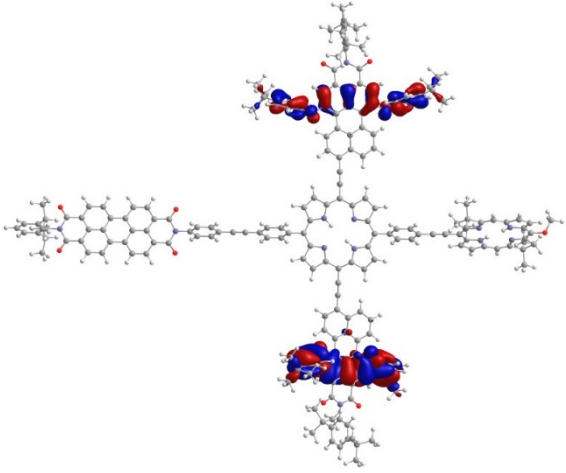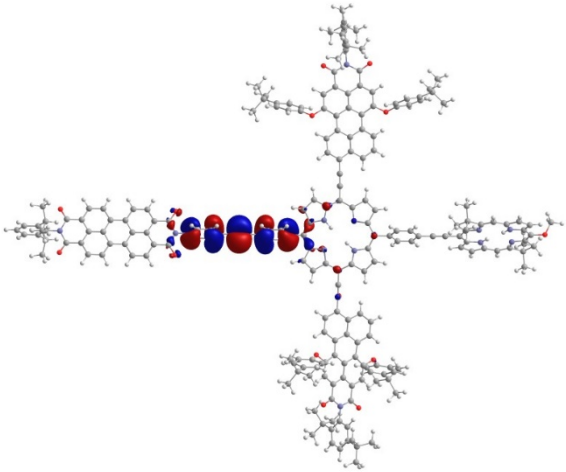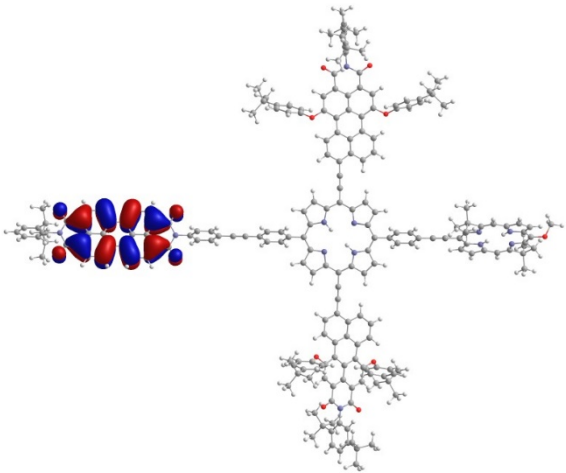
LUMO+6	-0.45	
LUMO+7	-0.26	
LUMO+8	-0.16	
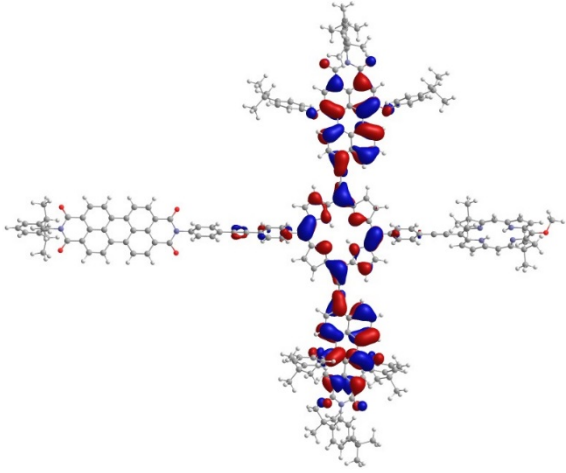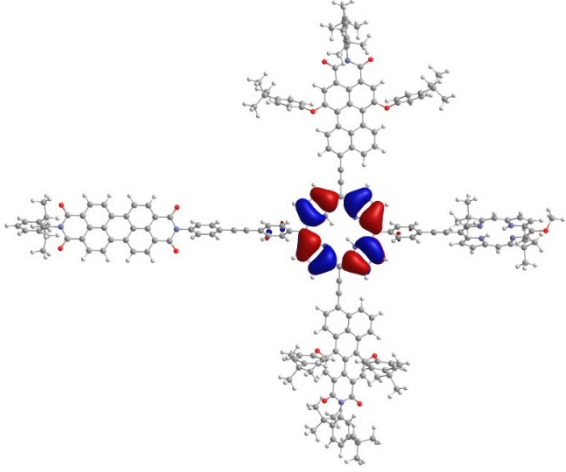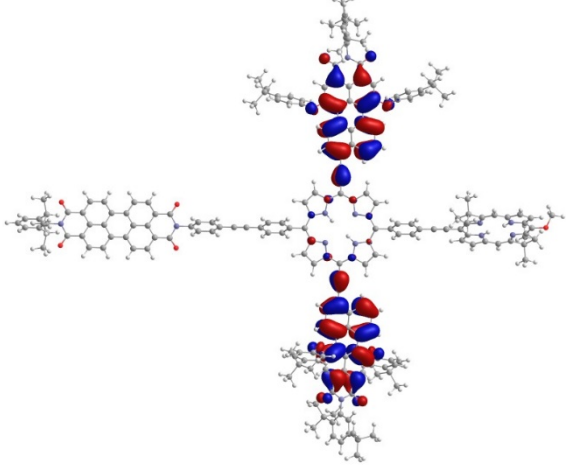
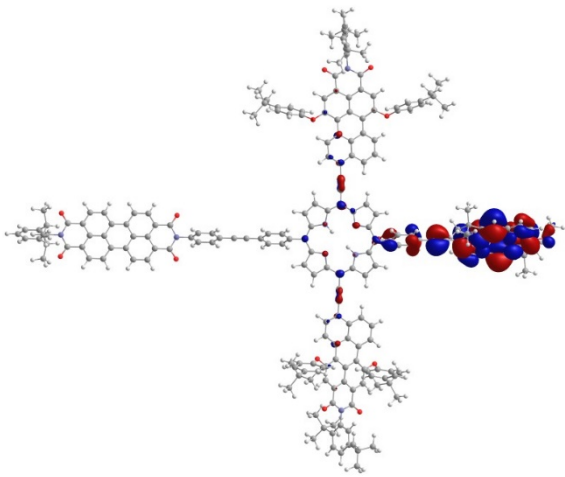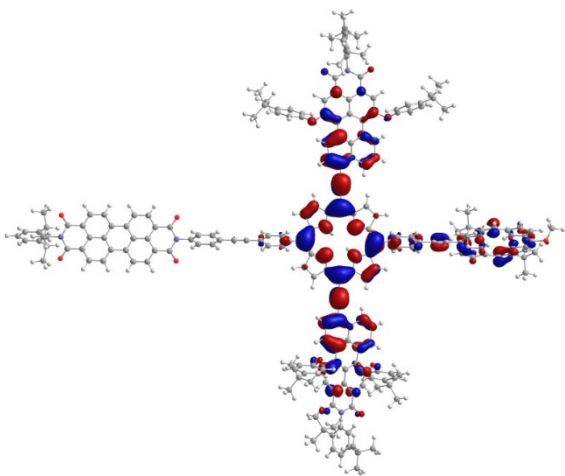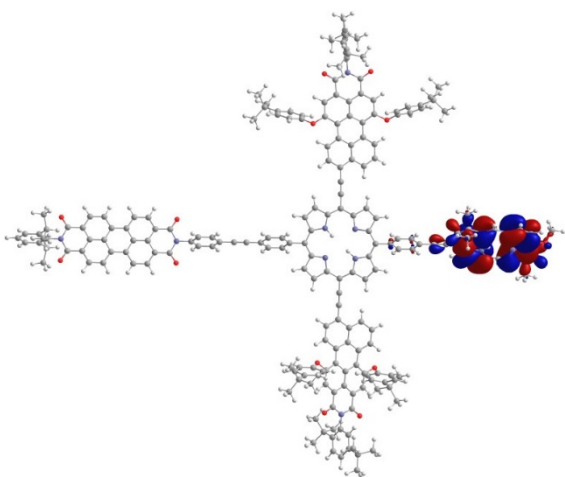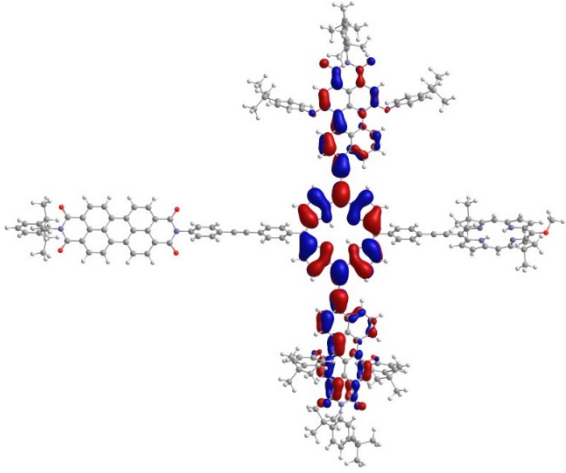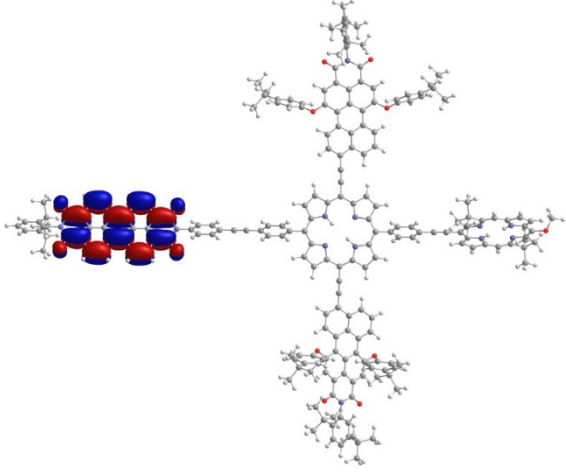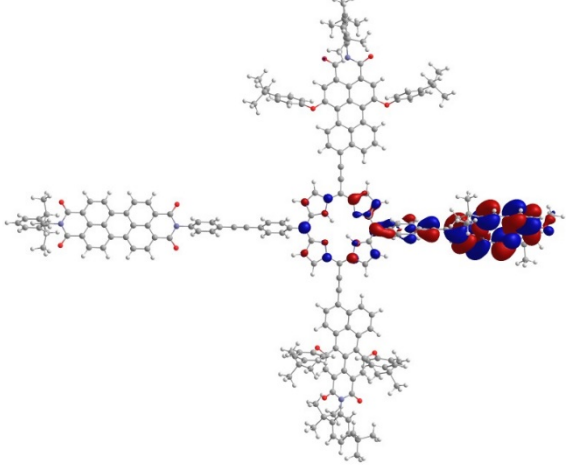|		
LUMO+9	-0.16	
LUMO+10	0.00	
LUMO+11	+0.18	

Table S2. MOs for pentad **BC-T-PDI** in DMSO.

MO	Energy (eV)	MO Image
HOMO-11	-8.61	
HOMO-10	-8.44	
HOMO-9	-8.30	
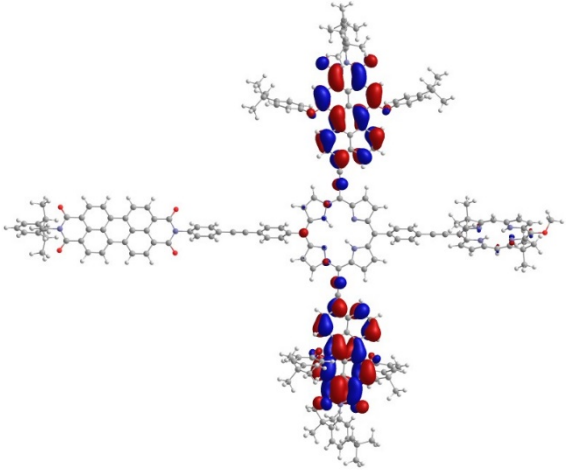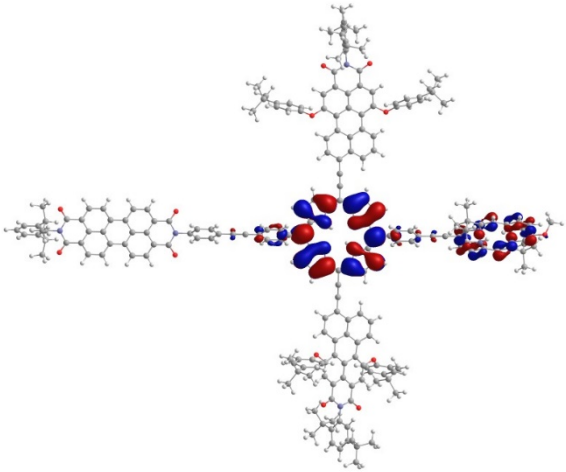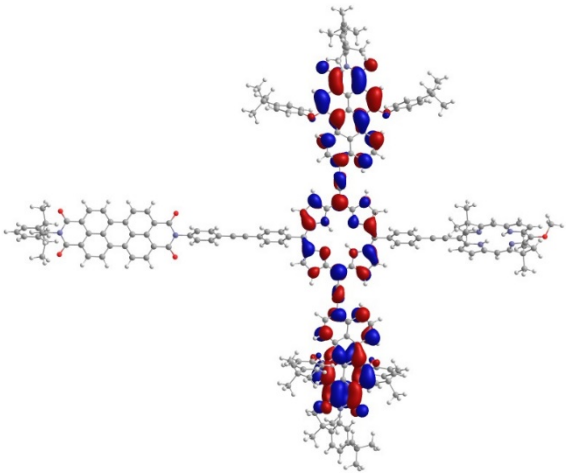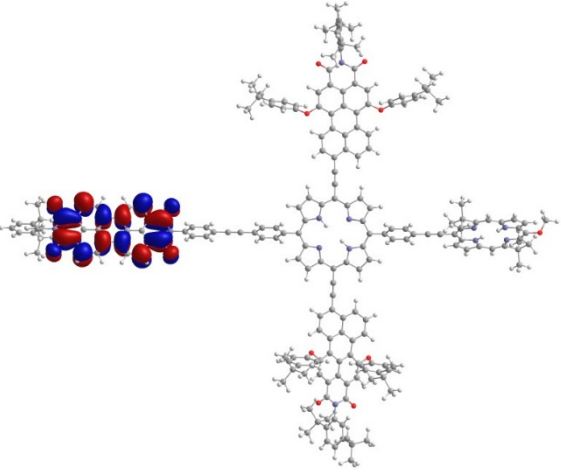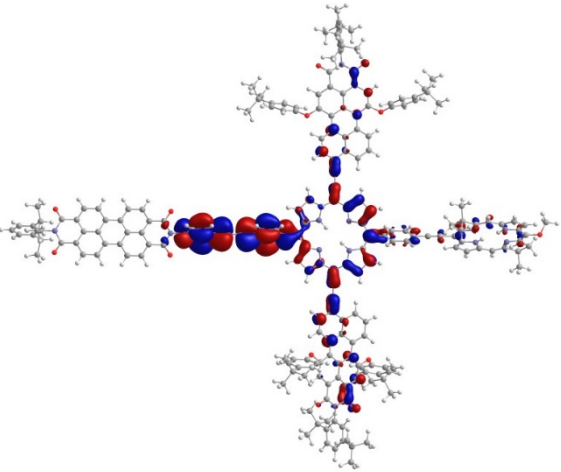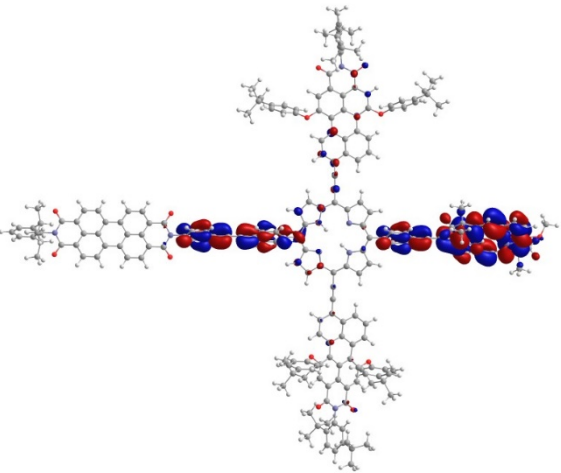
HOMO-8	-8.30	
HOMO-7	-8.16	
HOMO-6	-7.79	

HOMO-5	-7.55	
HOMO-4	-7.44	
HOMO-3	-7.24	

HOMO-2	-6.89	
HOMO-1	-6.66	
HOMO	-6.39	

LUMO	-2.27	
LUMO+1	-2.26	
LUMO+2	-1.81	

LUMO+3	-1.76	
LUMO+4	-1.61	
LUMO+5	-1.56	

LUMO+6	-0.42	
LUMO+7	-0.32	
LUMO+8	-0.19	

LUMO+9	-0.15	
LUMO+10	-0.13	
LUMO+11	+0.09	

Table S3. MOs for bacteriochlorin monomer **MeO-BC-1** in toluene.

LUMO+4 +1.13 eV	LUMO+5 +1.20 eV	LUMO+6 +1.35 eV	LUMO+7 +1.36 eV
LUMO -1.61 eV	LUMO+1 -0.01 eV	LUMO+2 +0.81 eV	LUMO+3 +1.06 eV

HOMO	HOMO-1	HOMO-2	HOMO-3
-6.24 eV	-6.69 eV	-8.25 eV	-9.22 eV
HOMO-4	HOMO-5	HOMO-6	HOMO-7
-9.30 eV	-9.41 eV	-9.46 eV	-9.65 eV
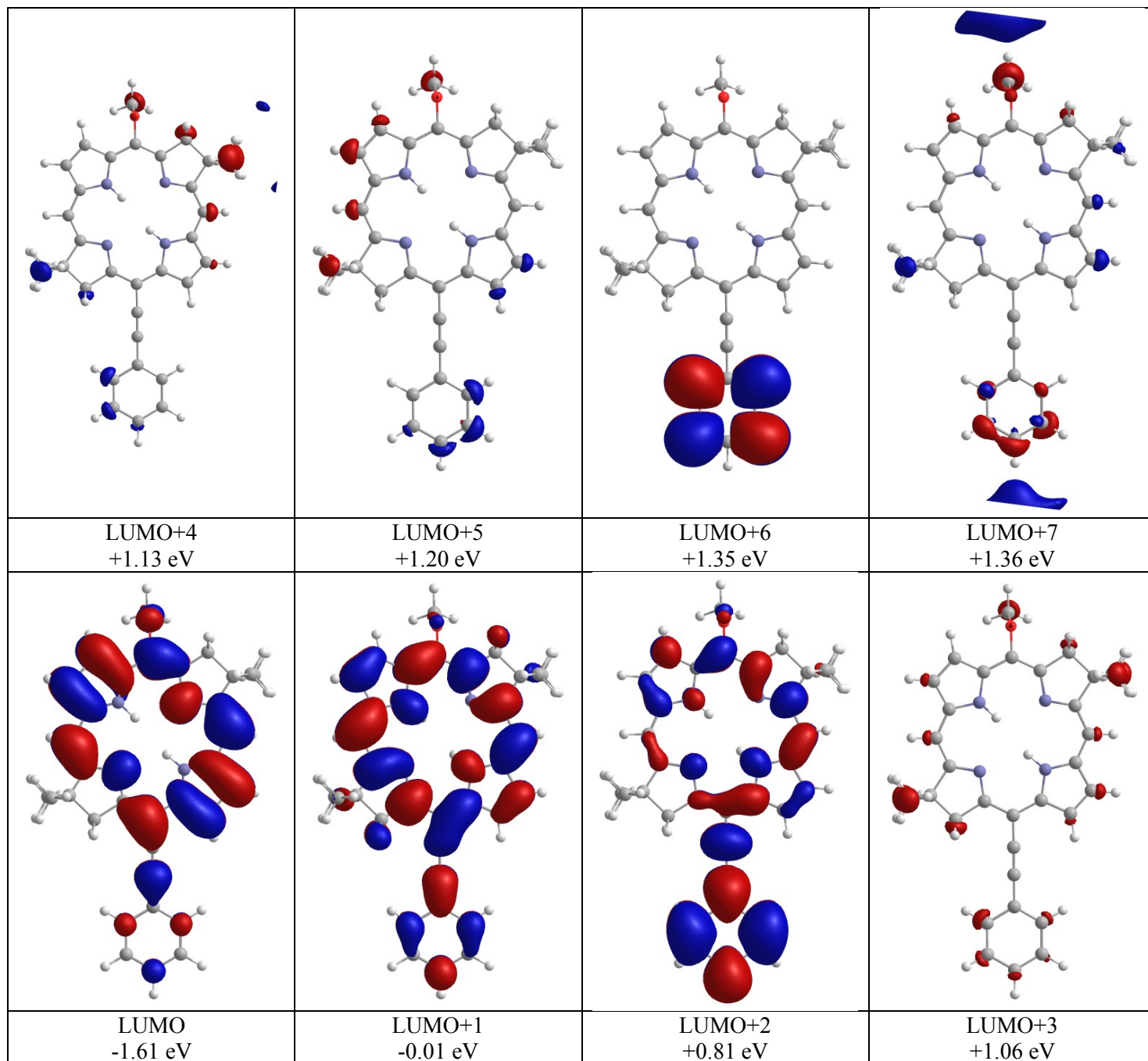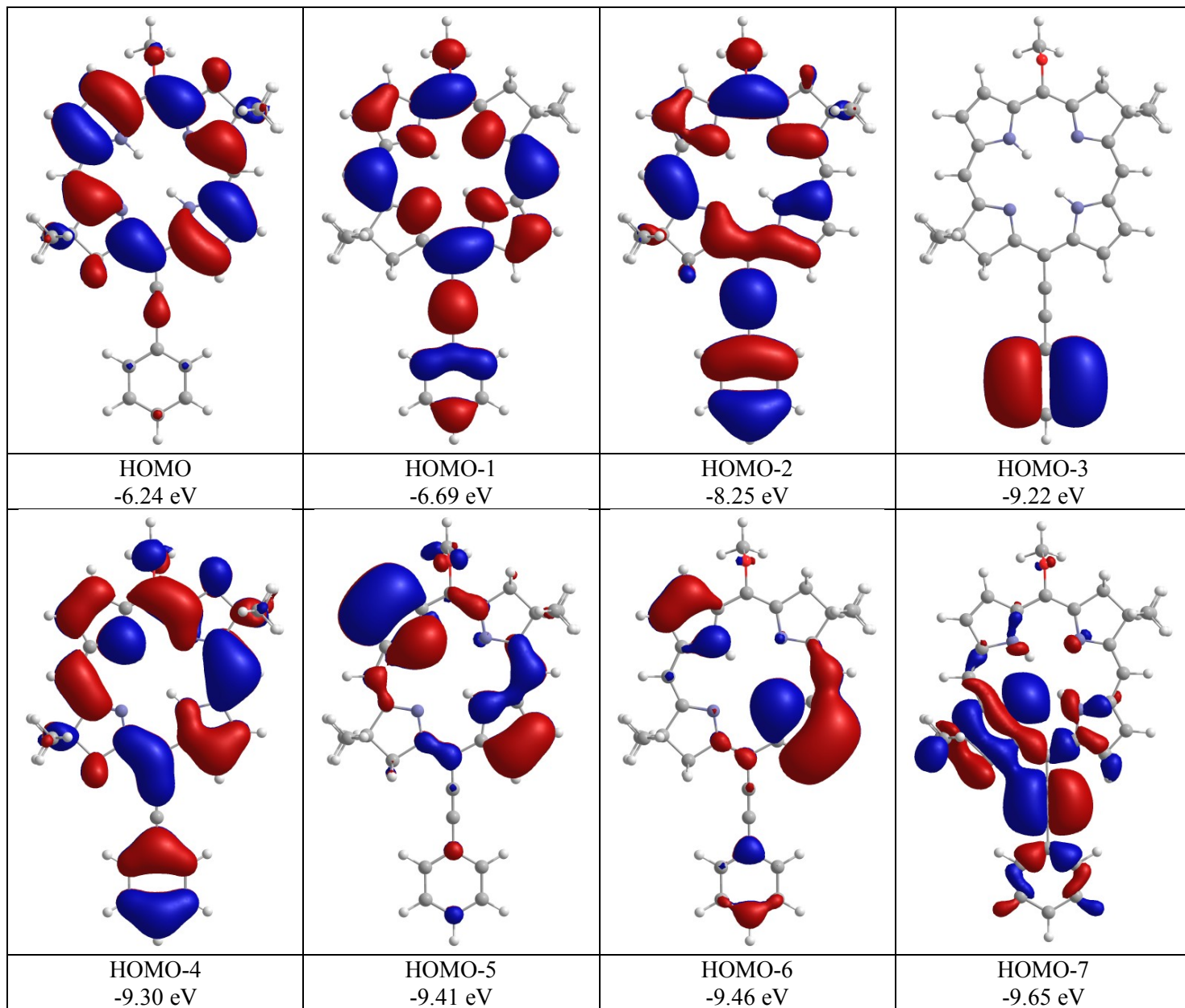
Table S4. Results of TDDFT calculations on pentad **BC-T-PDI** in toluene.[a]

State	λ (nm)	Shifted λ[b] (nm)	f	filled MO	empty MO	%
S$_1$	730	746	0.45	H-2	L+9	4
				H	L+2	81
				H	L+4	8
S$_2$	710	725	1.49	H-5	L+1	2
				H-5	L+5	3
				H-4	L+1	4
				H-4	L+4	9
				H-3	L+3	3
				H-2	L+1	4
				H-1	L+1	60
				H-1	L+4	3
				H-1	L+5	4
S$_3$	627	639	0.36	H-5	L+4	6
				H-4	L+1	33
				H-4	L+5	7
				H-2	L+4	2
				H-1	L+1	8
				H-1	L+2	5
				H-1	L+4	32
				H-2	L+2	66
				H-2	L+4	5
				H-1	L+2	8
				H	L+9	9
				H	L+10	2
S$_4$	566	575	0.63	H-2	L+2	66
				H-2	L+4	5
				H-1	L+2	8
				H	L+9	10
				H	L+10	2
S$_5$	505	513	0.022	H-5	L+3	15
				H-3	L+1	31
				H-3	L+5	15
				H-2	L+3	3
				H-1	L+3	26
S$_6$	497	505	2.61	H-5	L+1	16
				H-5	L+5	5
				H-4	L+2	2
				H-4	L+4	17
				H-3	L+3	30
				H-1	L+1	2
				H-1	L+5	17
S$_7$	485	492	1.46	H-6	L	2.2
S$_8$	428	433	2.19	H-5	L+4	3
				H-4	L+1	43
				H-4	L+5	6

				H-1	L+2	5
				H-1	L+4	31
S9	408	413	0.65	H-5	L+5	16
				H-4	L+2	7
				H-4	L+4	51
				H-3	L+3	9
				H-1	L+1	29
				H-1	L+5	7
S10	384	388	0.004	H-16	L+1	3
				H-3	L+1	7
				H-3	L+5	7
				H-2	L+1	4
				H	L+1	67
S11	383	387	0.001	H-16	L+1	8
				H-5	L+3	2
				H-3	L+1	25
				H-3	L+5	20
				H-1	L+3	3
				H	L+1	23
S12	364	368	0.44	H-16	L+1	2
				H-10	L+2	3
				H-5	L+3	10
				H-3	L+1	9
				H-2	L+2	3
				H-2	L+9	3
				H-1	L+2	3
				H-1	L+3	19
				H-1	L+8	3
				H-1	L+9	2
				H	L+9	11
				H	L+10	4
S13	360	364	0.35	H-10	L+2	2
				H-8	L+1	4
				H-8	L+3	7
				H-8	L+5	5
				H-5	L+1	3
				H-5	L+3	4
				H-2	L+1	4
				H-2	L+2	5
				H-1	L+3	8
				H-1	L+10	2
				H	L+9	19
				H	L+10	4
S14	358	362	0.20	H-25	L+3	2
				H-9	L+1	9
				H-9	L+3	10
				H-9	L+5	13
				H-8	L+3	9

				H	L+1	7
				H	L+9	7
S15	357	361	0.87	H-25	L+5	2
				H-24	L+3	2
				H-16	L+1	2
				H-9	L+3	15
				H-8	L+1	9
				H-8	L+3	10
				H-8	L+5	14
				H-5	L+3	2
				H-1	L+3	3
				H	L+9	4
S16	356	360	0.13	H-9	L+1	3
				H-9	L+3	4
				H-9	L+5	6
				H-8	L+3	5
				H-5	L+1	22
				H-2	L+1	16
				H-2	L+5	3
				H-1	L+5	12
				H	L+1	2
				H	L+9	2

[a] H = HOMO and L = LUMO. [b] Shifted by 300 cm^{-1} to improve overlap with the measured spectrum for plotting.

Table S5. Results of TDDFT calculations on pentad **BC-T-PDI** in DMSO.[a]

State	λ (nm)	Shifted λ[b] (nm)	f	filled MO	empty MO	%
S$_1$	729	745	0.43	H-2	L+8	4.7
				H	L+2	79
				H	L+4	8.6
S$_2$	711	726	1.57	H-5	L	2.2
				H-5	L+5	2.9
				H-4	L	4.2
				H-4	L+4	8.2
				H-3	L+3	3
				H-2	L	3.5
				H-1	L	61
				H-1	L+4	3.4
				H-1	L+5	3.3
S$_3$	625	637	0.35	H-5	L+4	6.2
				H-4	L	33
				H-4	L+5	6.1
				H-1	L	7.1
				H-1	L+2	5.6
				H-1	L+4	32
S$_4$	563	572	0.61	H-2	L+2	64
				H-2	L+4	6.1
				H-1	L+2	8
				H	L+8	9.6
				H	L+10	3
S$_5$	509	517	0.018	H-5	L+3	15
				H-3	L	31
				H-3	L+5	16
				H-2	L+3	2.9
				H-1	L+3	26
S$_6$	500	508	2.50	H-5	L	17
				H-5	L+5	4.8
				H-4	L+2	2.3
				H-4	L+4	17
				H-3	L+3	30
				H-1	L	2.1
				H-1	L+5	18
S$_7$	486	494	1.49	H-6	L	2.2
S$_8$	424	430	2.20	H-5	L+4	2.9
				H-4	L	43
				H-4	L+5	6.3
				H-1	L+2	5.7
				H-1	L+4	32
S$_9$	407	412	0.68	H-5	L+5	5.5
				H-4	L+2	7.4
				H-4	L+4	49
				H-3	L+3	8.7

				H-1	L	9.9
				H-1	L+5	7
S_{10}	387	392	0.006	H-2	L	4.9
				H	L	84
S_{11}	386	390	0.001	H-16	L	9.9
				H-5	L+3	2.7
				H-3	L	32
				H-3	L+5	25
				H-1	L+3	4.7
				H-1	L+7	2.4
				H	L	6.0
S_{12}	364	368	0.45	H-9	L+3	11
				H-8	L	5.3
				H-8	L+5	7.7
				H-5	L+3	8.8
				H-3	L	7.4
				H-1	L+3	16
				H-1	L+7	2.4
				H	L+8	3.0
S_{13}	360	367	0.12	H-29	L+3	2.3
				H-9	L	12
				H-9	L+5	17
				H-8	L+3	29
				H-5	L	2.8
S_{14}	362	365	0.007	H-10	L+2	2.3
				H-9	L+3	18
				H-9	L+5	2.2
				H-8	L	6.7
				H-8	L+5	9.9
				H-5	L+3	2.2
				H-2	L+2	2.5
				H-1	L+3	2.9
				H	L+8	8.1
				H	L+10	3.1
S_{15}	359	363	0.067	H-8	L+3	3.0
				H-5	L	27
				H-2	L	22
				H-2	L+5	3.1
				H-1	L+3	2.2
				H-1	L+5	12
				H	L	2.9
S_{16}	357	361	1.3	H-16	L	2.7
				H-10	L+2	3.4
				H-5	L	3.1
				H-5	L+3	5.0
				H-2	L+2	8.3
				H-1	L+3	9.7
				H-1	L+10	2.4

				H	L+7	2.2
				H	L+8	28
				H	L+10	8.0

[a] H = HOMO and L = LUMO. [b]Shifted by 300 cm^{-1} to improve overlap with the measured spectrum for plotting for the pentad in toluene (to use a consistent shift).

Table S6. Results of TDDFT calculations on bacteriochlorin monomer **MeOBC-1** in toluene.[a]

State	λ (nm)	Shifted λ[b] (nm)	f	filled MO	empty MO	%
S$_1$	727	738	0.41	H-1	L+1	5.1
				H	L	91
S$_2$	564	570	0.41	H-1	L	83
				H	L+1	14
S$_3$	359	361	1.6	H-2	L	6.5
				H-1	L	14
				H-1	L+1	6.1
				H	L+1	68
				H	L+2	4.0
S$_4$	337	340	1.4	H-2	L	5.3
				H-2	L+2	2.2
				H-1	L+1	73
				H	L	5.4
				H	L+1	10
S$_5$	317	319	0.17	H-6	L	2.9
				H-4	L	7.0
				H-2	L	70
				H-1	L+1	9.0
				H	L+1	3.8
S$_6$	286	287	0.006	H-10	L	41
				H-9	L	3.6
				H-8	L	44
S$_7$	283	284	0.05	H-6	L	76
				H-5	L	6.9
				H-1	L+2	5.2
				H	L+2	2.4
S$_8$	278	279	0.0002	H-10	L	16
				H-8	L	19
				H-7	L	53
S$_9$	277	278	0.005	H-9	L	3.9
				H-6	L	6.9
				H-5	L	37
				H-4	L	33
				H-1	L+1	4.1
S$_{10}$	273	274	0.13	H-6	L	2.8
				H-5	L	14
				H-2	L	4.1

				H-2	L+1	5.5
				H-2	L+2	3.6
				H-1	L+2	25
				H	L+2	33
S_{11}	262	264	0.001	H-9	L	10
				H-6	L	2.1
				H-5	L	19
				H-4	L	15
				H-2	L+1	3.8
				H-1	L+2	7.0
				H	L+2	16
				H	L+3	5.7
				H	L+12	2.1
				H	L+15	2.3
S_{12}	261	262	0.004	H-5	L	2.7
				H-4	L	2.7
				H	L+3	44
				H	L+4	4.1
				H	L+5	3.5
				H	L+9	2.8
				H	L+12	20
				H	L+28	3.3
S_{13}	253	254	0.002	H-10	L	21
				H-8	L	20
				H-8	L+2	2.4
				H-7	L	25
				H-7	L+1	3.6
				H-7	L+2	5.5
				H-4	L	2.5
				H-1	L+2	3.8
				H	L+2	2.3
S_{14}	253	254	0.013	H-9	L	6.7
				H-8	L	4.0
				H-7	L	5.6
				H-5	L	5.6
				H-4	L	9.5
				H-3	L+2	2.6
				H-2	L+6	3.3
				H-1	L+2	21
				H-1	L+6	3.3
				H	L+2	15
S_{15}	252	253	0.001	H-4	L	2.1
				H-4	L+6	2.9
				H-3	L	8.7
				H-3	L+1	4.1
				H-3	L+2	17
				H-2	L+6	20
				H-1	L+2	4.2

				H-1	L+6	22
				H	L+2	3.2
				H	L+6	4.7
S$_{16}$	242	243	0.0001	H-2	L+3	2.1
				H	L+4	54
				H	L+5	18
				H	L+8	2.9
				H	L+7	5.9

[a] H = HOMO and L = LUMO. [b]Shifted by 200 cm^{-1} to improve overlap with the measured spectrum for plotting.
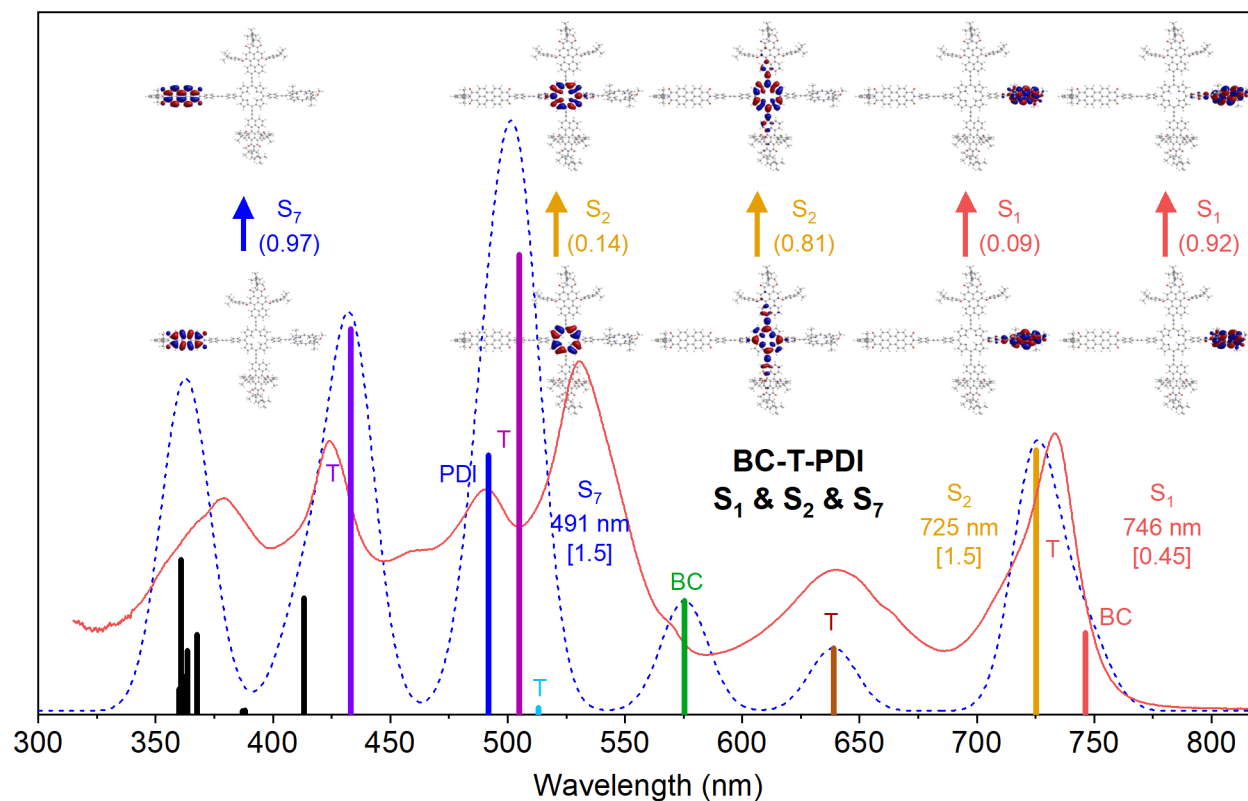
Figure S18. Absorption spectra calculated by TDDFT (colored sticks and blue dashed lines using 10-nm Gaussian skirts) are given along with pairs of occupied and virtual NTOs for absorption from S_0 to S_1 and S_2 and S_7 for pentad **BC-T-PDI** in toluene. The calculated spectra are shifted to lower energy by 300 cm^{-1} to best align with the measured spectrum (red solid line). The eigenvalue (weight) for each pair of natural transition orbitals that contribute to a transition is indicated in parenthesis. The calculated wavelength and oscillator strength (in square brackets) for each transition are given at the bottom of each panel.
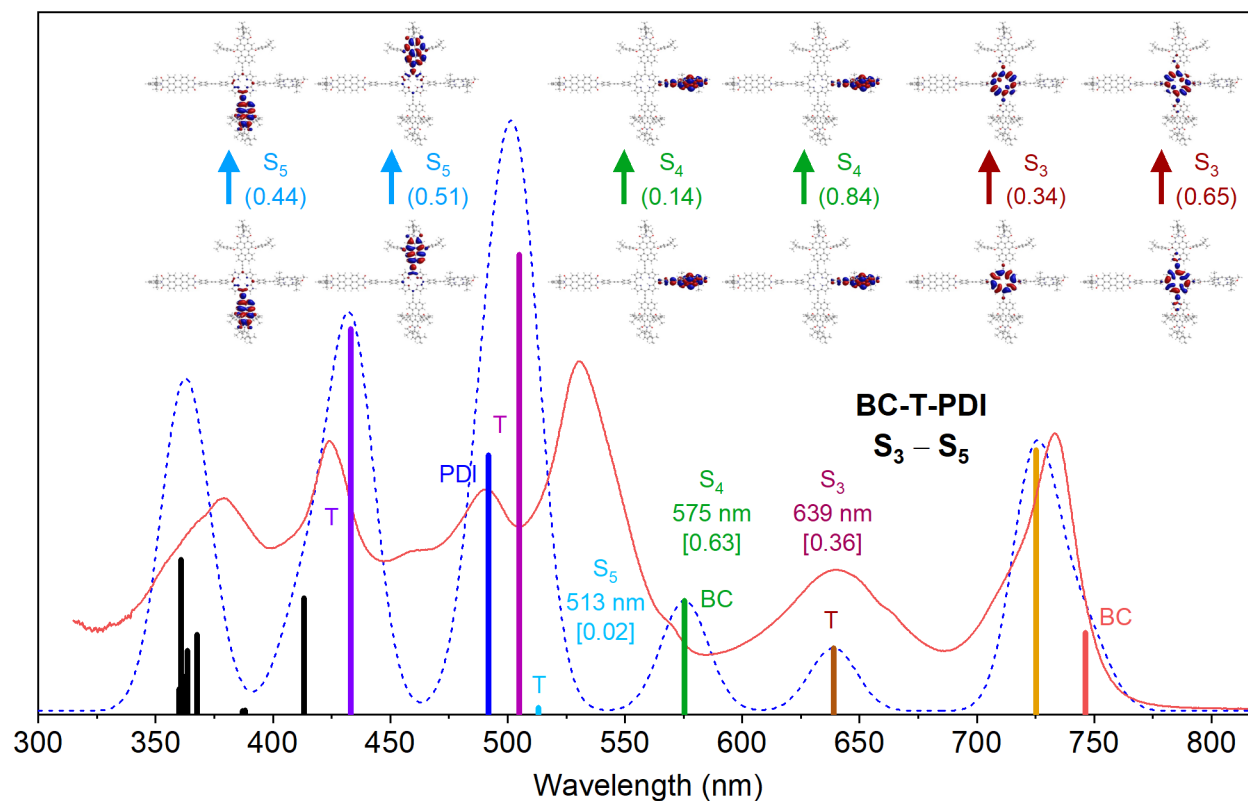
Figure S19. Absorption spectra calculated by TDDFT (colored sticks and blue dashed lines using 10-nm Gaussian skirts) are given along with pairs of occupied and virtual NTOs for absorption from S_0 to $S_3 - S_5$ for pentad **BC-T-PDI** in toluene. The calculated spectra are shifted to lower energy by 300 cm^{-1} to best align with the measured spectrum (red solid line). The eigenvalue (weight) for each pair of NTOs that contribute to a transition is indicated in parenthesis. The calculated wavelength and oscillator strength (in square brackets) for each transition are given at the bottom of each panel.
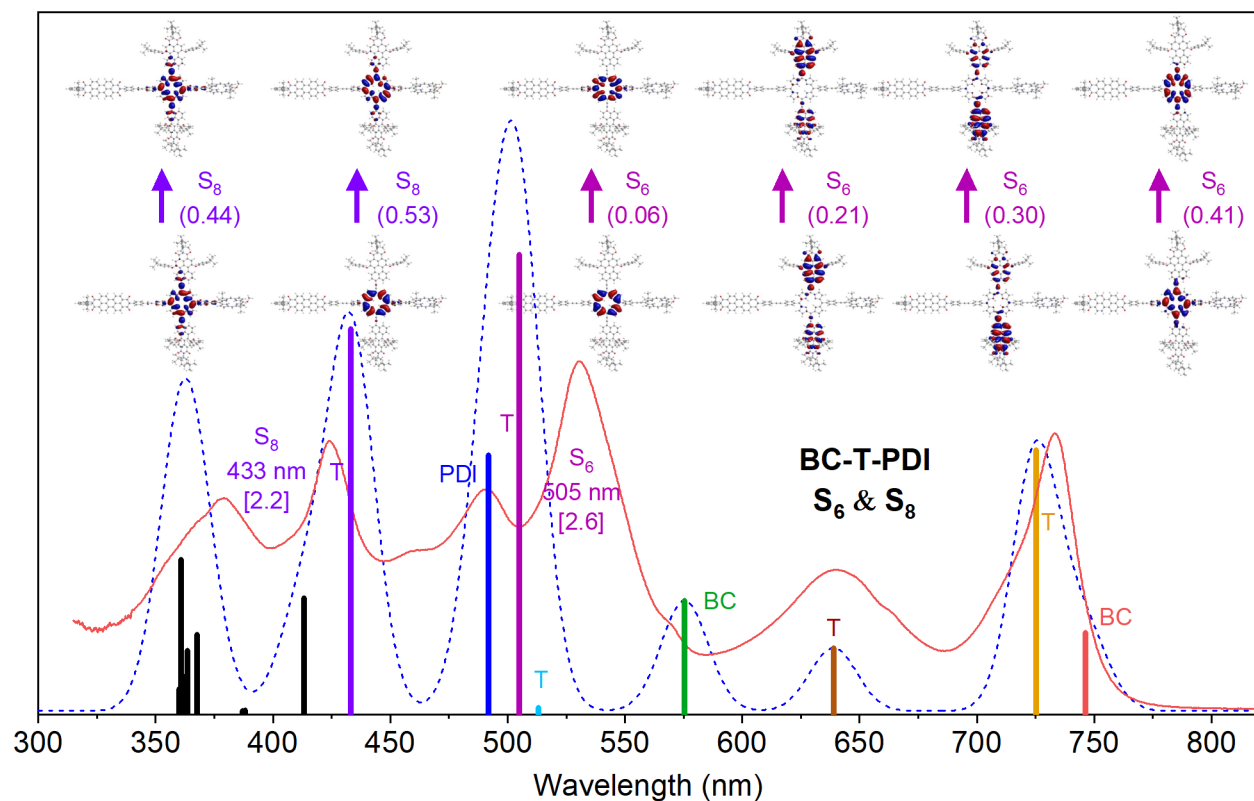
Figure S20. Absorption spectra calculated by TDDFT (colored sticks and blue dashed lines using 10-nm Gaussian skirts) are given along with pairs of occupied and virtual NTOs for absorption from S_0 to S_6 and S_8 for pentad **BC-T-PDI** in toluene. The calculated spectra are shifted to lower energy by 300 cm^{-1} to best align with the measured spectrum (red solid line). The eigenvalue (weight) for each pair of NTOs that contribute to a transition is indicated in parenthesis. The calculated wavelength and oscillator strength (in square brackets) for each transition are given at the bottom of each panel.
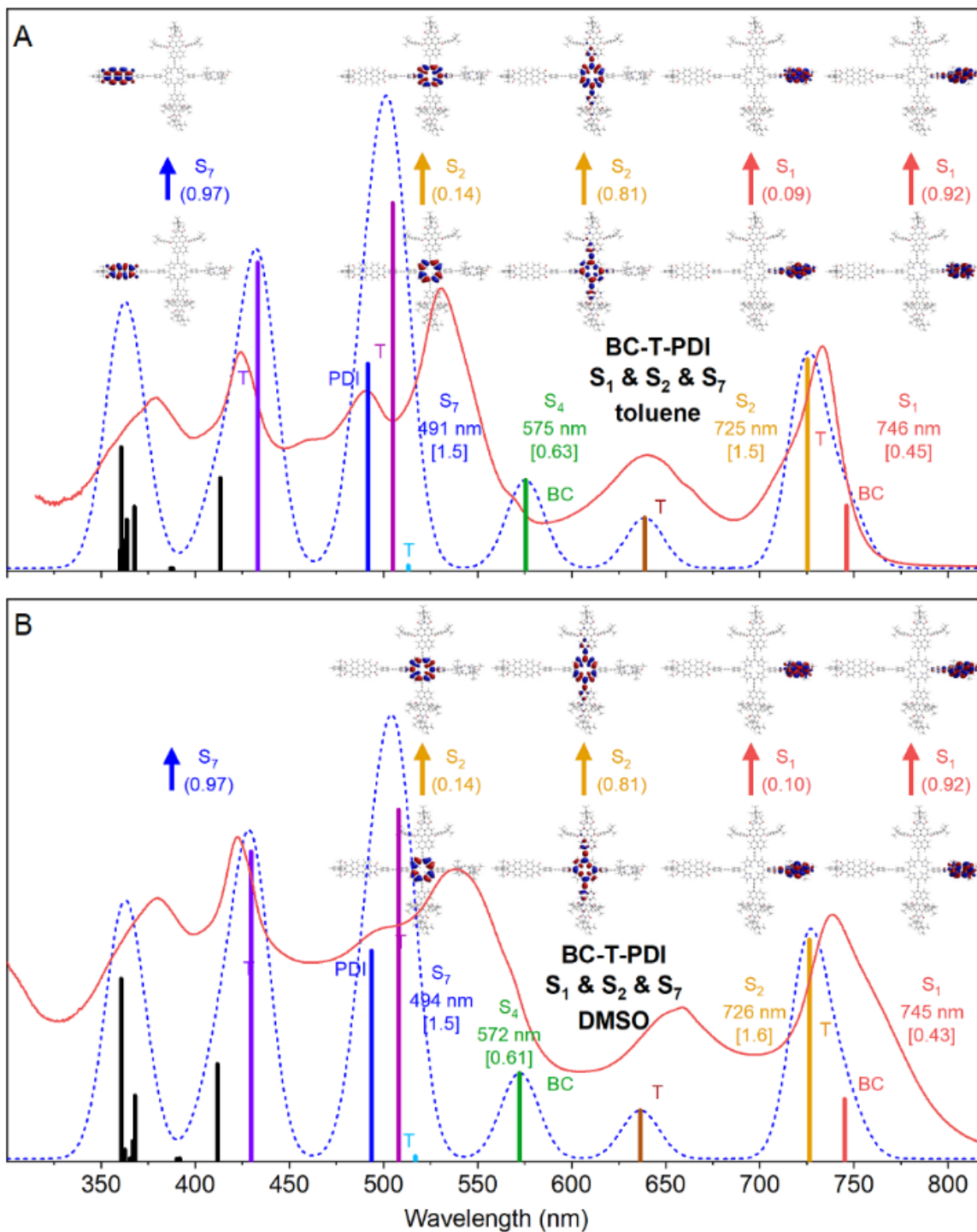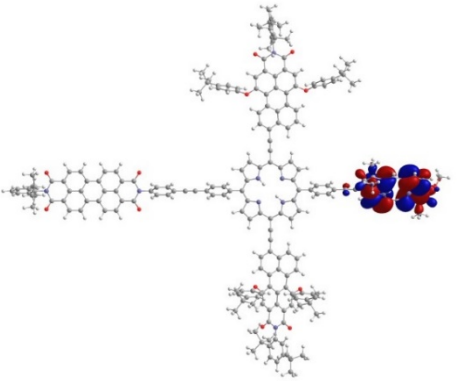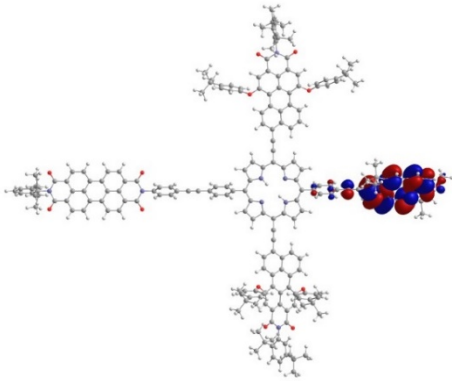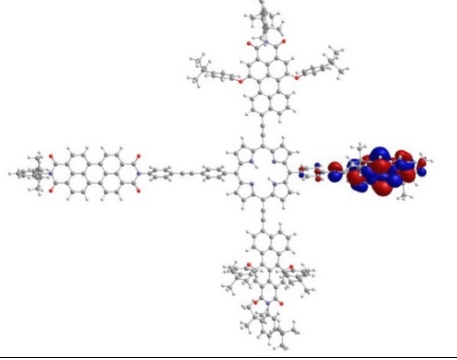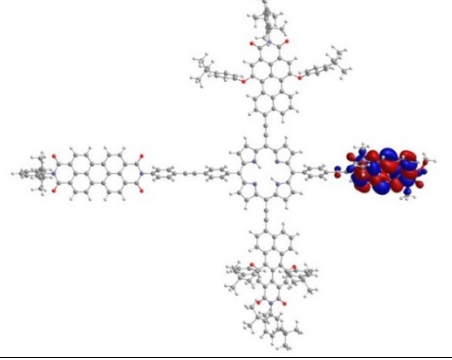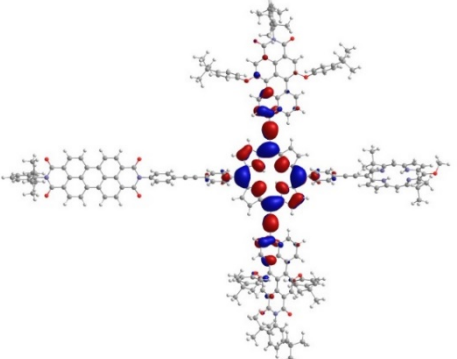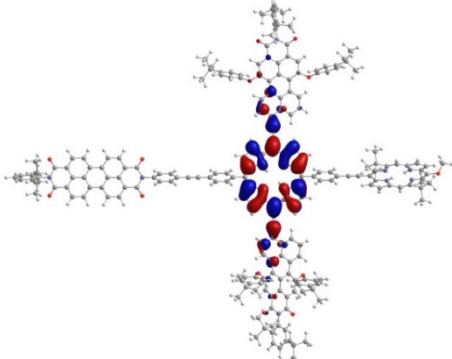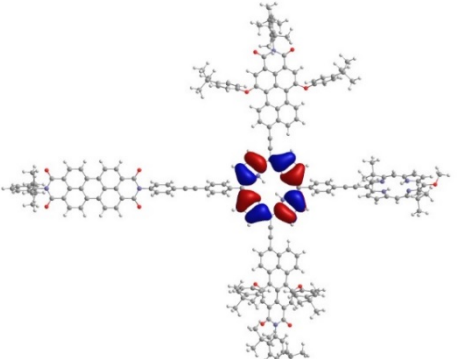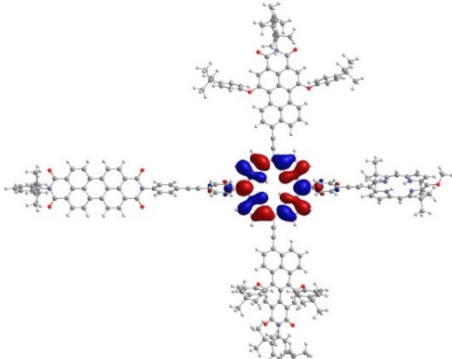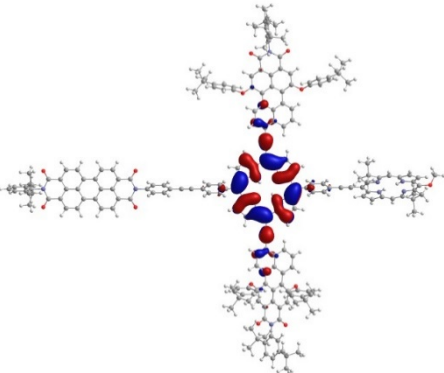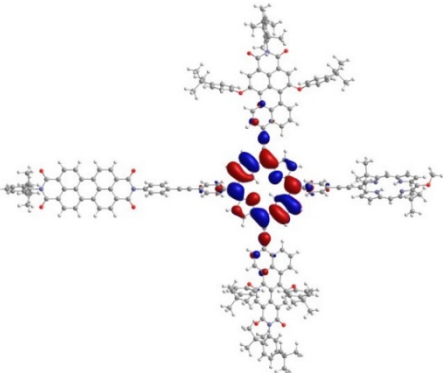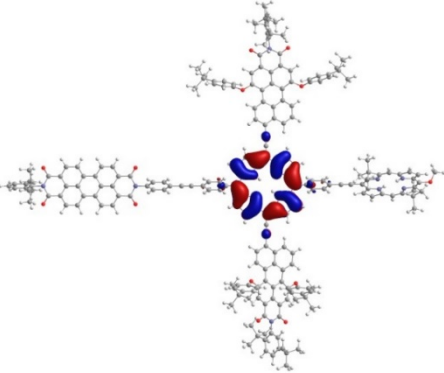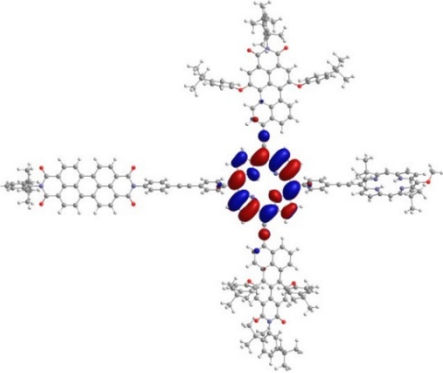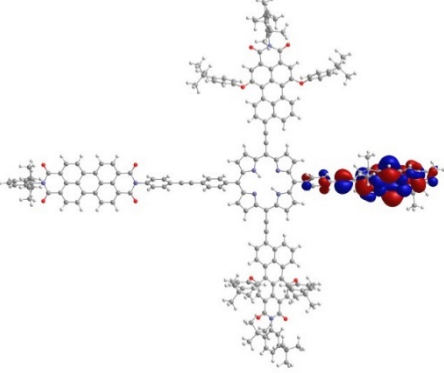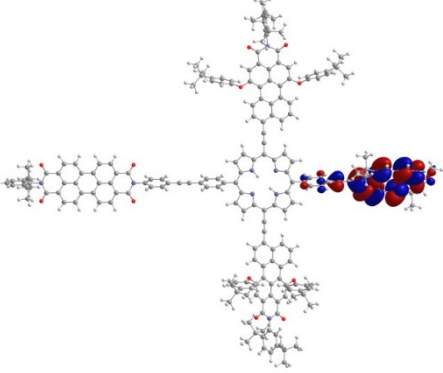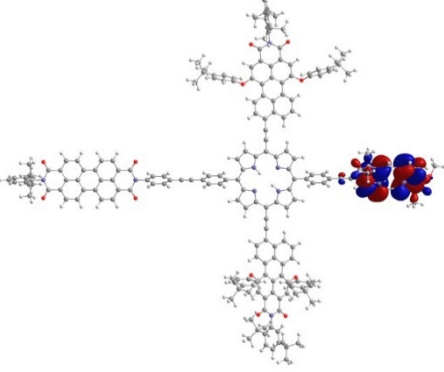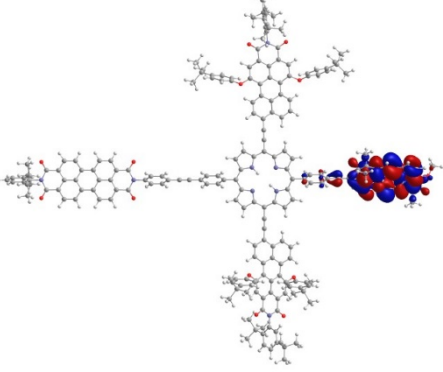
Figure S21. Absorption spectra calculated by TDDFT (colored sticks and blue dashed lines using 10-nm Gaussian skirts) are given along with pairs of occupied and virtual NTOs for absorption from S_0 to S_1 and S_2 for pentad **BC-T-PDI** in toluene (A) and DMSO (B). The calculated spectra are shifted to lower energy by 300 cm^{-1} to best align with the measured spectrum (red solid line) in toluene. The eigenvalue (weight) for each pair of NTOs that contribute to a transition is indicated in parenthesis. The calculated wavelength and oscillator strength (in square brackets) for various transitions are given at the bottom of each panel.
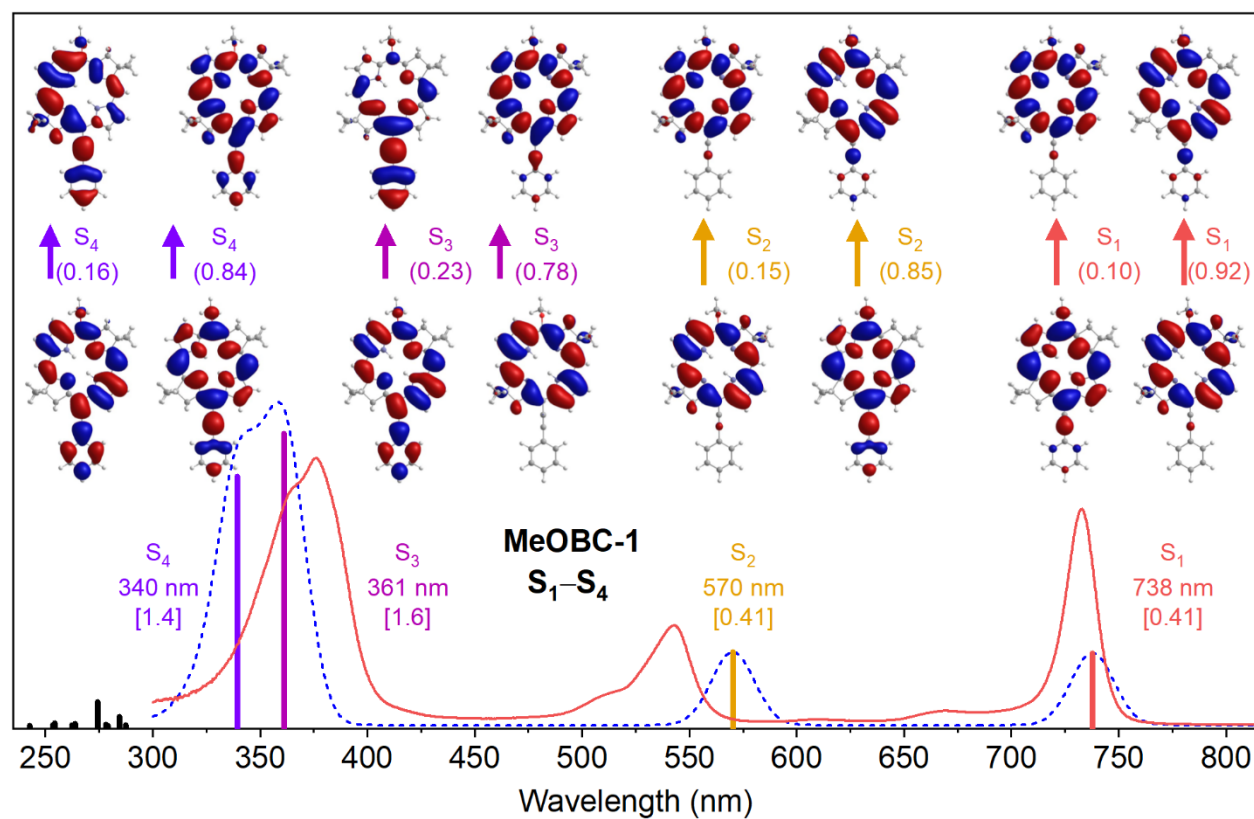
Figure S22. Absorption spectra calculated by TDDFT (colored sticks and blue dashed lines using 10-nm Gaussian skirts) are given along with pairs of occupied and virtual NTOs for absorption from S_0 to S_1 and S_2 for pentad **MeOBC-1** in toluene. The calculated spectra are shifted to lower energy by 200 cm^{-1} to best align with the measured spectrum (red solid line) in toluene. The eigenvalue (weight) for each pair of NTOs that contribute to a transition is indicated in parenthesis. The calculated wavelength and oscillator strength (in square brackets) for various transitions are given at the bottom of each panel.
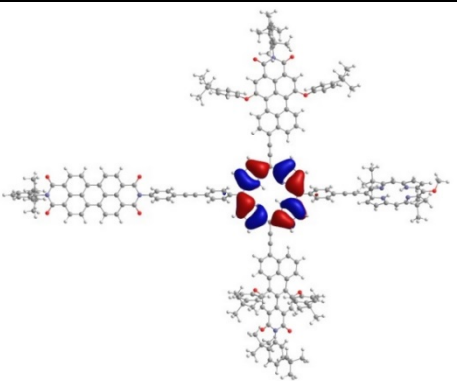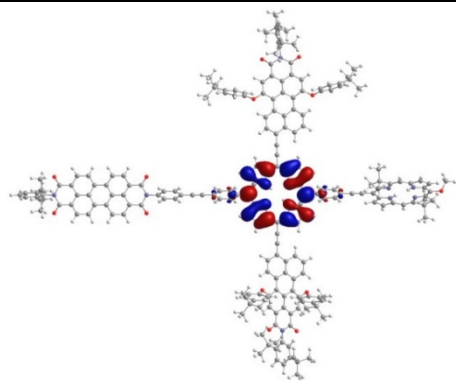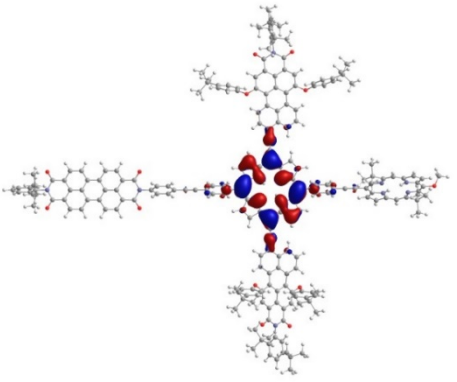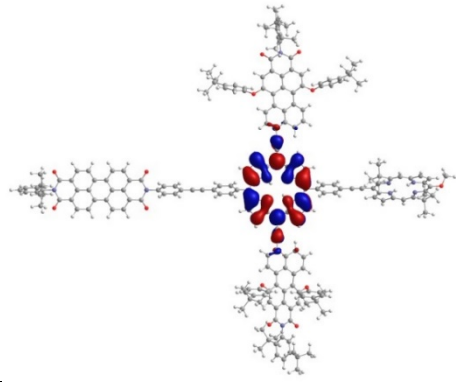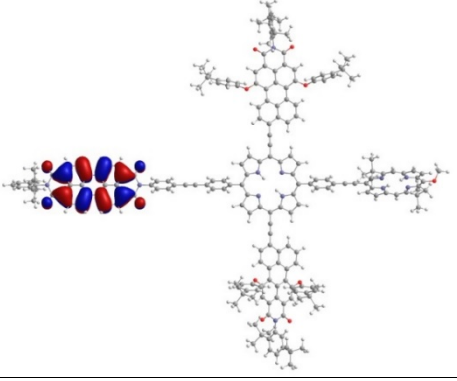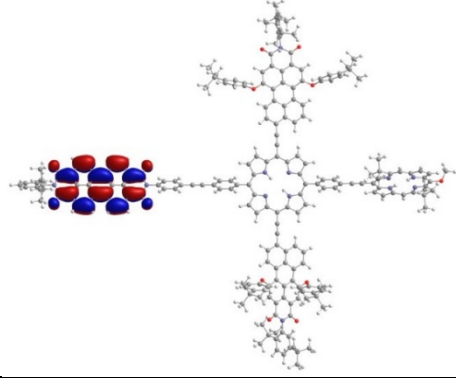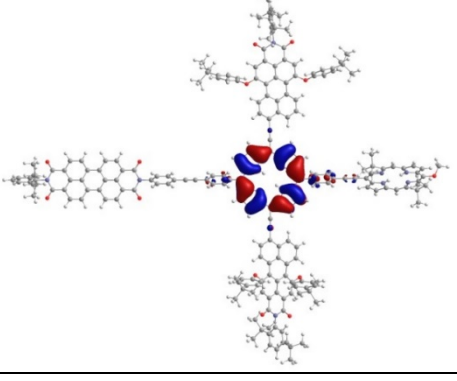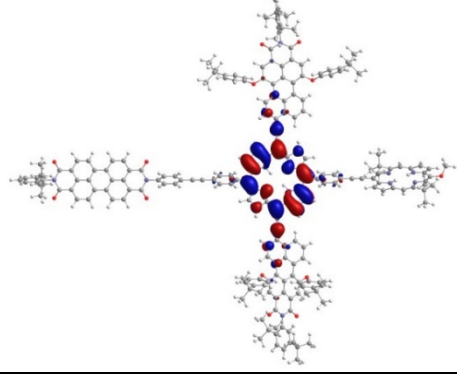
Table S7. NTO pairs for pentad **BC-T-PDI** in toluene.
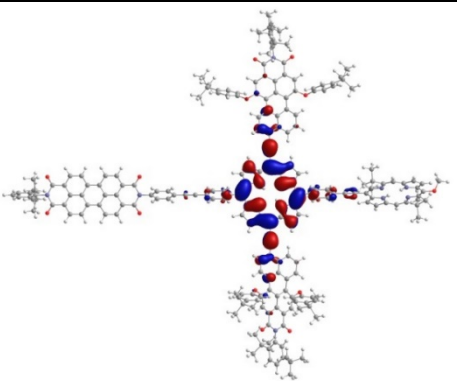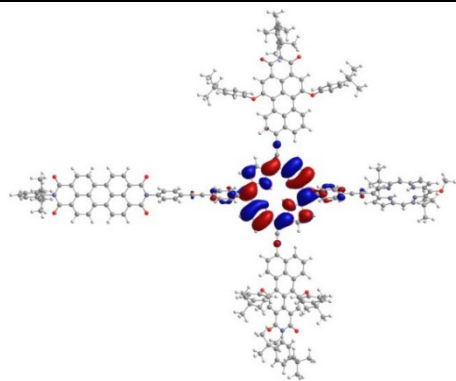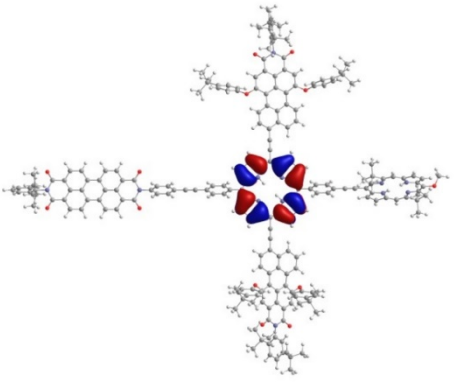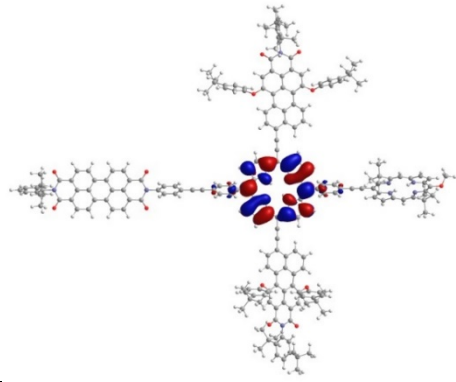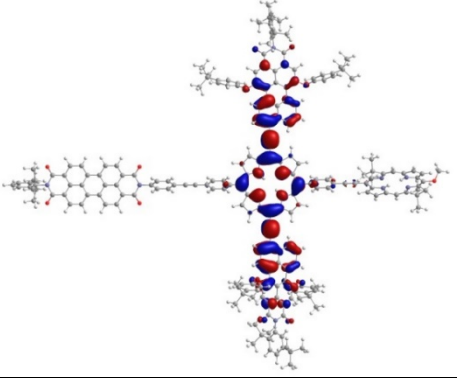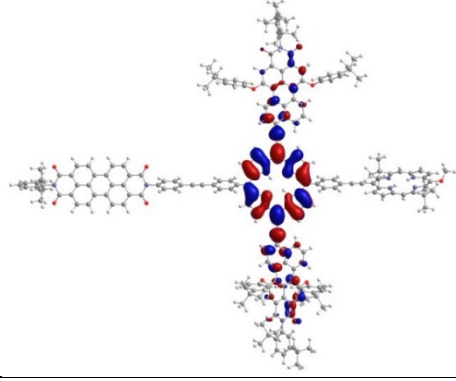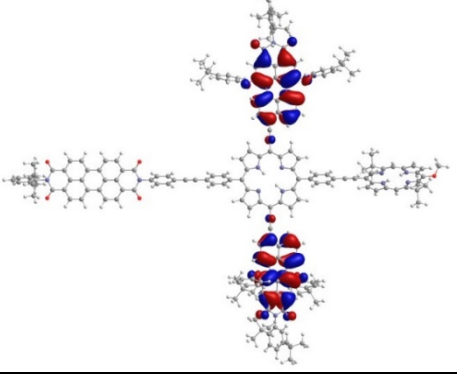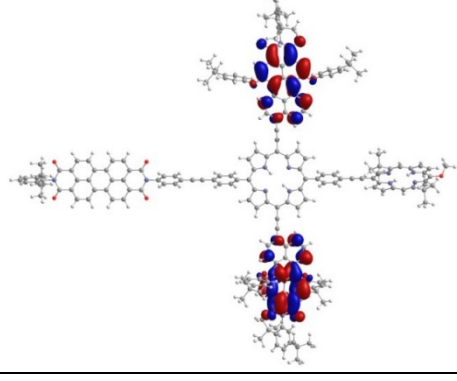
State	Eigenvalue	From NTO	To NTO
S1	0.92158		
S1	0.09370		
S2	0.81032		
S2	0.13869		

S3	0.64670		
S3	0.33934		
S4	0.84175		
S4	0.14032		
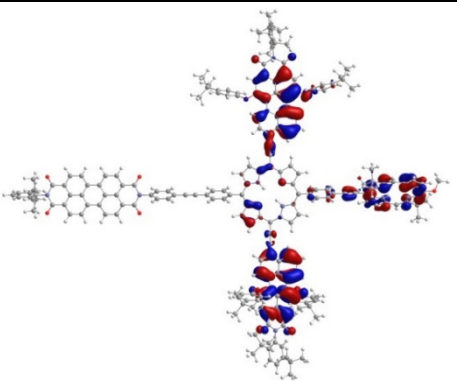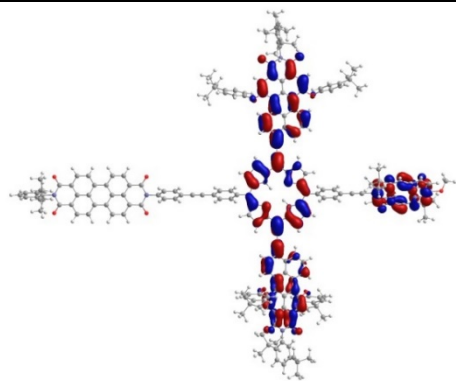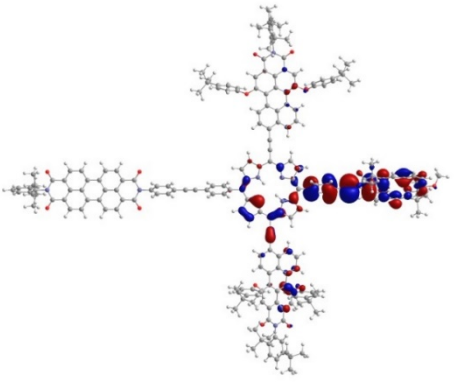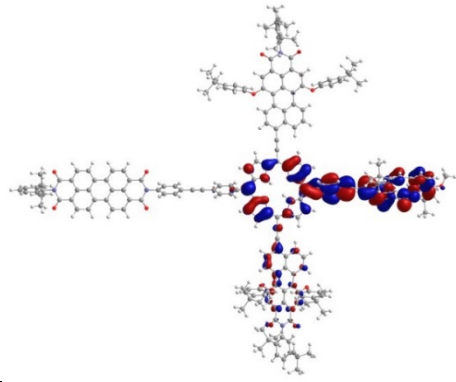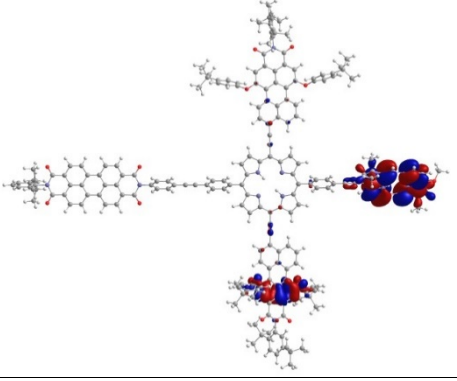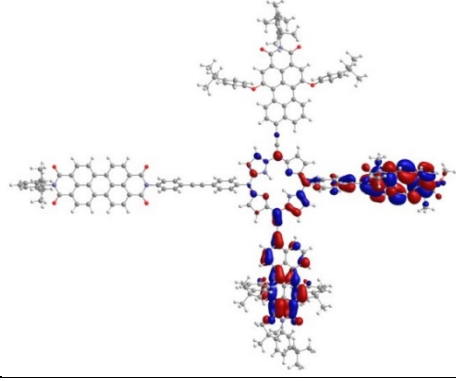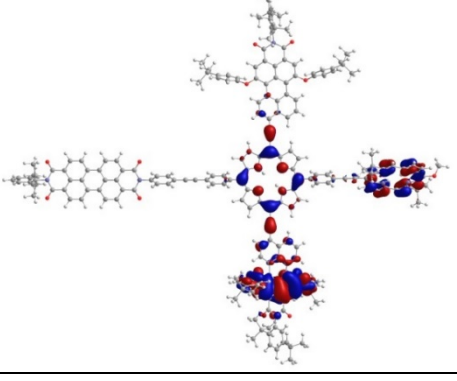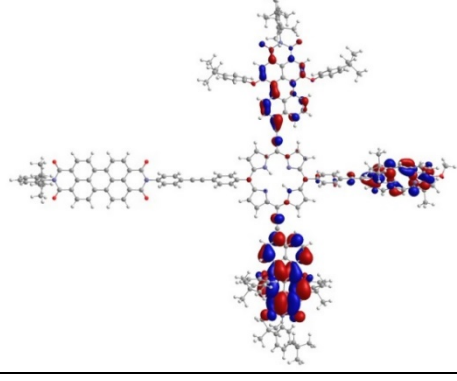
S5	0.50656		
S5	0.43913		
S6	0.41263		
S6	0.30094		
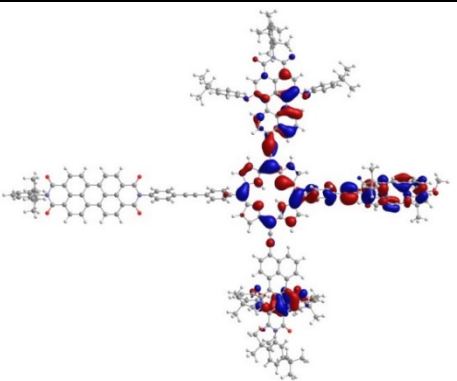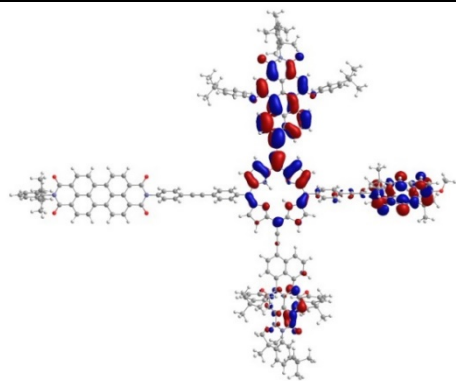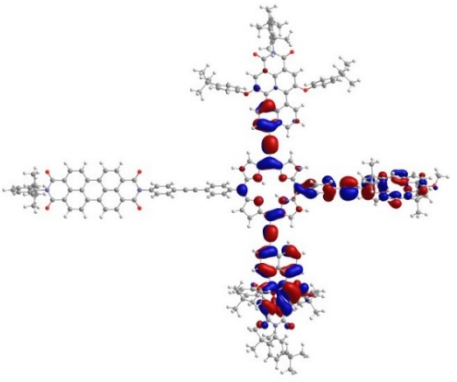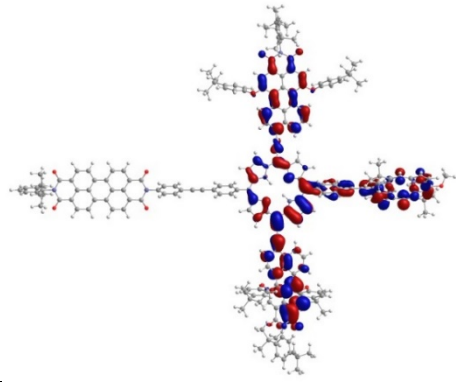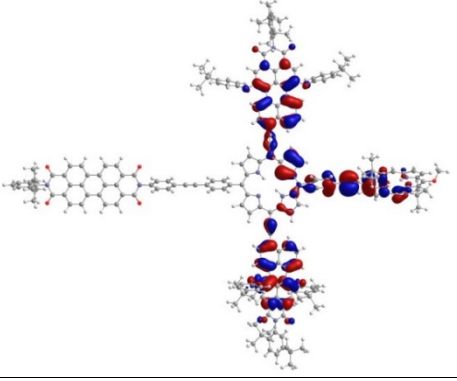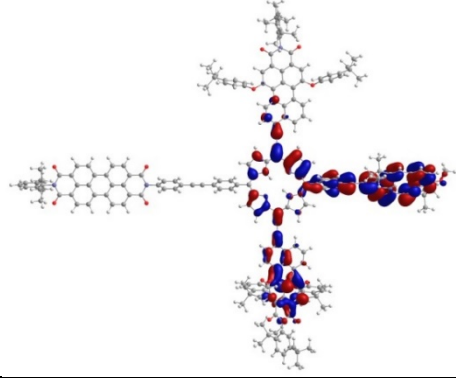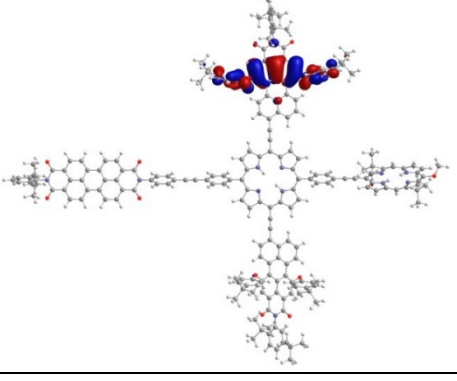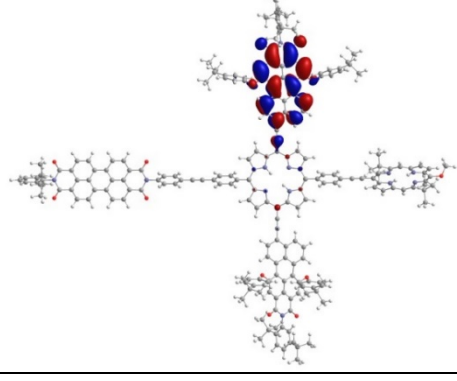
S6	0.20695		
S6	0.06277		
S7	0.96892		
S8	0.52573		

S8	0.43847		
S9	0.61401		
S9	0.19527		
S9	0.11185		

S9	0.08547		
S10	0.88583		
S10	0.06738		
S11	0.75216		

S11	0.13610		
S11	0.07588		
S12	0.44458		
S12	0.24299		

S12	0.13934		
S12	0.09808		
S13	0.34095		
S13	0.26974		
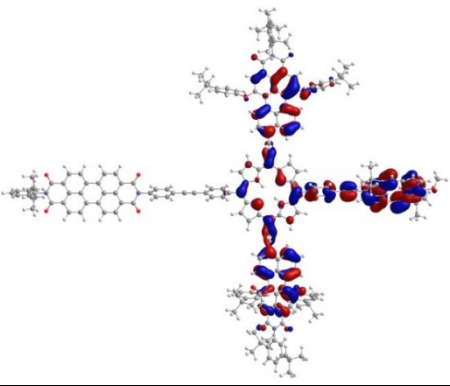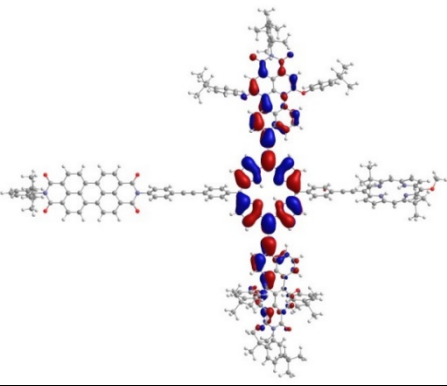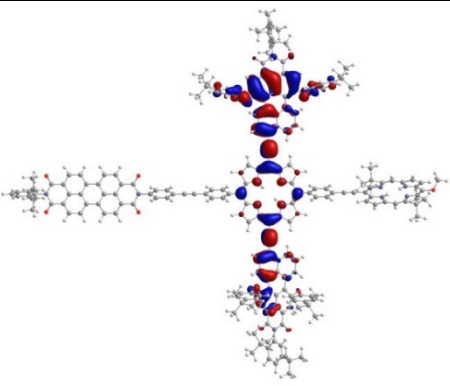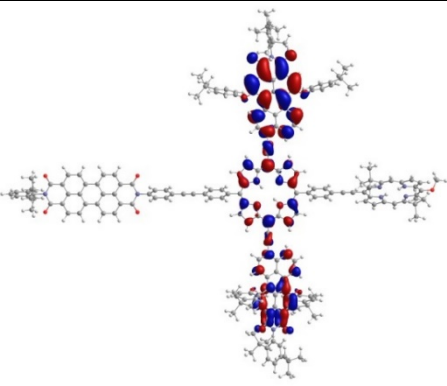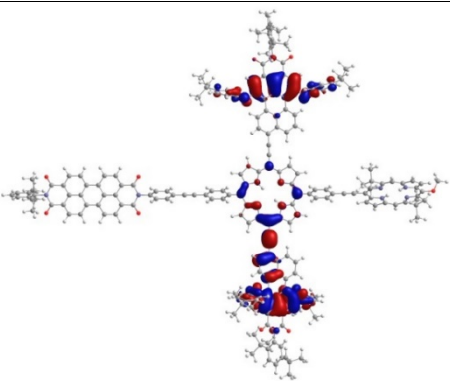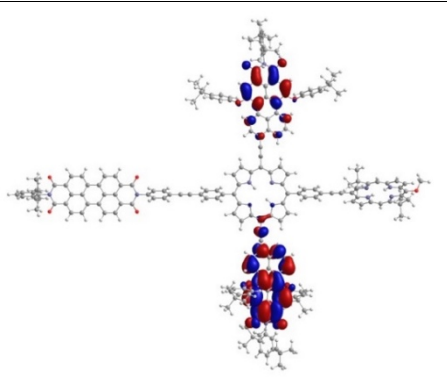
S13	0.17603		
S13	0.10373		
S13	0.05944		
S14	0.45092		

S14	0.18903		
S14	0.13802		
S14	0.09683		
S14	0.05804		
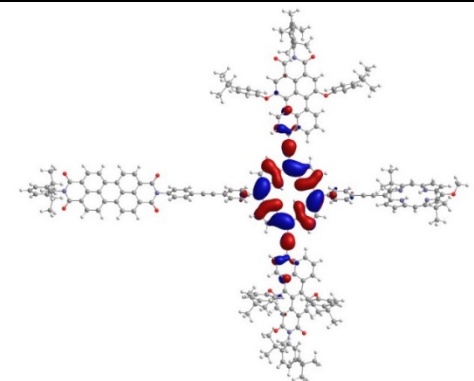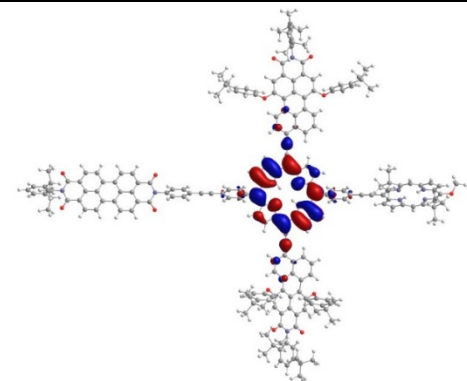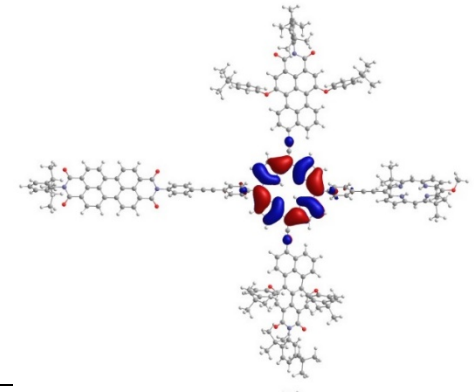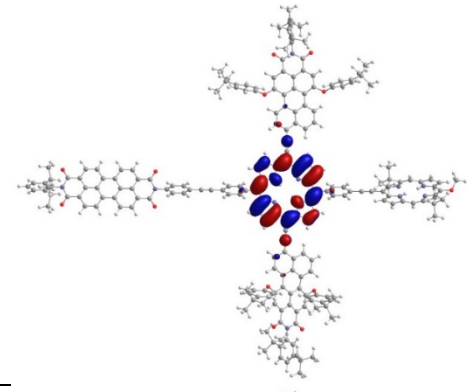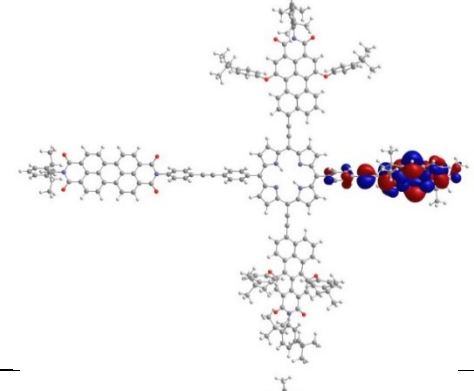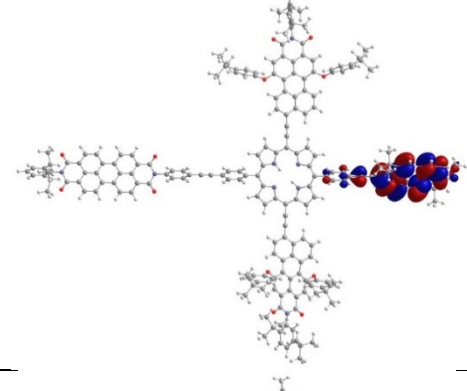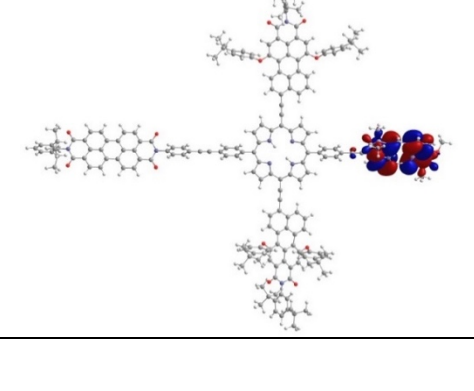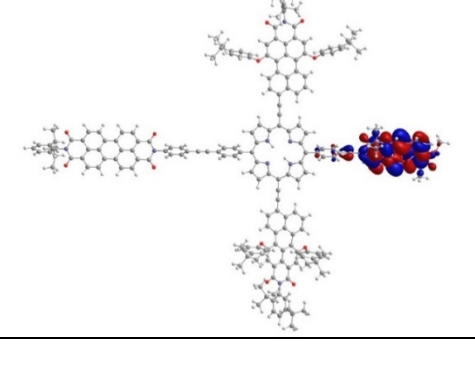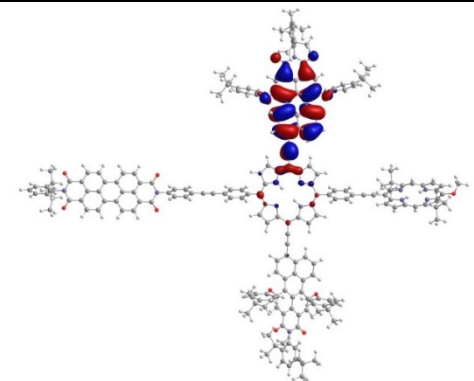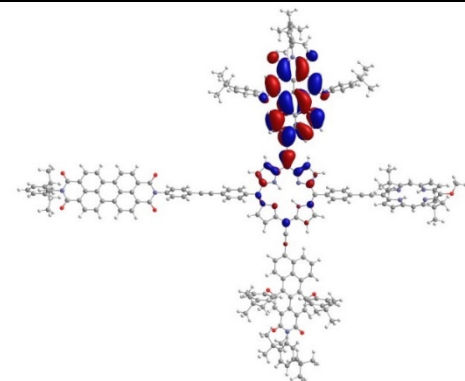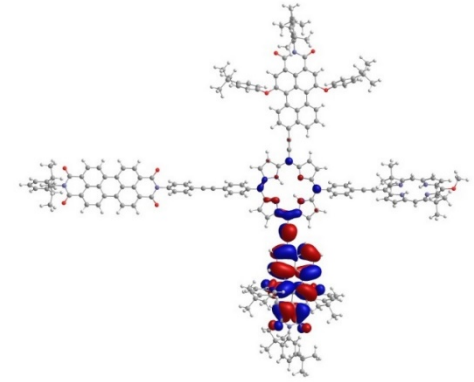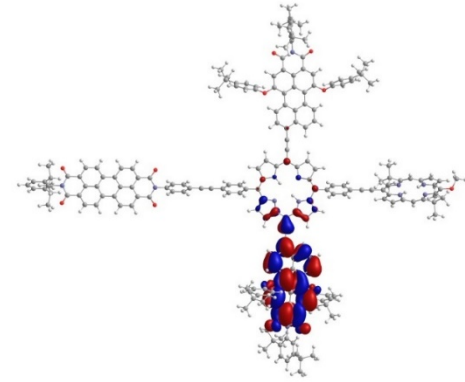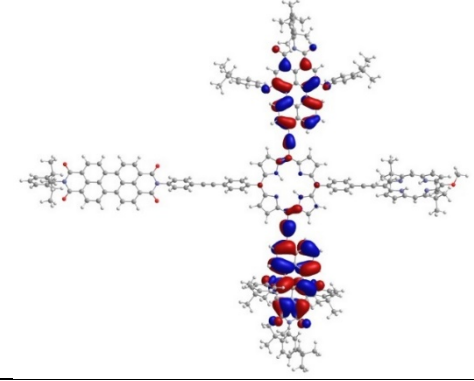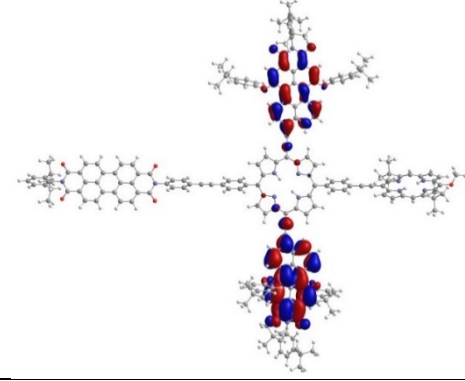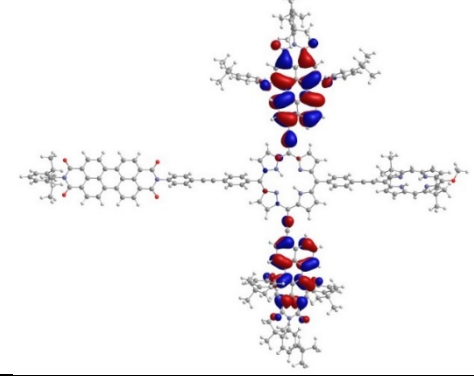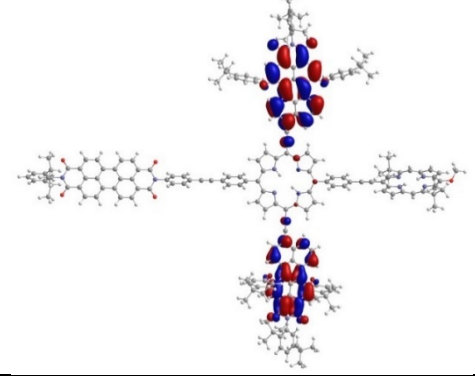
S15	0.48389		
S15	0.29019		
S15	0.05884		
S15	0.05085		

S16	0.50794		
S16	0.26255		
S16	0.12759		

Table S8. NTO pairs for pentad **BC-T-PDI** in DMSO.

S#	Eigenvalue	From NTO	To NTO
S1	0.91904		
S1	0.09587		
S2	0.80848		
S2	0.13559		

S3	0.63700		
S3	0.34831		
S4	0.83433		
S4	0.14562		

S5	0.49275		
S5	0.45143		
S6	0.40403		
S6	0.31023		

S6	0.20052		
S6	0.06915		
S7	0.96767		
S8	0.52801		

S8	0.43500		
S9	0.60414		
S9	0.20758		
S9	0.11303		
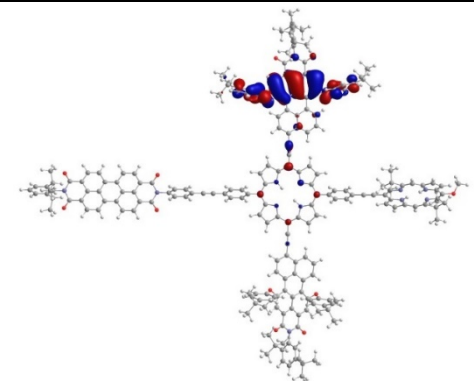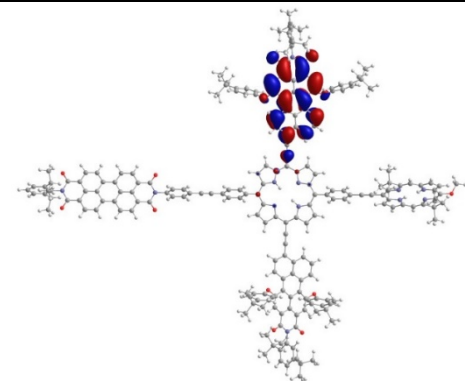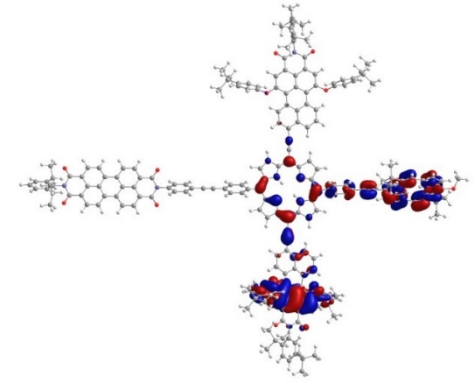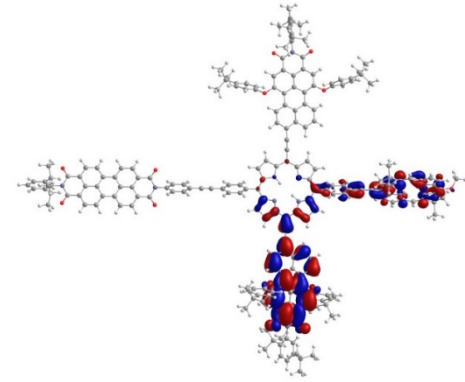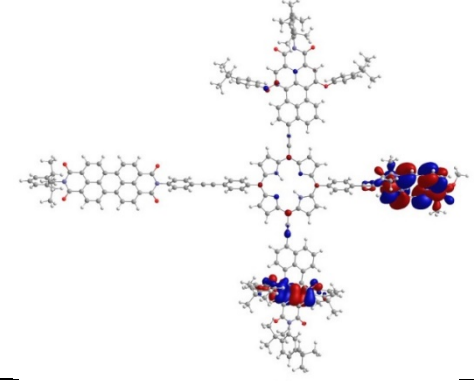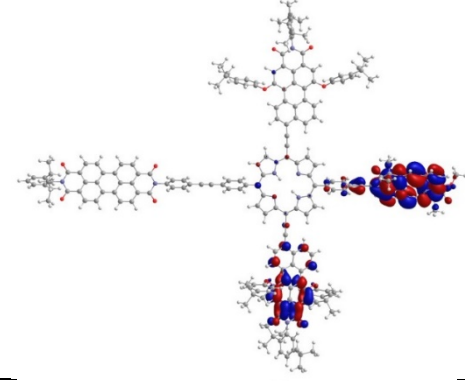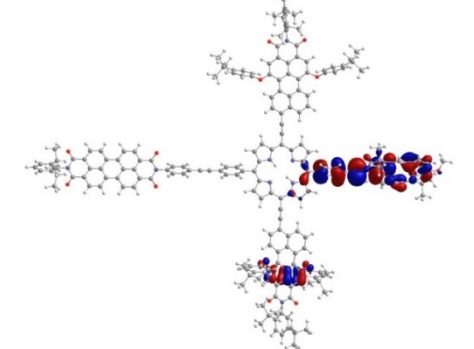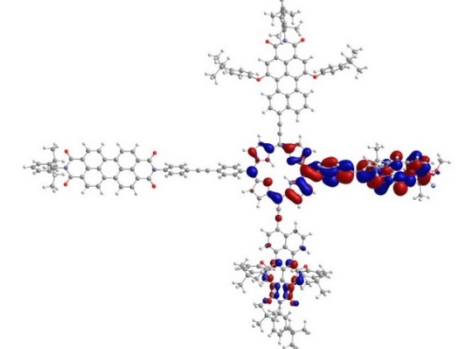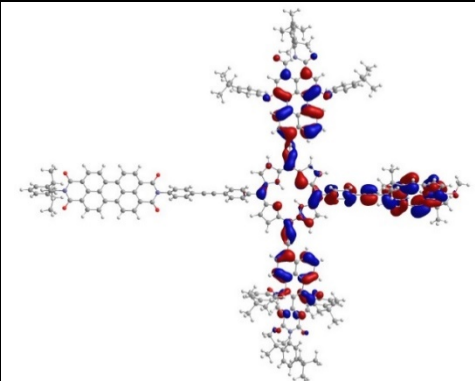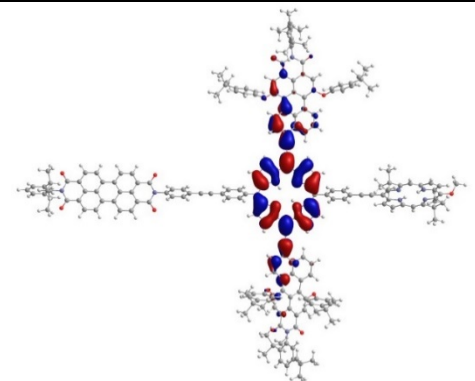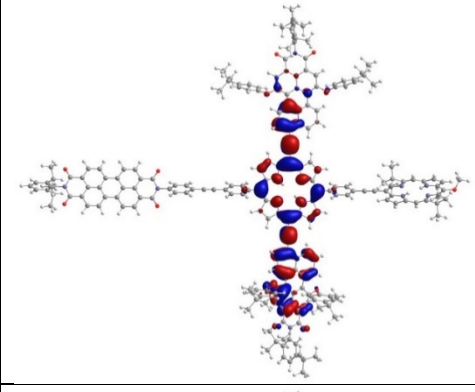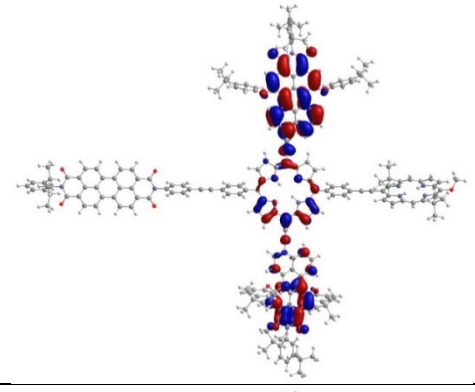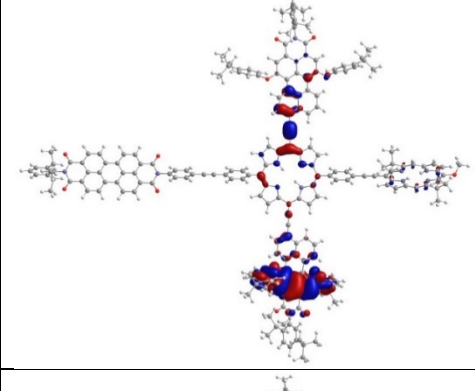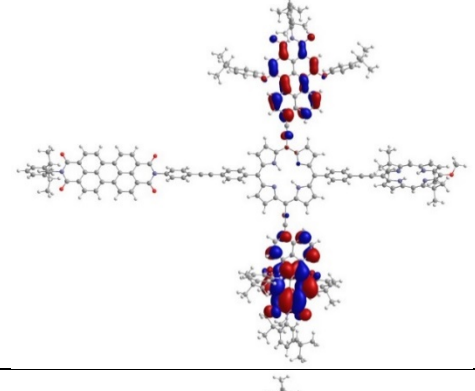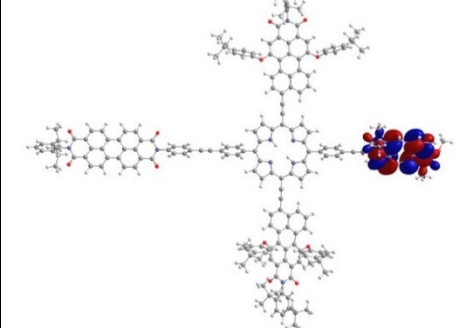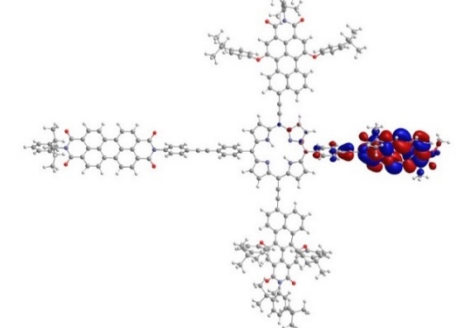
S9	0.08115		
S10	0.96195		
S11	0.74446		
S11	0.16773		
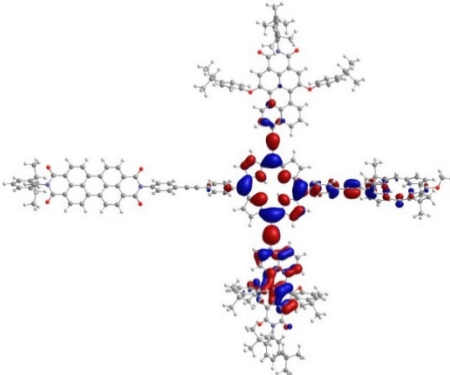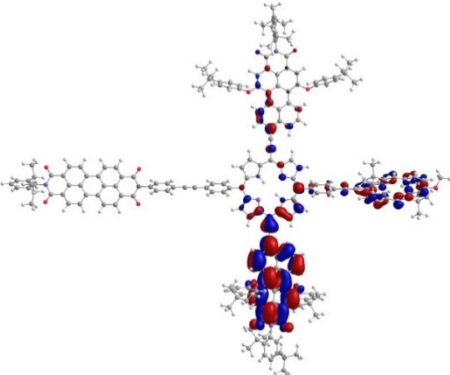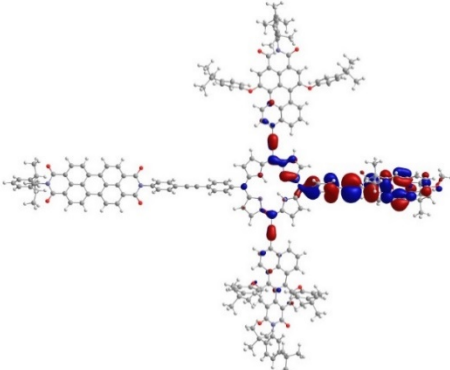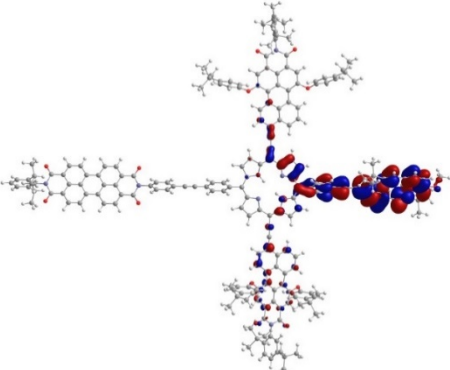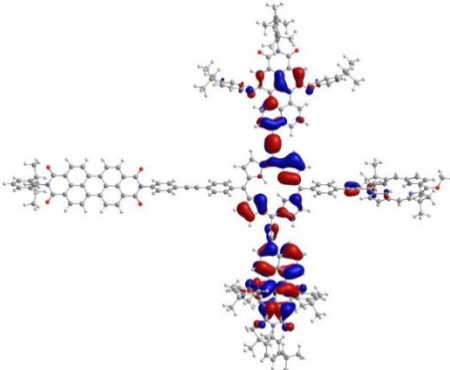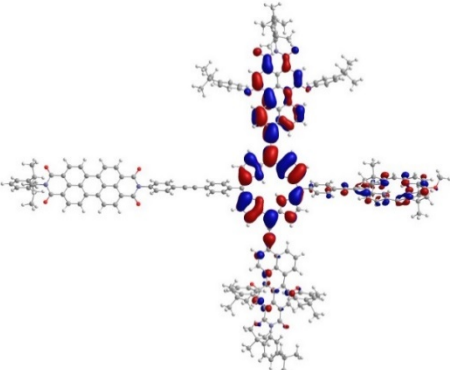
S12	0.47266		
S12	0.26140		
S12	0.07850		
S12	0.05103		
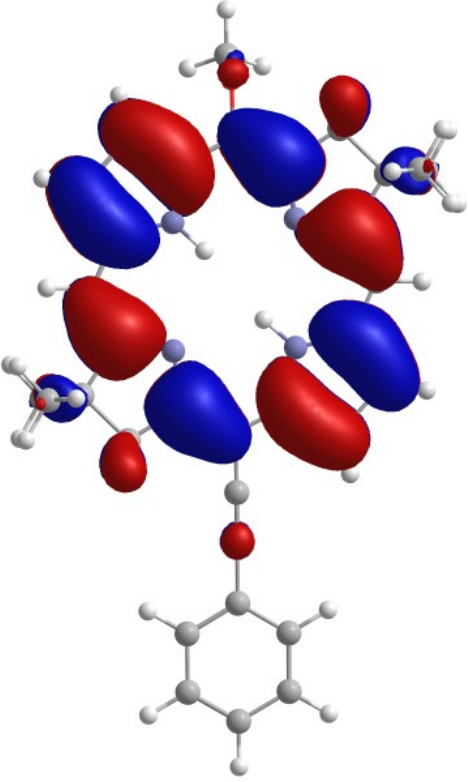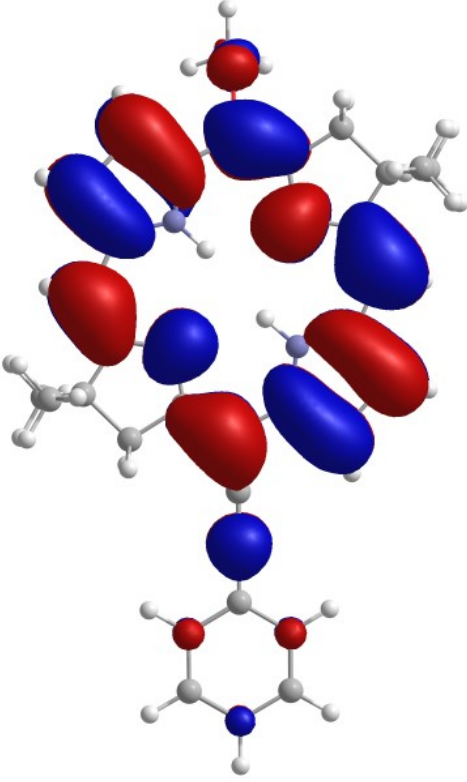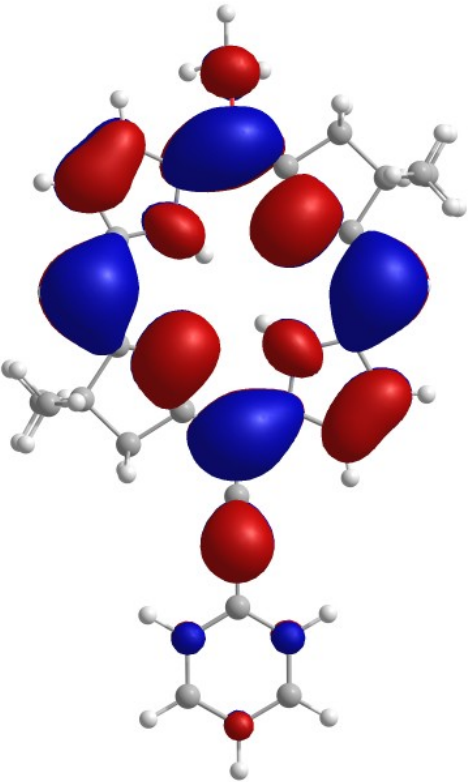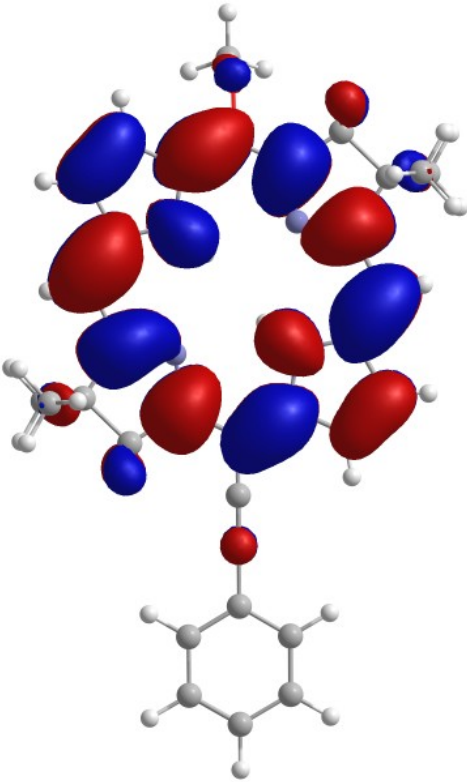
S13	0.49612		
S13	0.30981		
S13	0.09105		
S13	0.05224		

S14	0.40651		
S14	0.22562		
S14	0.16135		
S14	0.07991		
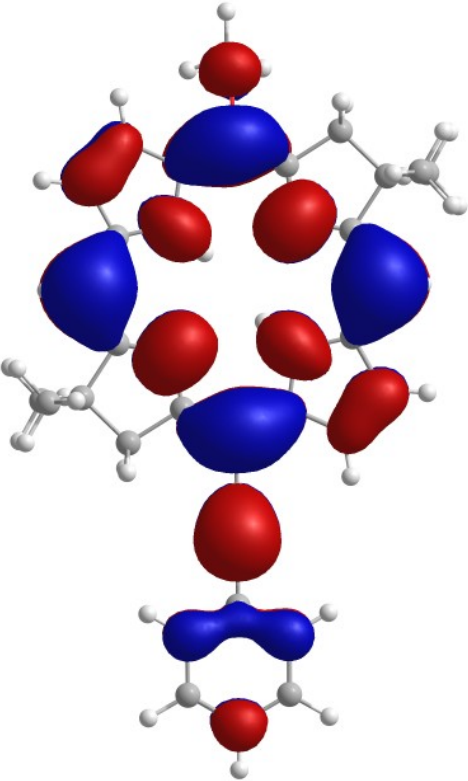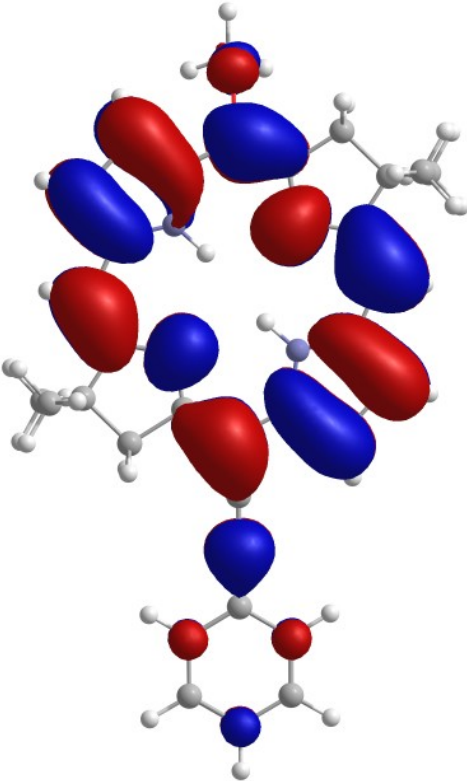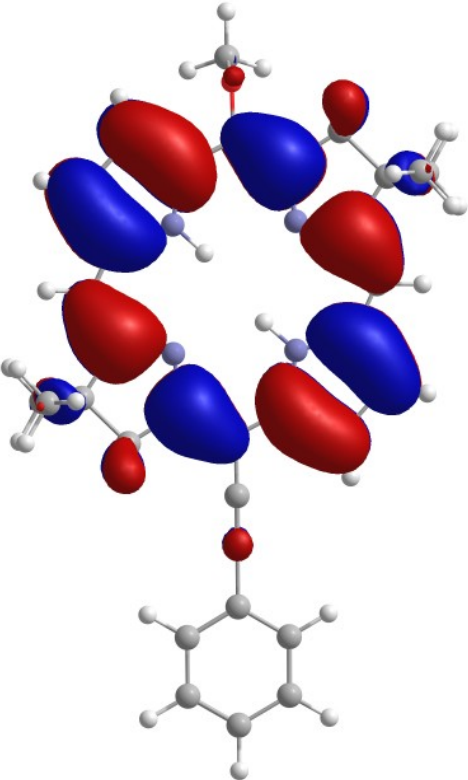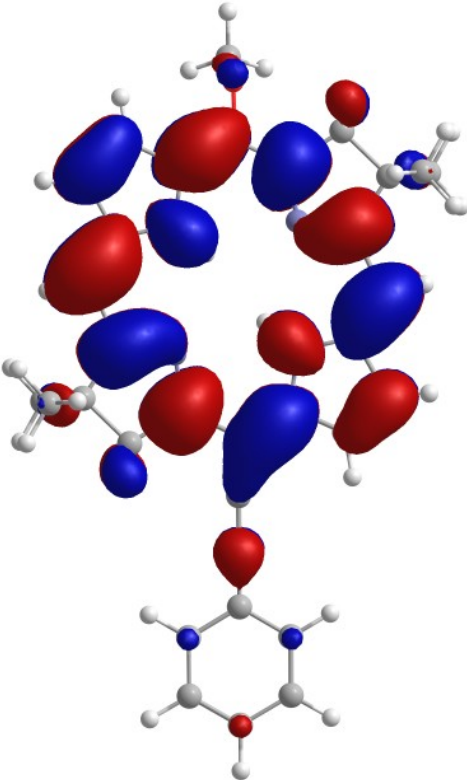
S15	0.63162		
S15	0.21480		
S15	0.08598		
S16	0.46780		
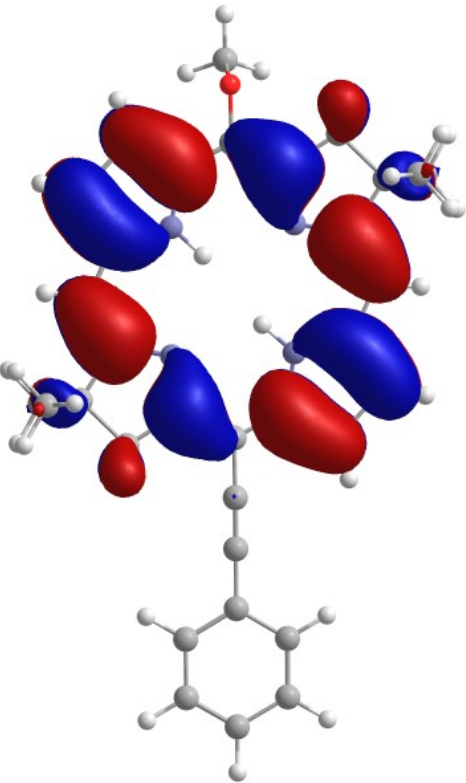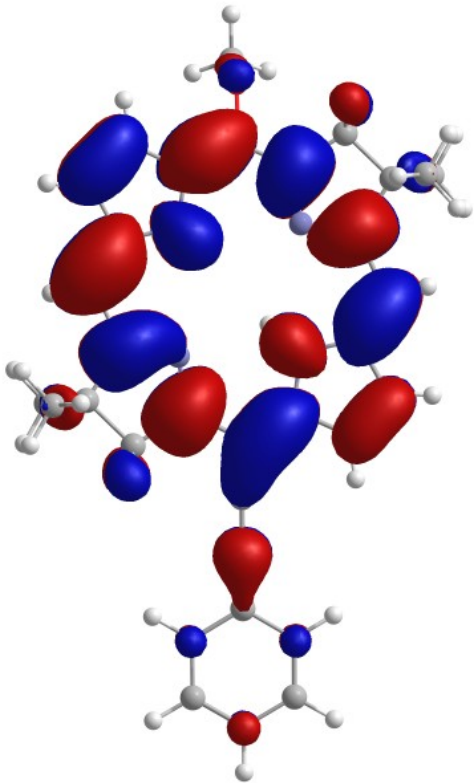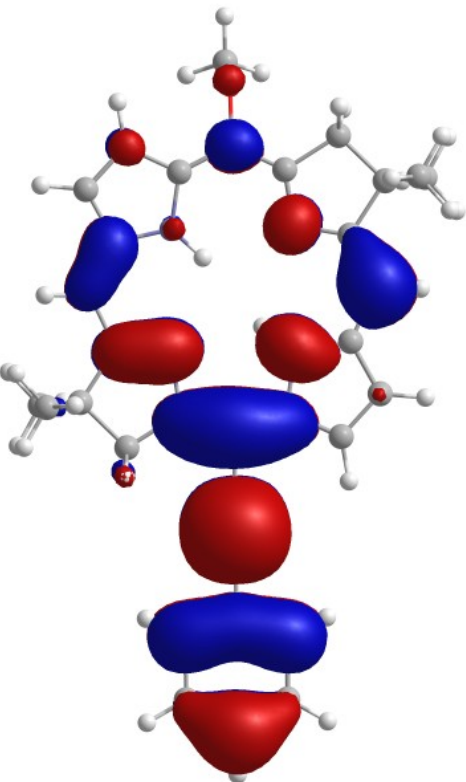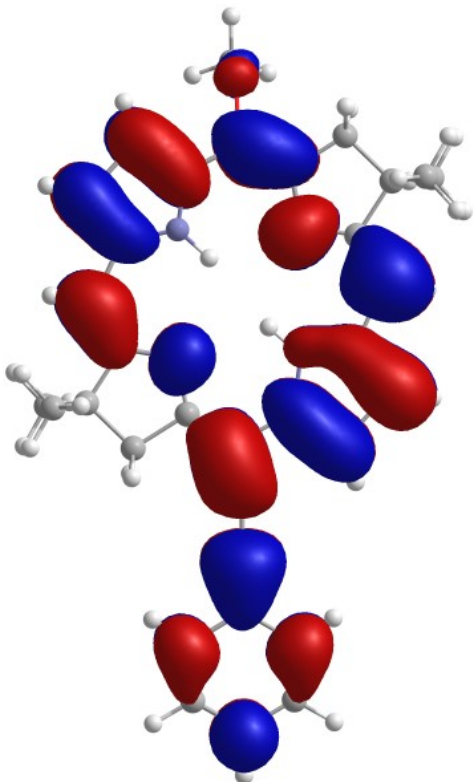
S16	0.25716		
S16	0.12978		
S16	0.08085		

Table S9. NTOs for bacteriochlorin monomer **MeO-BC-1** in toluene.
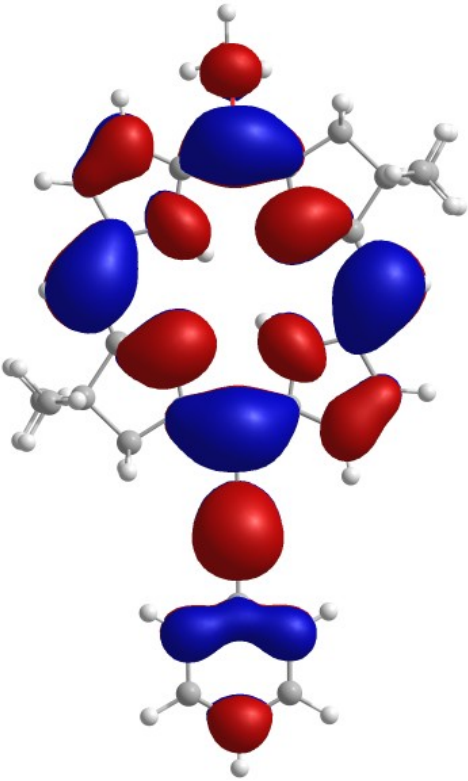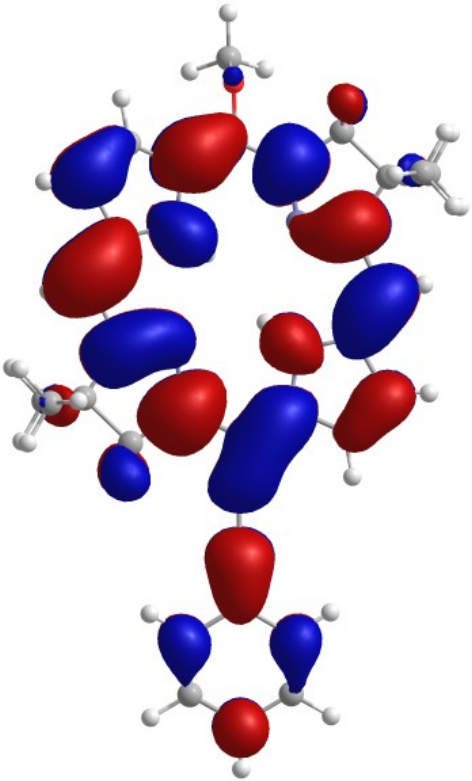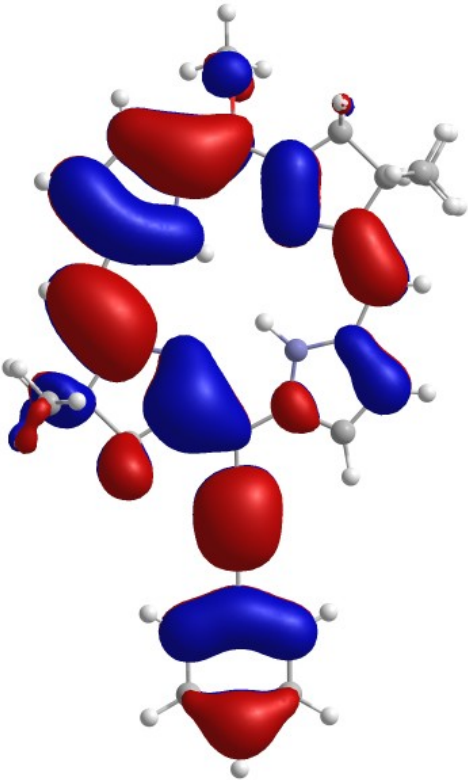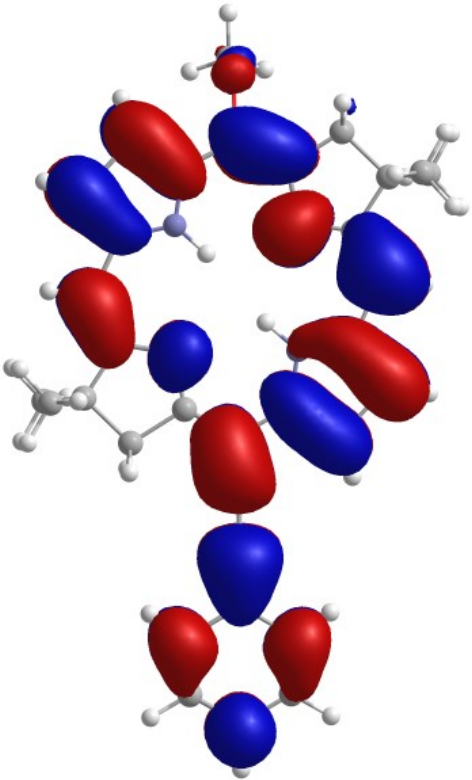
S#	Eigenvalue	From NTO	To NTO
S1	0.92091		
S1	0.09594		
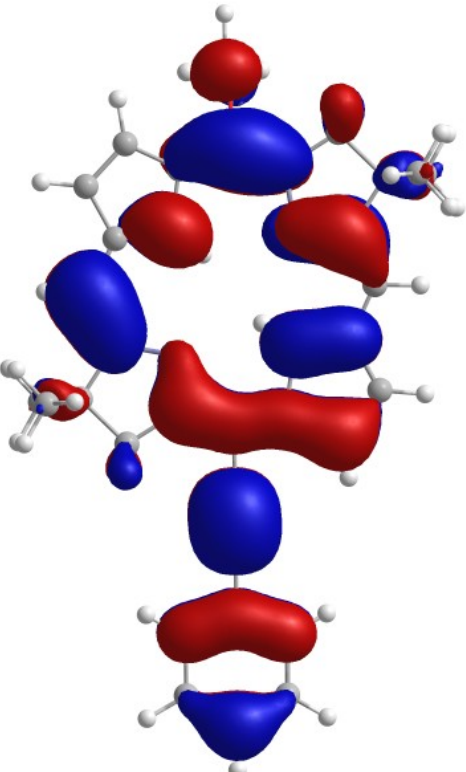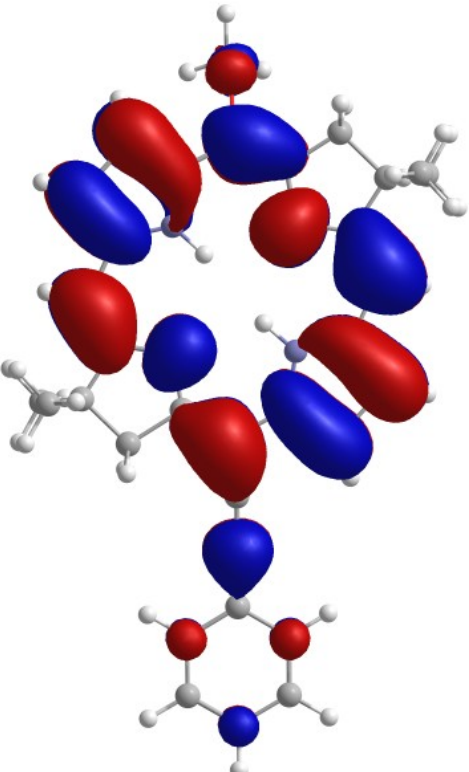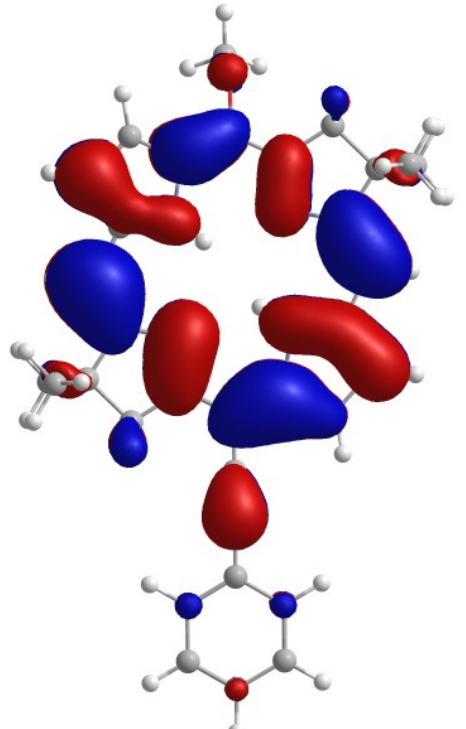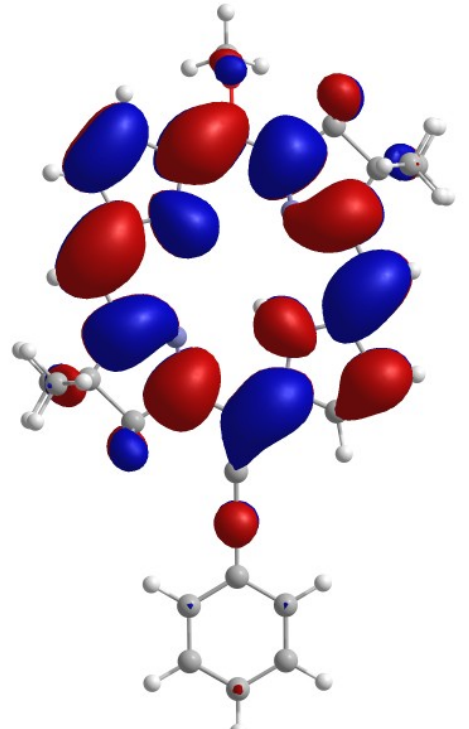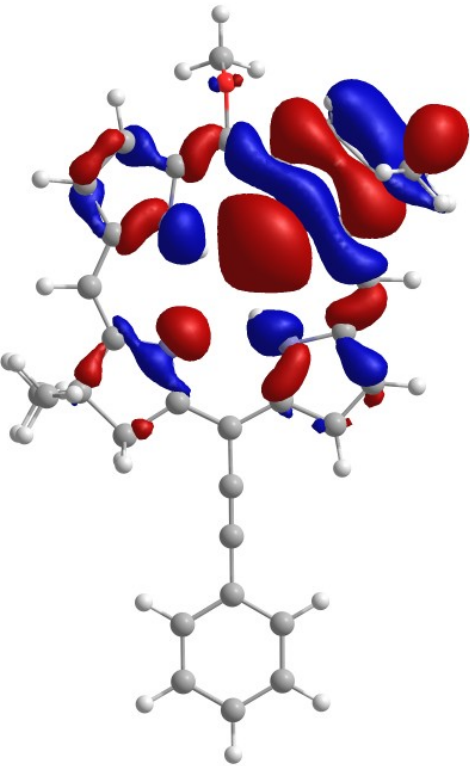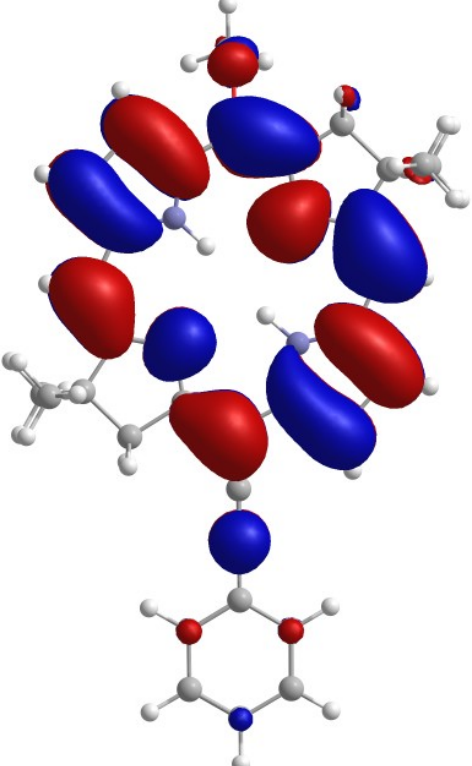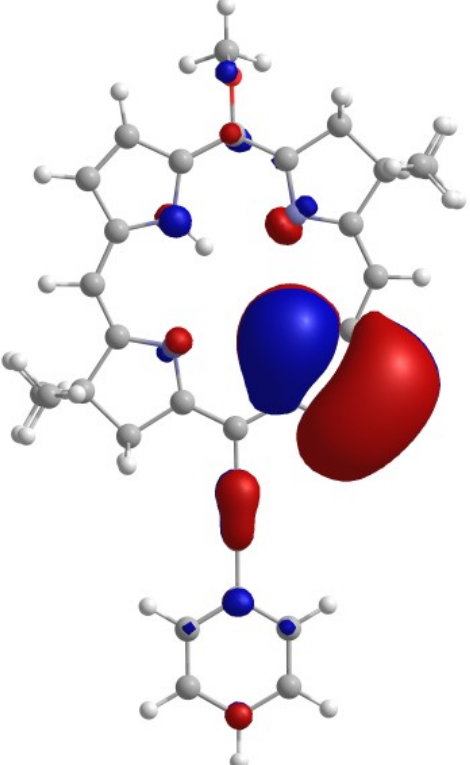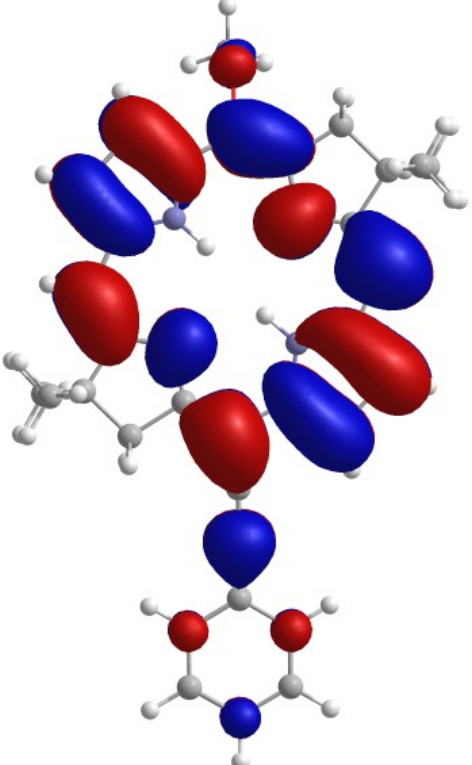
S2	0.85488		
S2	0.14559		
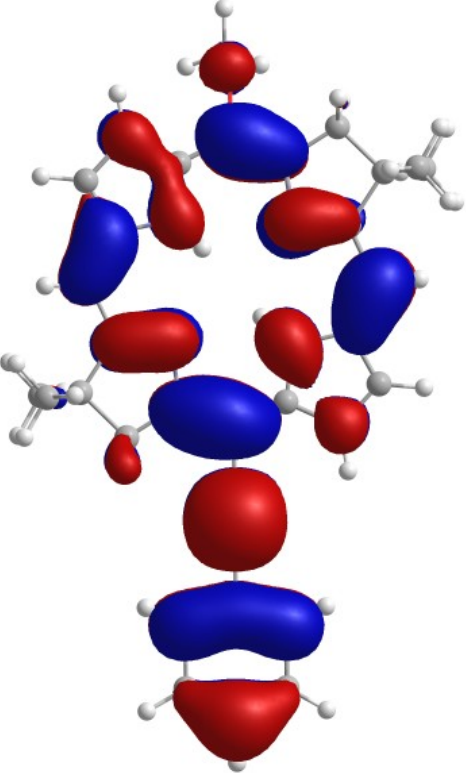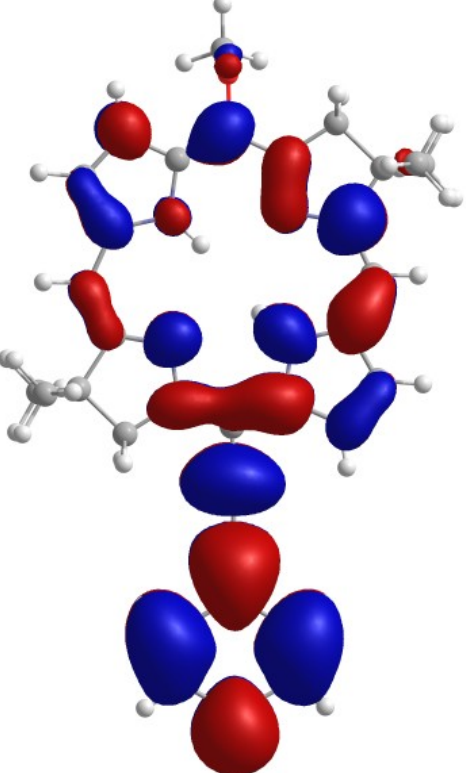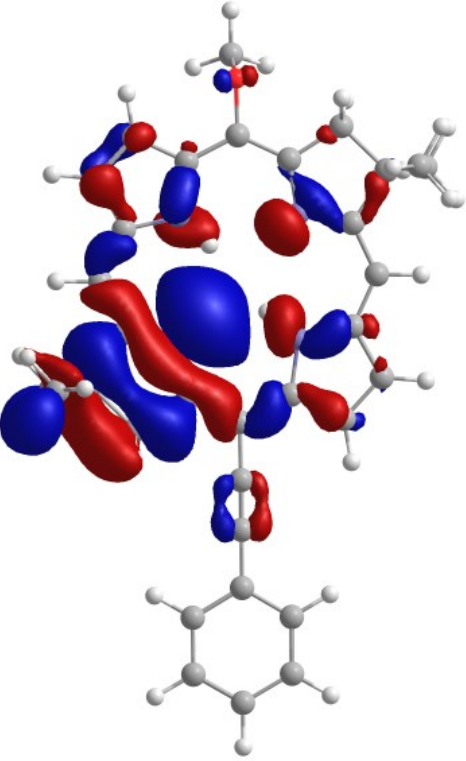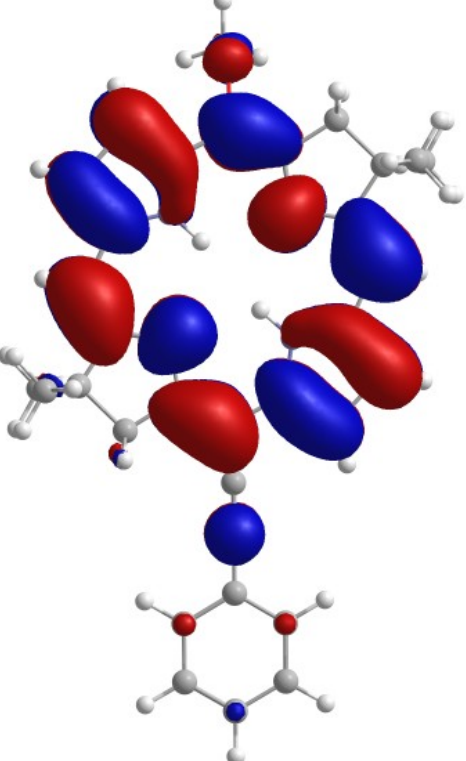
S3	0.78147		
S3	0.22902		
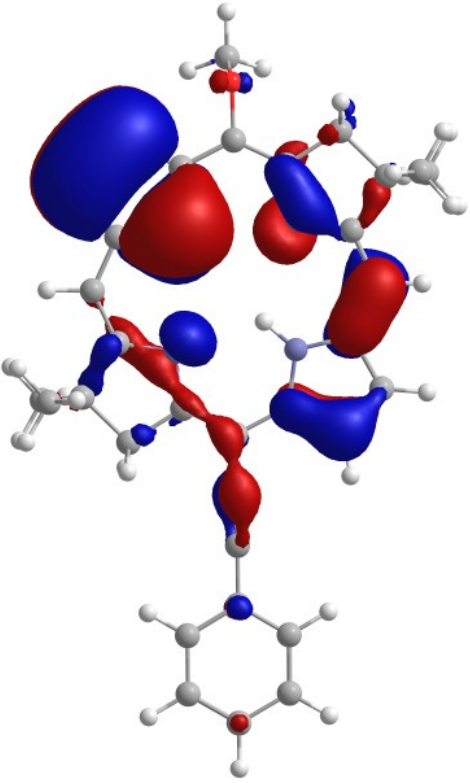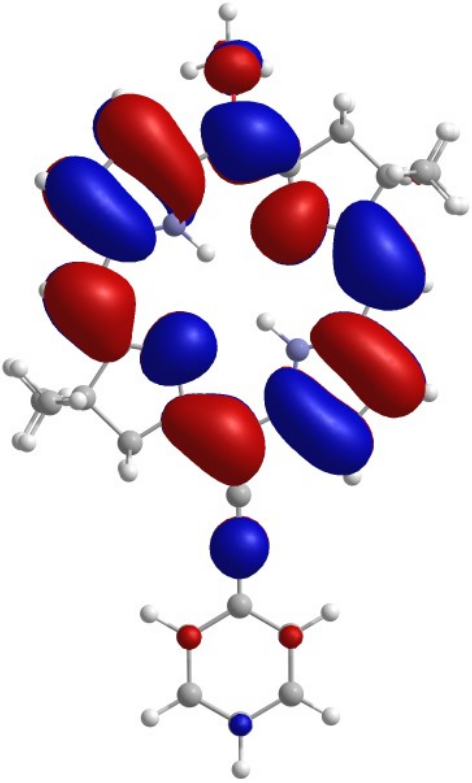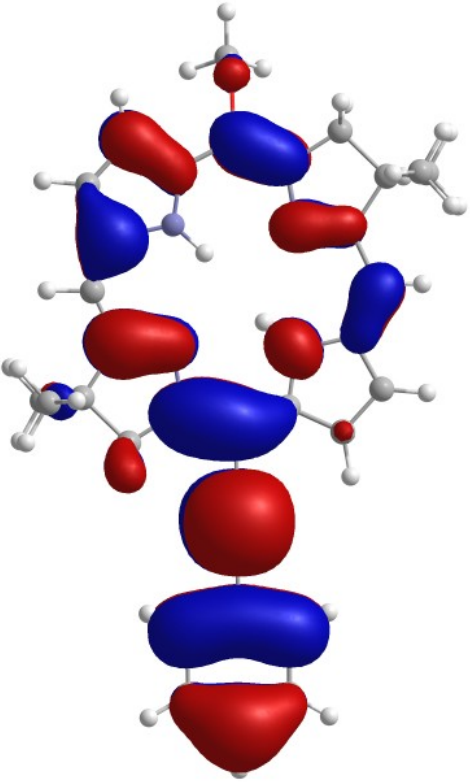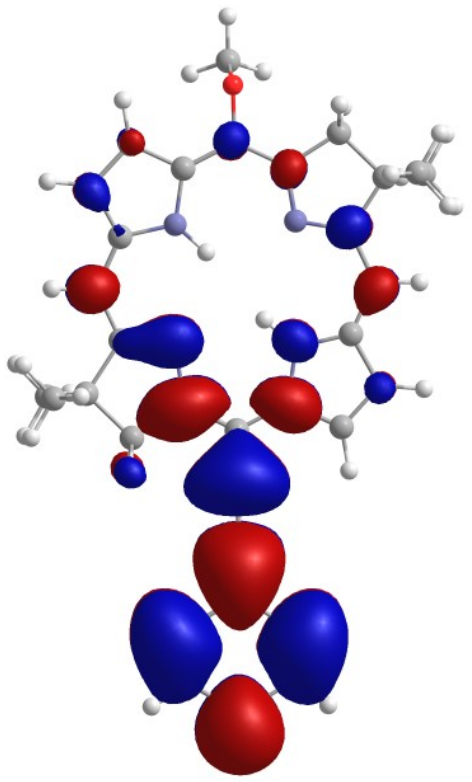
| S4 | 0.84023 | | |
| S4 | 0.16305 | | |
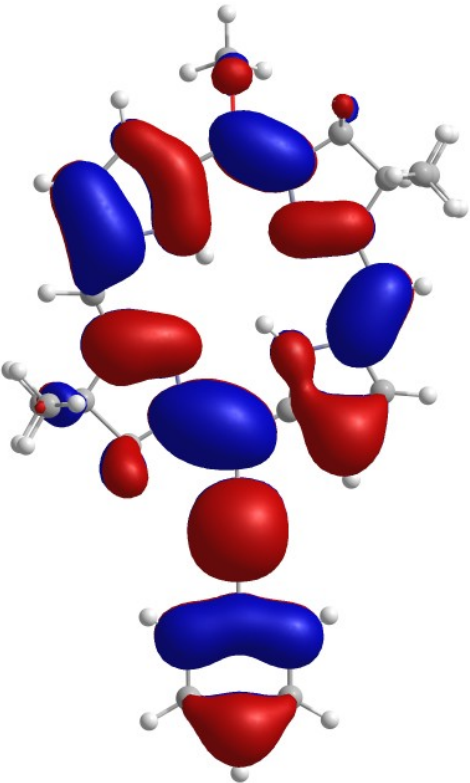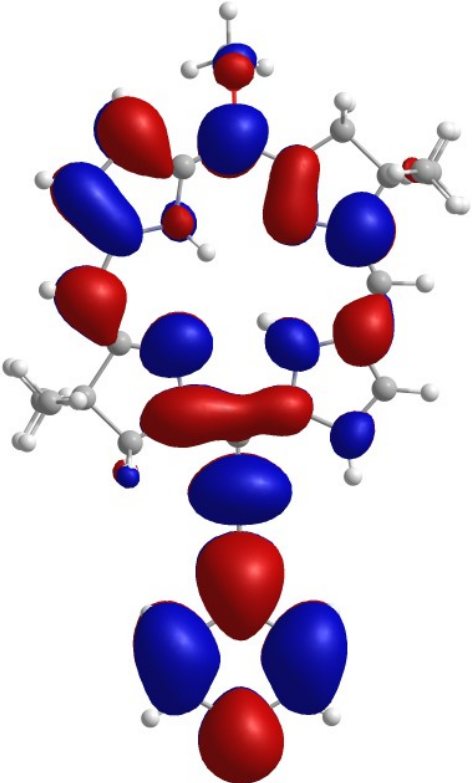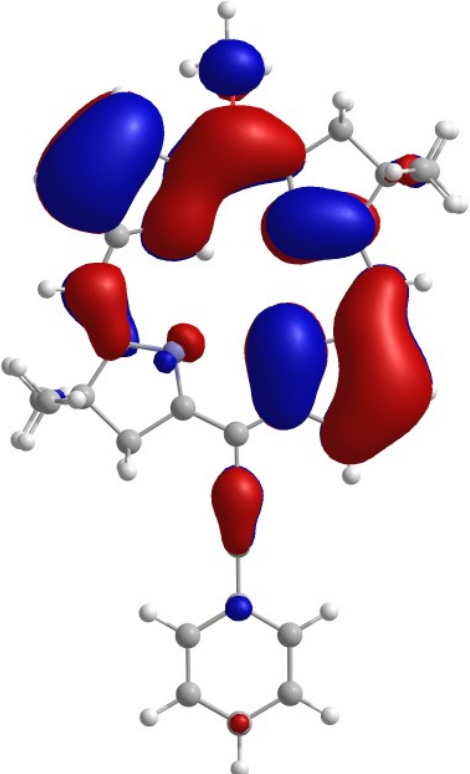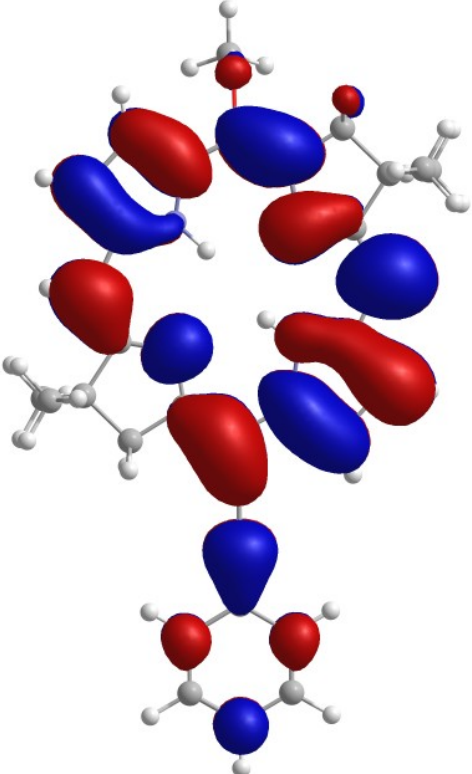
S5	0.83656		
S5	0.14879		
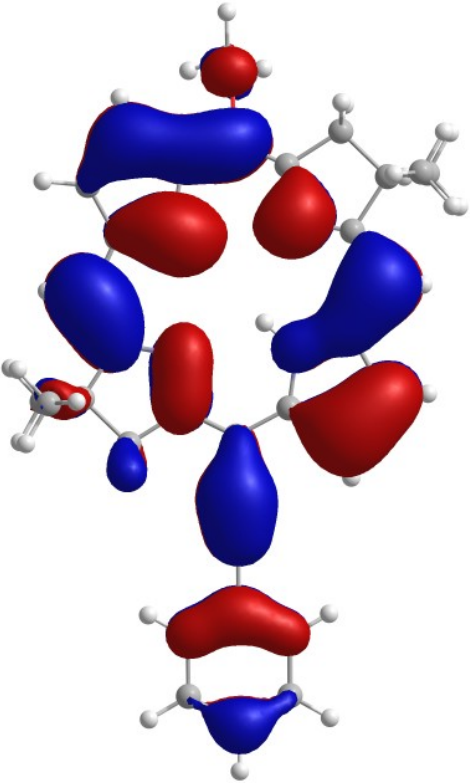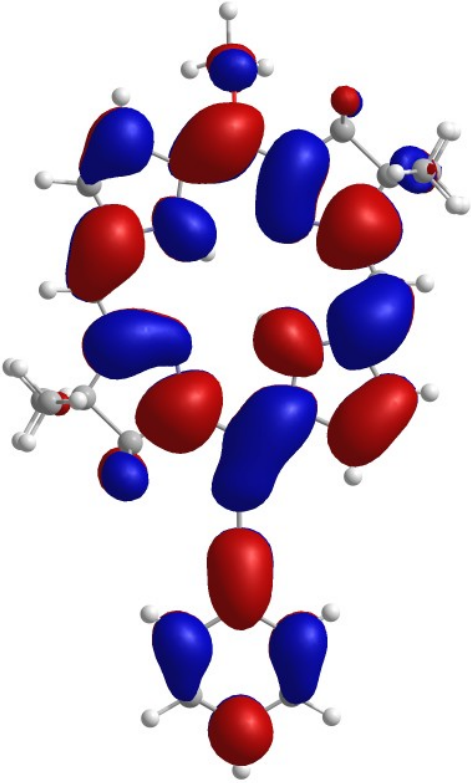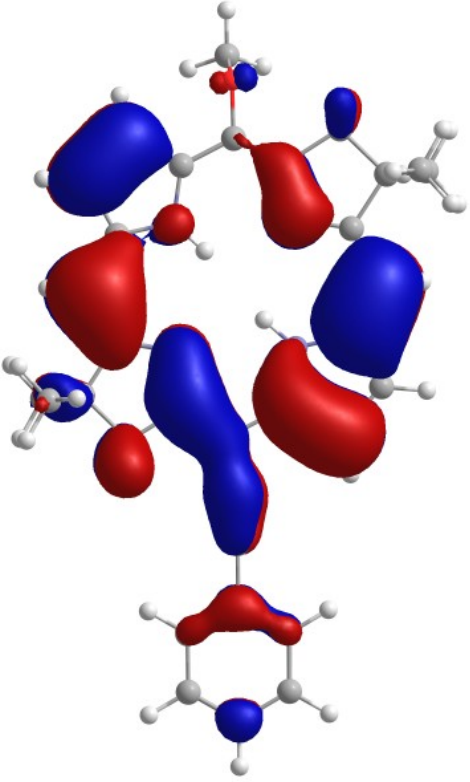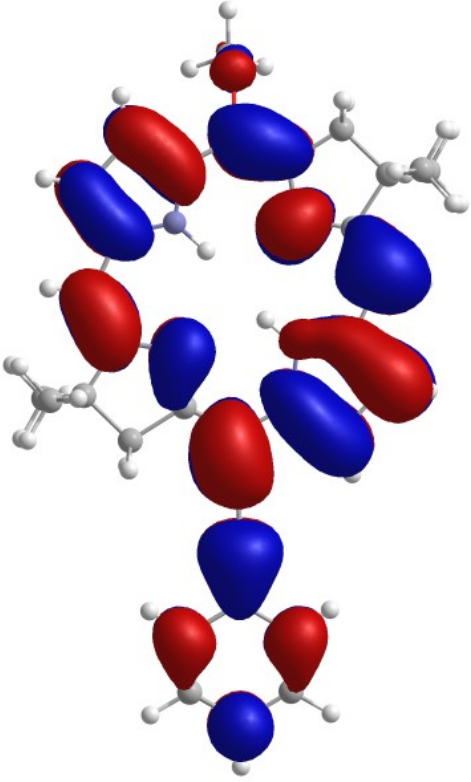
S6	0.99127		
S7	0.88777		
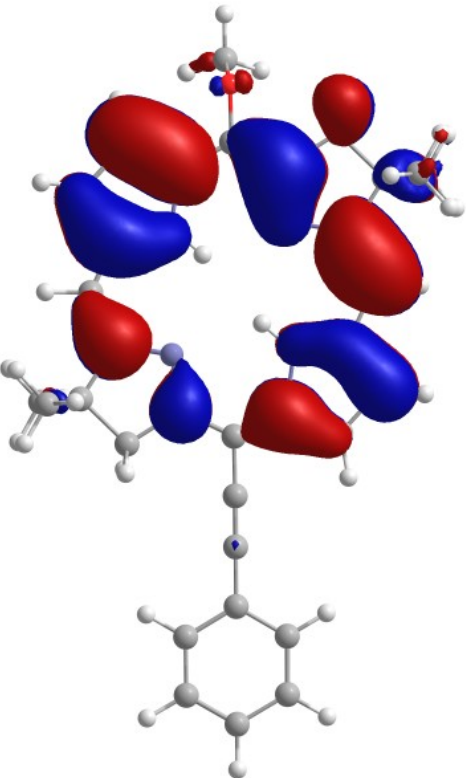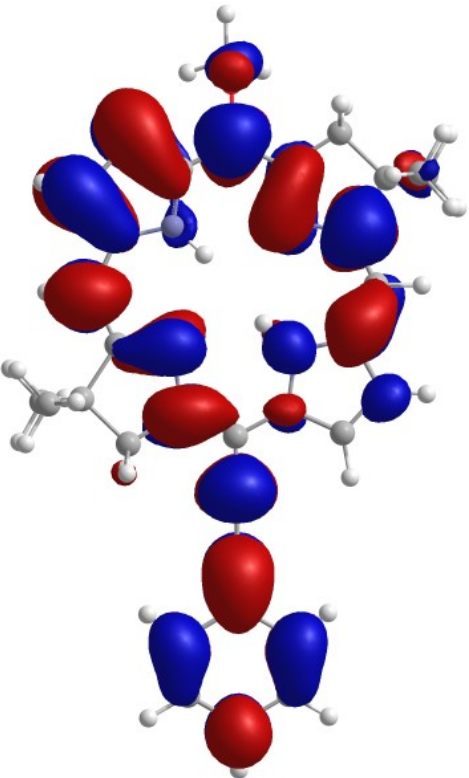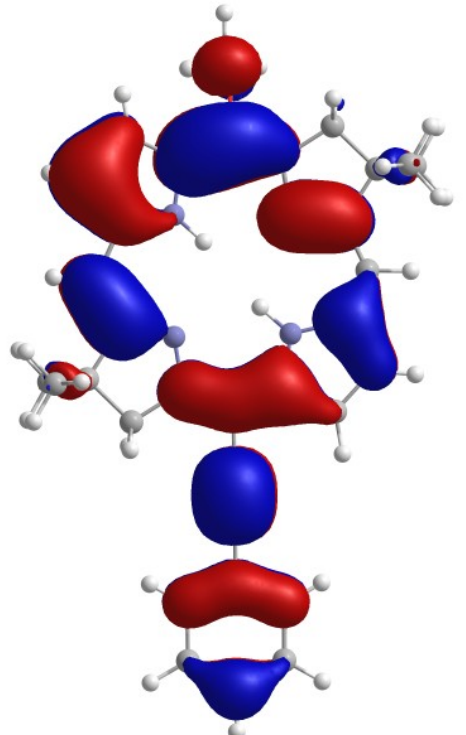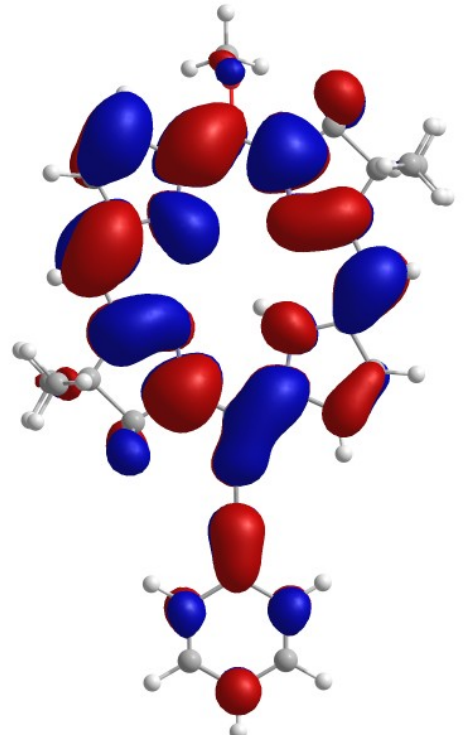
| S7 | 0.08718 | | |
| S8 | 0.98602 | | |
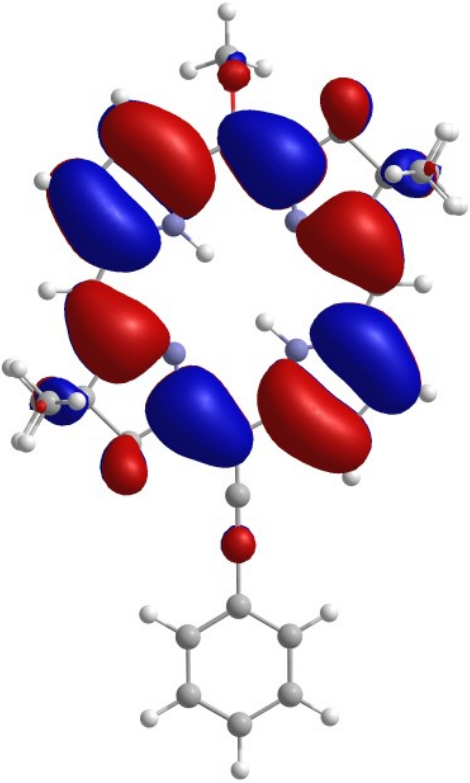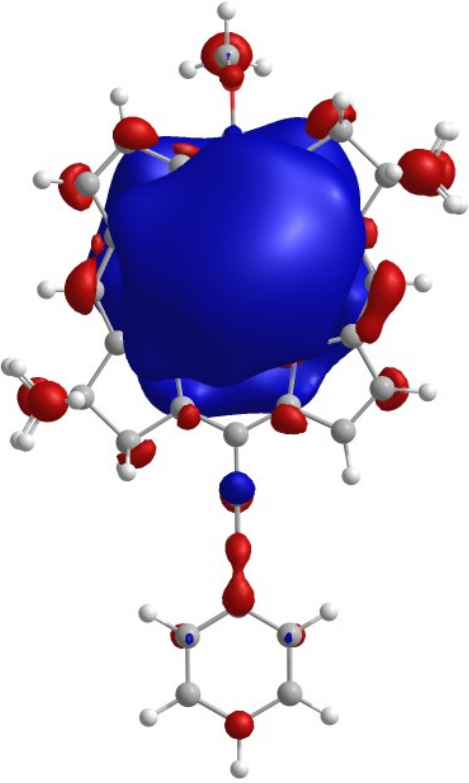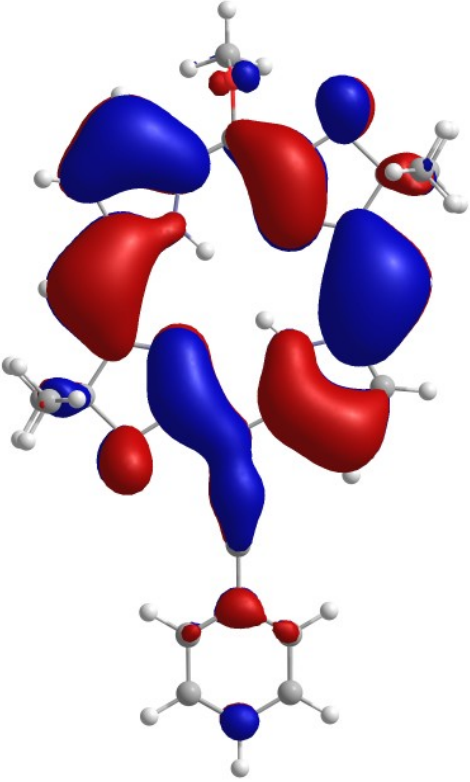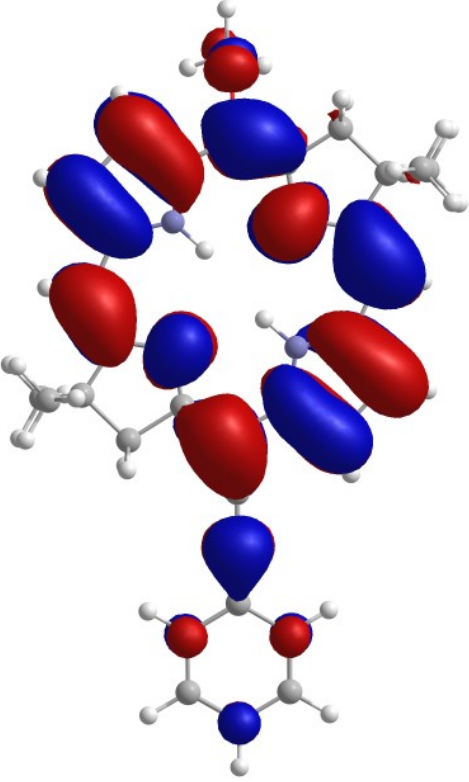
S9	0.88684		
S9	0.07873		
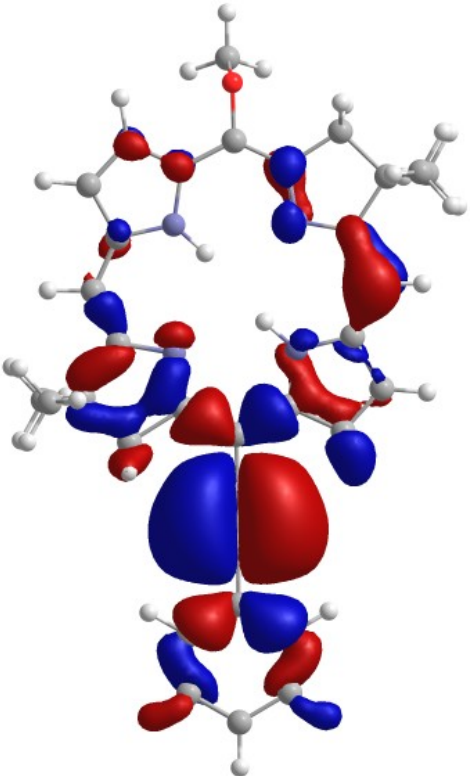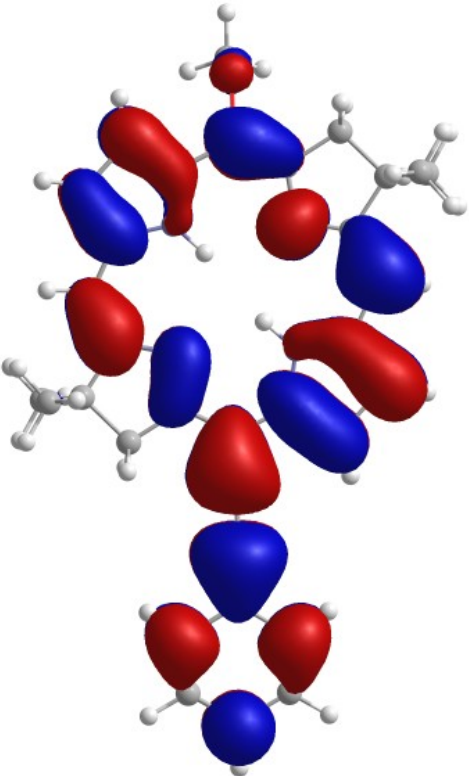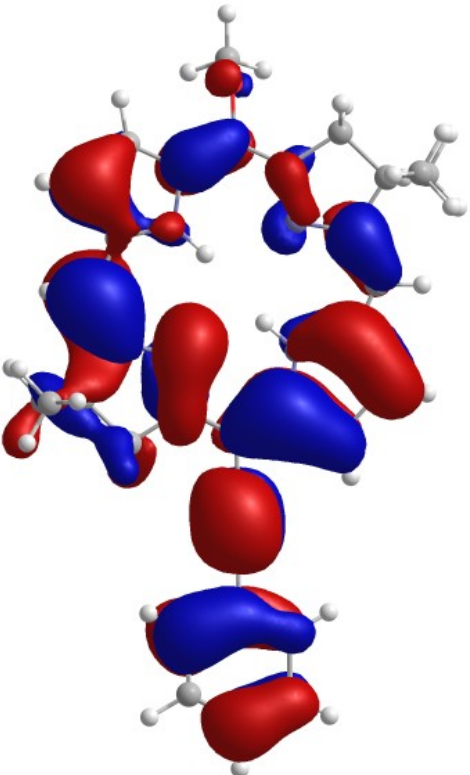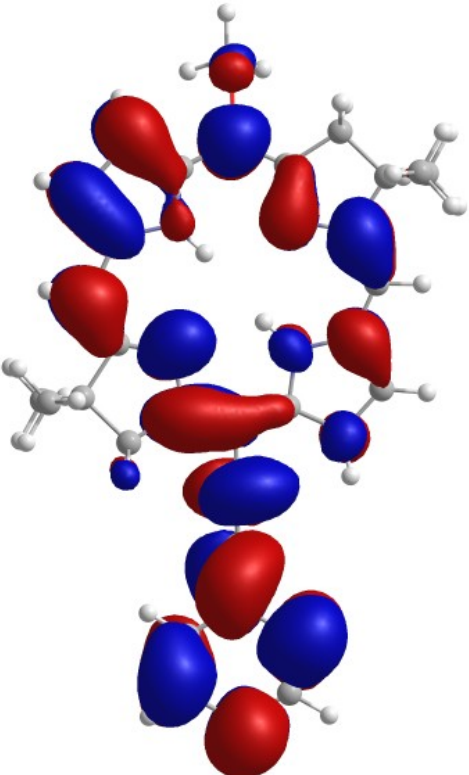
S10	0.68442		
S10	0.21745		
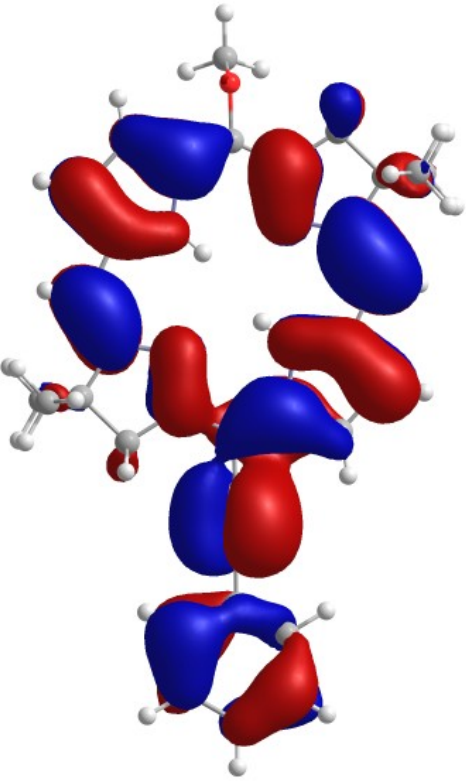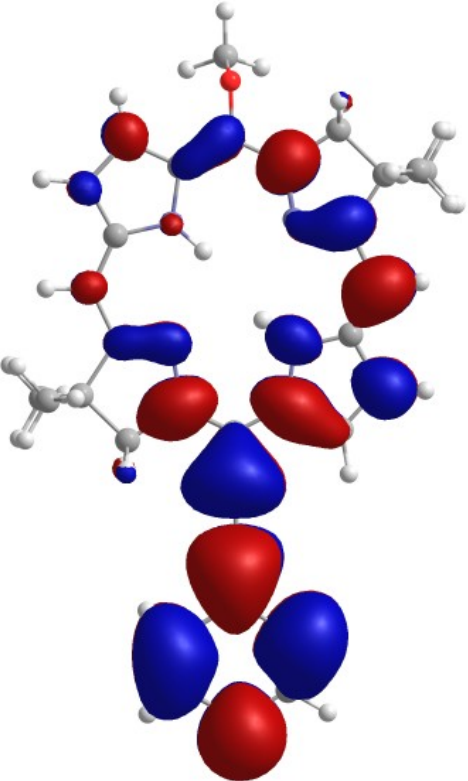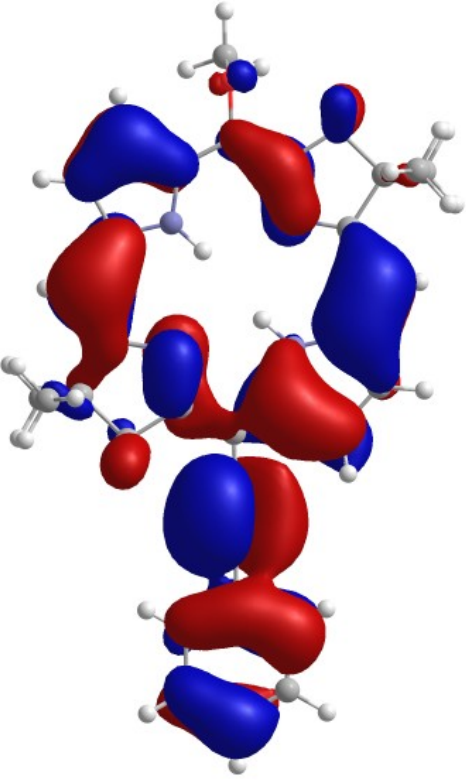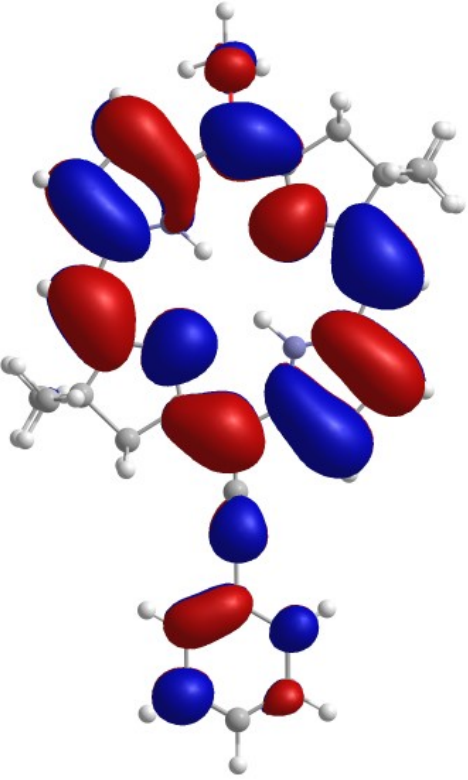
S10	0.05889		
S11	0.48945		
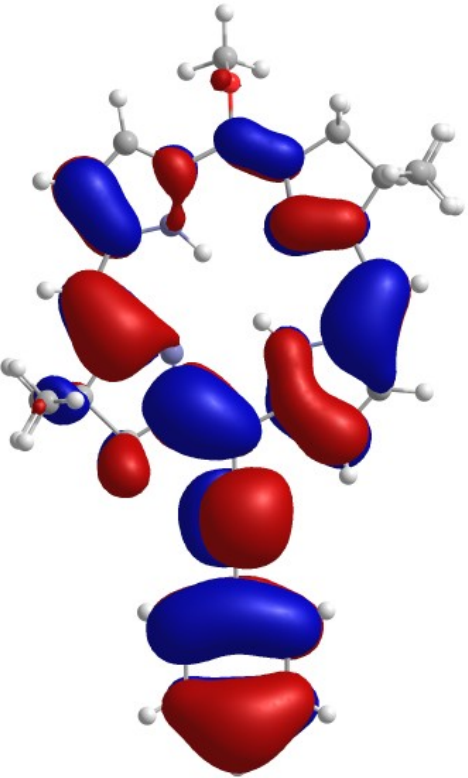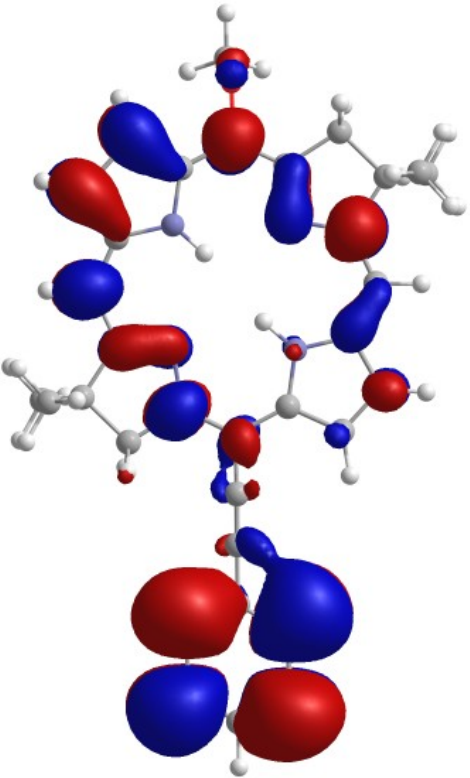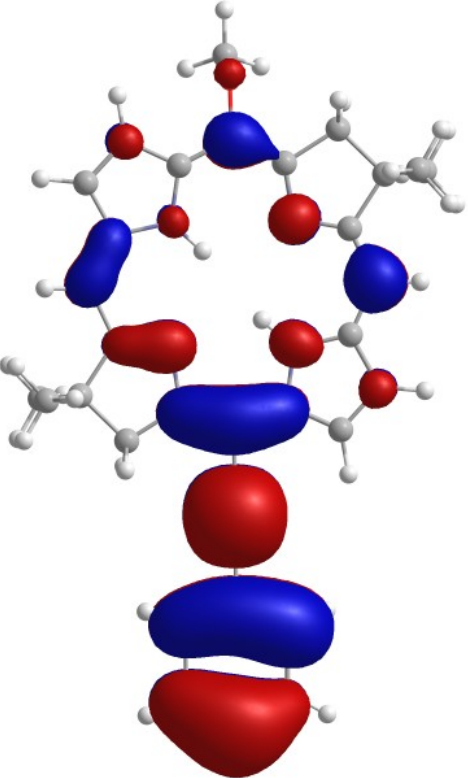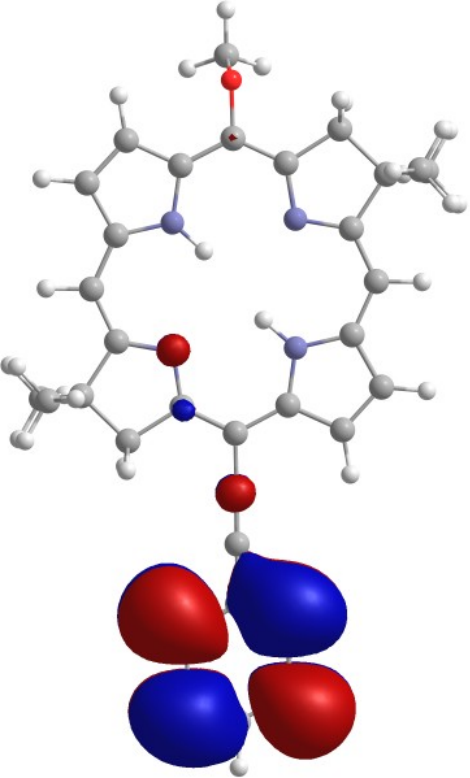
S11	0.40633		
S11	0.05233		
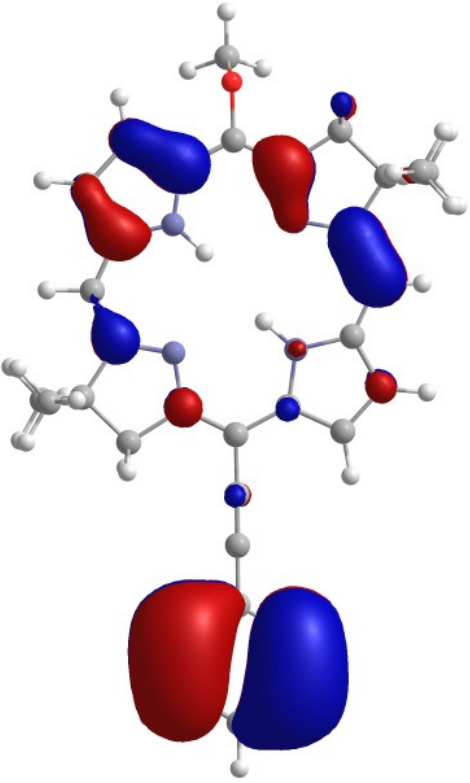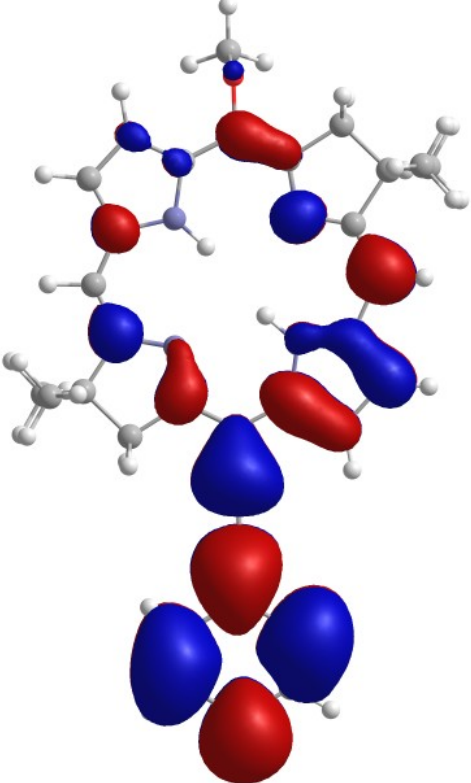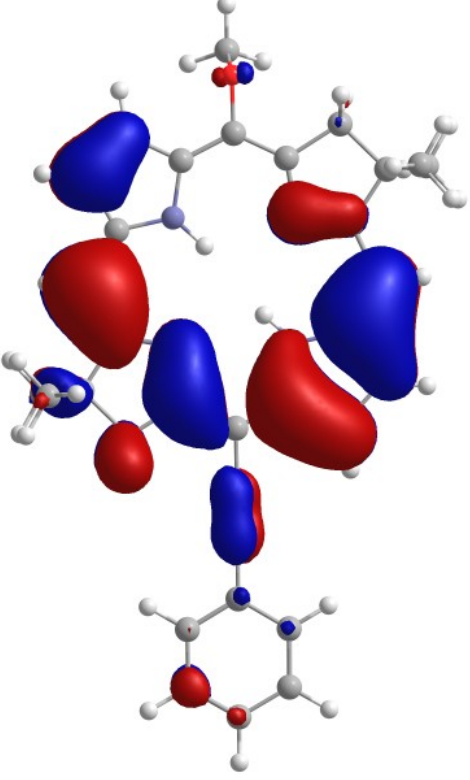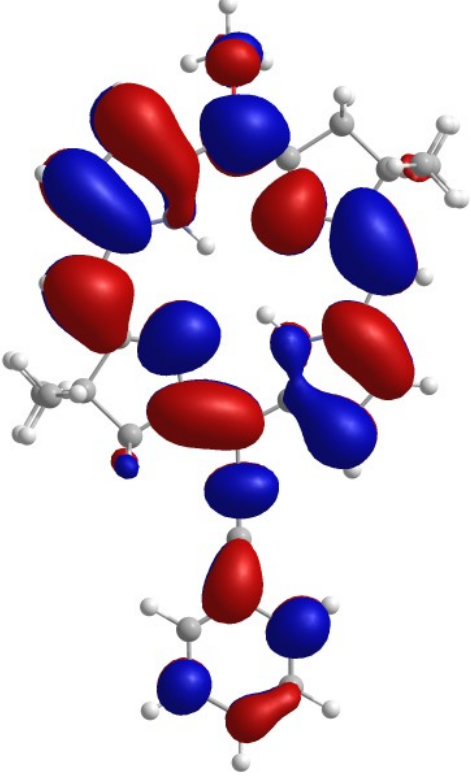
| S12 | 0.87902 | | |
| S12 | 0.08726 | | |
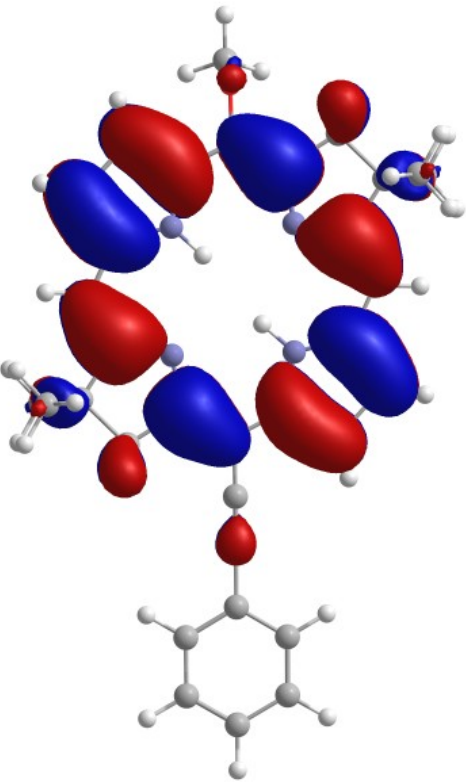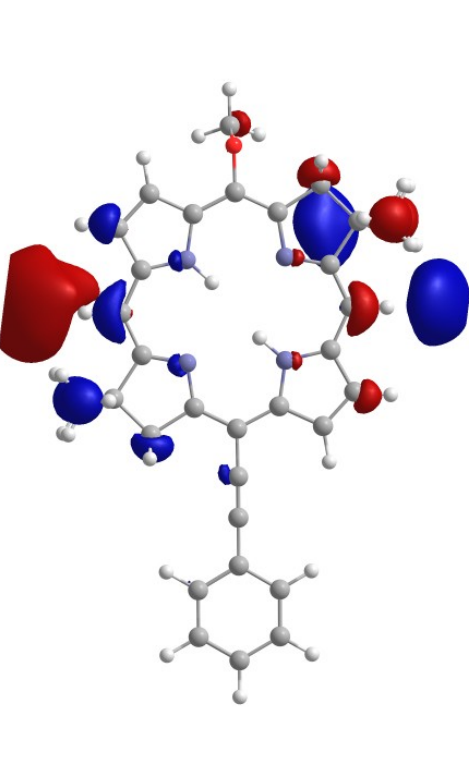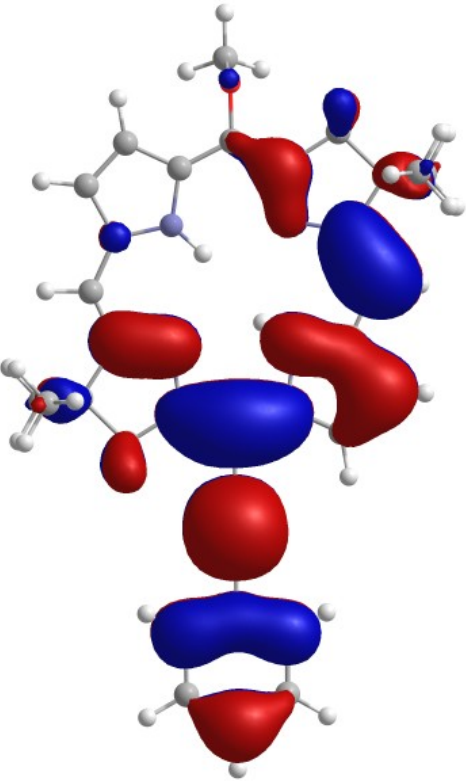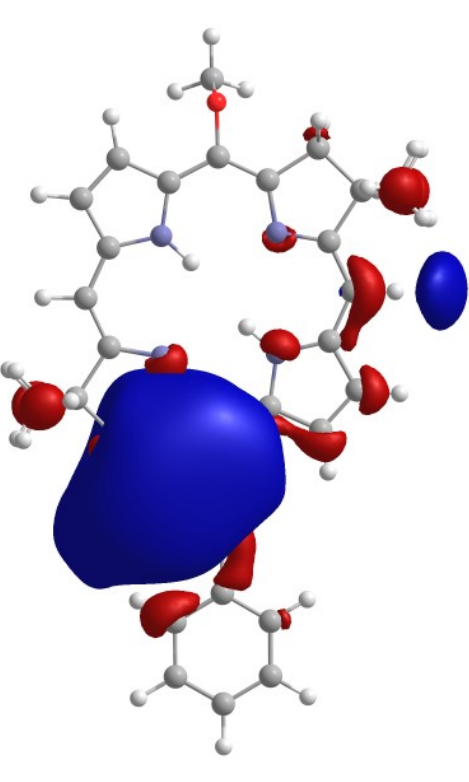
S13	0.88332		
S13	0.08596		

S14	0.48636		
S14	0.39102		

S14	0.08086		
S15	0.55612		

S15	0.36149		
S15	0.05920		

S16	0.90735		
S16	0.05767		